

**FULL SCALE LIMITED VENTILATION FIREROOM
FIRE EXPERIMENTS**

BY

DARIN JOHN MILLAR

Supervised by

Dr Charles M. Fleischmann

**Fire Engineering Research Report 95/4
August 1995**

This report was presented as a project report
as part of the M.E.(Fire) degree at the University of Canterbury

School of Engineering
University of Canterbury
Private Bag 4800
Christchurch, New Zealand

Phone 643 366-7001
Fax 643 364-2758

ABSTRACT

The purpose of this project was to investigate the conditions that exist in a typical residential compartment fire when subject to limited ventilation. Emphasis was on the conditions that leads to a backdraft from natural fuel and the circumstances prior to a smoke explosion. Also included within this report is a comparison of the results with those expected from CFAST, a computer zone model.

The first phase of the project was to design a full scale apparatus to safely carry out the experiments. The second phase consisted of seven experiments with variations in ventilation size and location, and fuel elevation. The fuel used was timber cribs that provided a fuel load density of 340 MJ/m^2 . Temperatures, mass loss, pressures and O_2 concentration within the compartment were monitored. The areas used to represent leakage ranged from 0.0154m^2 to 0.0079m^2 . Ventilation was modelled using two horizontal circular vents located at lowest and highest practical points. In each experiment the vent at the bottom was twice the area of that at the top.

Under the conditions experimented no backdraft occurred. During one experiment (number 6) a smoke explosion occurred that caused an instantaneous temperature rise of 140°K and pressure increase of 30 Pa . Further research in this phenomena is required. Comparisons made with CFAST indicate that it is inadequate in coping with limited ventilation fires in a single compartment situation.

ACKNOWLEDGMENTS

My most sincere gratitude goes to my supervisor and friend Charley Fleischmann who sacrificed many of his personal hours to help complete this project and supplied endless encouragement, enthusiasm and homebrew. Many thanks also go to Andy Buchanan. Without Andy this course would not exist. Thanks to Ivan Bolliger for his friendship, patience, and effort throughout the project. The Fire Service played an important role in both having the foresight to fund the course and in their unlimited support during the construction of the container, especially Steve Rule, Dave Berry and the guys from the workshop.

This project would not have been possible without the dedication and persistence of Shane Gorinski, Simon Johnson and the I.F.E Wellington. Their perseverance enabled most of the materials to be donated by the following:

Winstone Wallboards

Wormalds

Forman Insulation

Christchurch City Council

Thanks to all the technicians especially Geoff Hill, Trevor Berry, Ray Allen and Paul Fuller

Thanks to Carol Caldwell who let Charley stay out and play during the nights. Also our cheerleader, secretary and cue card model Catherine Price. Special thanks to my classmates, Ivan Bolliger, Tony Enright, Faran Rahmanian, Hanz Gerlich, Brady Cosgrove and all my friends.

Finally, thanks to my family who have supported me right through my academic career and always been there for me.

TABLE OF CONTENTS

ABSTRACT.....	i
ACKNOWLEDGEMENTS	ii
TABLE OF CONTENTS	iii
LIST OF FIGURES, PHOTOS AND TABLES	vi
NOMENCLATURE	ix
1. INTRODUCTION	1
2. EXPERIMENTAL APPARATUS	5
2.1. CONTAINER.....	5
2.2. STRENGTH.....	7
2.2.1. WALLS	7
2.2.2. ROOF	8
2.3. PRESSURE RELIEF	11
2.3.1. PRESSURE RELIEF PANEL.....	11
2.3.2. SIZE OF THE PRESSURE RELIEF PANEL	11
2.3.3. CONSTRUCTION	13
2.3.4. OPENING FORCE.....	14
2.3.5. INTERIOR WALL VENTS.....	16
2.4. WINDOW	17
2.4.1. HIGH TEMPERATURE RESISTANCE	17
2.4.2. STRENGTH OF THE GLASS	18
2.4.3. CONSTRUCTION	21
2.5. FRONT OPENING	21
2.6. INTERNAL INSULATION	23
2.6.1. LINING CONFIGURATION	23
2.6.2. LINING MATERIALS	24
2.6.2.1. GYPSUM PLASTER BOARD.	24
2.6.2.2. CALCIUM SILICATE BOARD.	25
2.6.3. TASEF ANALYSIS	25
2.6.3.1. THERMAL PROPERTIES OF MATERIALS	27
2.6.3.2. HEAT TRANSFER CO-EFFICIENTS	28
2.6.4. TASEF RESULTS.....	28
2.7. IGNITER	29
2.8. LEAKAGE VENTS	31
3. INSTRUMENTATION	32
3.1. TEMPERATURE.....	32
3.1.1. COMPARTMENT TEMPERATURES	32
3.1.2. WALL LINING TEMPERATURES.....	33
3.2. PRESSURE.....	33
3.3. FRONT VENT FLOW VELOCITIES	33
3.4. GAS ANALYSIS	35
3.4.1. OXYGEN ANALYSIS	36
3.4.2. GAS CHROMATOGRAPHY.....	37

3.5. AMBIENT CONDITIONS	38
3.6. LOAD CELL	39
3.7. DATA ACQUISITION METHOD	40
4. EXPERIMENTAL PROGRAM	41
5. FUEL DESIGN, LAYOUT AND IGNITION.....	45
5.1. INTRODUCTION	45
5.2. CRIB DESIGN	45
5.3. LAYOUT AND IGNITION SOURCE.....	46
6. METHOD OF RESULTS ANALYSIS	49
6.1. ANALYSIS	49
6.2. MASS FLOW RATES.....	49
6.3. LAYER HEIGHT AND TWO ZONE TEMPERATURES.....	51
7. EXPERIMENTAL RESULTS AND DISCUSSION	53
7.1. CONSISTENCY	54
7.2. REDUCED VENT AREAS.....	54
7.3. CHANGE IN ELEVATION OF THE TOP VENT.....	55
7.4. ELEVATION OF THE FUEL	55
7.5. PILOT FLAME DURATION.....	56
7.6. DISCUSSION OF RESULTS.....	56
7.6.1. REDUCED VENT AREA	60
7.6.2. LOWERED ELEVATION OF THE TOP VENT.....	60
7.6.3. ELEVATION OF THE FUEL.....	61
7.6.4. EXTENDING THE DURATION OF THE PILOT FLAME.....	64
7.6.5. SMOKE EXPLOSION.....	65
8. COMPUTER MODELS.....	67
8.1. INTRODUCTION	67
8.2. CFAST	67
8.2.1. PREVIOUS COMPARISONS	68
8.2.2. ESTIMATIONS OF UNKNOWNNS	68
8.2.2.1. GAS COMPOSITION.....	69
8.2.3. CFAST CALIBRATION.....	71
9. COMPARISON BETWEEN EXPERIMENTS AND CFAST.....	74
9.1. DISCUSSION	75
9.1.1. MASS LOSS WITH TIME	75
9.1.2. COMPARTMENT TEMPERATURE.....	75
9.1.3. INTERFACE HEIGHTS.....	77
9.1.4. MASS FLOWS	77
9.1.5. OXYGEN CONCENTRATION HISTORY.....	79
10. CONCLUSIONS.....	80
11. FUTURE RESEARCH.....	81
12. REFERENCES	82
13. BIBLIOGRAPHY.....	85

APPENDIX A

APPENDIX B

APPENDIX C

APPENDIX D

FIGURES, PHOTOS AND TABLES

Figure 2.1 Schematic of the completed test container	6
Figure 2.2 Roof element.....	9
Figure 2.3 Free body of roof element	9
Figure 2.4 Photo of pressure relief panel	13
Figure 2.5 Glass specimen.....	18
Figure 2.6 Window frame construction	21
Figure 2.7 Lining configurations.....	23
Figure 2.8 Lining systems A and B analysed using TASEF	26
Figure 2.9 Simplified TASEF geometry.....	26
Figure 2.10 Comparison of lining options.....	29
Figure 2.11 Location of the electrodes	31
Figure 2.12 Location of vents	31
Figure 3.1 Thermocouple locations throughout the container	32
Figure 3.2 Gas sample line, from fire compartment to oxygen analyser	36
Figure 3.3 Load transfer frame.....	39
Figure 4.1 Plan view of crib layout.....	47
Figure 4.2 Elevation of the set up.....	48
Figure 7.1 Consistency between temperatures and layer height.....	57
Figure 7.2 Temperature history of experiment 6	58
Figure 7.3 Compartment flow history for experiment 5.....	59
Figure 7.4 Compartment flow history for experiment 6.....	59
Figure 7.5 Temperature and layer height for experiments 2 and 3	60
Figure 7.6 Temperature and layer height for experiments 5 and 6	61
Figure 7.7 Temperature and layer height for experiments 2 and 3	62
Figure 7.8 Temperature and layer height for experiments 4 and 5	62
Figure 7.9 Temperature and layer height for experiments 6 and 7	64
Figure 7.10 Compartment pressure history of experiment 6.	65
Figure 7.11 Mass yield of CO ₂ at the top port during experiment 6.....	66
Figure 7.12 Mass yield of O ₂ at the top port during experiment 6	66
Figure 9.1 Comparison of layer temperatures in scenario 2.....	76
Figure 9.2 Comparison of layer temperatures in scenario 3	76

Figure 9.3 Comparison of layer temperatures in scenario 7.....	77
Figure 9.4 Comparison of mass flow out in scenario 2.....	78
Figure 9.5 Oxygen history for scenario 4.....	79
Photo 1.1 I.F.E Backdraft demonstration.....	3
Photo 2.1 Completed compartment.....	6
Photo 2.2 Pressure panel failure mechanism.....	14
Photo 2.3 Testing of the pressure relief panel.....	15
Photo 2.4 Pressure relief panel held open by a spring and chain system	16
Photo 2.5 The vent in the fully opened position.....	22
Photo 2.6 Steel runners for lining fixing.....	24
Photo 2.7 Location of the electrodes with respect to the fuel	30
Photo 3.1 Installed bi-directional probes	35
Photo 4.1 Partial involvement of the fuel.....	43
Photo 5.1 Shredded paper for ease of ignition.....	47
Photo 5.2 Layout of timber cribs.....	48
Photo 7.1 Partial involvement of the fuel.....	57
Photo 7.2 Developement of smoke layer	63
Photo 7.3 Consistent dense smoke layer.....	63
Table 2.1 FMS (Table 3) Table required to determine the minimum internal over pressure vent area	12
Table 2.2 Factors C2 and C3 for plate bending.....	20
Table 2.3 Thermal properties of 16mm gypsum plasterboard.....	27
Table 2.4 Thermal properties of steel	27
Table 2.5 Thermal properties of Promatect H.....	27
Table 2.6 Heat transfer co-efficients at the boundaries	28
Table 4.1 Description of each experimental set up.....	42
Table 7.0 Experimental conditions	54
Table 7.1 Comparison of experiments 3 and 4.....	54
Table 7.2 Effect of reduced vent areas	55
Table 7.3 Change in location of the top vent	55
Table 7.4 Elevation of the fuel	55
Table 7.5 Effect of pilot flame duration.....	56

Table 8.1 CFAST sensitivity to variables.....	72
Table 9.1 Comparisons of CFAST estimations and experimental results	74

NOMENCLATURE

a	short window dimension (m)
A	cross-sectional area (m ²)
A _v	vent area (m ²)
A _s	internal surface area of enclosure (m ²)
b	long window dimension (m)
C	fuel characteristic constant (kPa ^{1/2})
C(Re)	empirical calibration constant (being a function of the Reynolds number)
D	burner diameter (m)
c _p	specific heat (J/kgK)
Fr	froude number (dimensionless)
g	acceleration of gravity (m/s)
H	compartment height (m)
ΔH	heat of combustion (MJ/kg)
k	thermal conductivity (W/mK)
L	half thw width of the container (1.175m)
L ₃	longest dimension of the enclosure (m)
M	moment (Nm)
M _w	molecular weight (kg)
\dot{m}''	mass loss rate (kg/m ² s)
p	pressure within compartment (kPa)
P	perimeter of cross-section (m)
P _{red}	Max. internal overpressure that can be withstood by the weakest structural element (kPa)
ΔP	pressure difference across bidirectional probe (Pa)
q	force per metre width
R	universal gas constant (8314 J/kg.mol.K)
t	thickness (m)
T	temperature (K)
U	Gas flow rate (m/s)
V	velocity (m/s)
w	glass width (m)

x_1	interface height (m)
Z	section modulus (m ³)
ε	emissivity of gas and boundary (dimensionless)
β	convective heat transfer coefficient (W/m ² K)
σ	Stefan-Boltzman constant (5.67×10^{-8} W/m ² K ⁴)
σ_{failure}	bending stress (Mpa)
γ	convective heat transfer power (dimensionless)
ρ	density (kg/m ³)
α	thermal expansion coefficient (3.25×10^{-6} /K)

SUBSCRIPTS

a	air
c	combustion
g	gas
l	lower layer
o	ambient
s	surface
u	upper layer
x	short dimension
y	long dimension

1. INTRODUCTION

BACKDRAFT. A phenomenon of fire that has taken the lives of many firefighters. Unfortunately most don't even know what it is.

Backdrafts occur in closed compartments where the fire, starved for oxygen, releases large amounts of excess pyrolozates into the space. When the compartment is vented (eg. door opened by a firefighter), oxygen in the form of a gravity current combines with the pyrolozates and produces a flammable mixture of gas. An ignition source, now completes the fire triangle. Within seconds of ignition, a rapid combustion process ignites the flammable mixture within the compartment producing a large fireball outside the opening. Also of concern for any firefighter, is the time from when the door is opened, to ignition. During such time the firefighter moves in deeper to the compartment. If still alive, escape could become impossible.

The first documented accounts of the backdraft phenomena was in the early 1900's (CROFT 1980). Since then, several reports by fire service have been produced, most give a graphic description of the event but none attempt to quantify. The National Fire Protection Association (NFPA), define Backdraft as

“The explosive or rapid burning of heated gases that occurs when oxygen is introduced into a building that has not been properly ventilated and has a depleted supply of oxygen due to fire”(Chitty 1993)

Similar to backdraft is a smoke explosion. The same principle of a oxygen starved fire applies, instead of oxygen entering as a gravity current, leakage allows feeding of oxygen to the smouldering fuel and the compartment gases. The outcome is an ignition of the flammable gases resulting in an explosion

For a firefighter entering a room there are few if any signs to warn them of the impending danger. They need to be shown the phenomena first hand and have the circumstances leading to this potential catastrophe explained.

The primary ingredient for a backdraft or smoke explosion is a compartment with low ventilation. Due to the reform of fire safety codes in many countries, emphasis has been towards protecting occupants during evacuation and protecting neighbouring buildings. In doing so passive fire protection measures are installed. Most significant in this case is fire resistant glazing that could have a 120 minute fire rating (SCHOTT). Normal glass in a compartment has no rating and will break early on in the fires growing stage. The fire will then grow to flashover and beyond. However, if the window does not break, the excess pyrolyzates accumulate within the room setting up a potential backdraft situation.

Commercial buildings are by no means the only compartments of concern. Energy efficient homes are on the increase. With the installation of double glazing and tighter construction practices, the potential for backdraft within a residential fire may also increase.

Between 1907-1976 a total of 127 fires involving explosions were documented in the available literature within the United Kingdom, United States and Canada. A total of 70 people were killed, that equates to one in every second explosion (CROFT 1980). In a later survey, Chitty 1993 highlighted the lack of work carried out in Backdraft. To date, the only experimental work to understand the phenomena was done at The University of California, Berkeley, USA. At Berkeley, Fleischmann et al carried out a program where both half residential scale experiments and salt water modelling were used to quantify backdraft. Although this was a thorough analysis, it was limited to one fuel source and as with all research projects, raises many more questions.

Many of the firefighters today are not professional but volunteers who undergo very limited training. Hence, the first objective of this project is to design and build a test set up, scaled to represent a typical residential compartment, in which both backdraft and post flashover experiments can be safely conducted.

Once the set up was completed, an experimental program investigating the ventilation effects on wooden crib fires was undertaken:

- i) What conditions within the compartment are influenced most significantly from the variation in ventilation size and location, and fuel elevation. Do any of these variations enhance conditions required for a backdraft.

ii) Under low ventilation is there enough production of pyrolyzates and incoming oxygen for a smoke explosion within the container before any simulated opening.

iii) Do computer zone models effectively represent the conditions in a low ventilated compartment.

It was intended that the Institution of Fire Engineers, Wellington Group, construct a similar set up in order to demonstrate to members of the Fire Service and Engineers involved in fire design (eventually the public) the difference between Flashover and Backdraft (see photo 1.1).

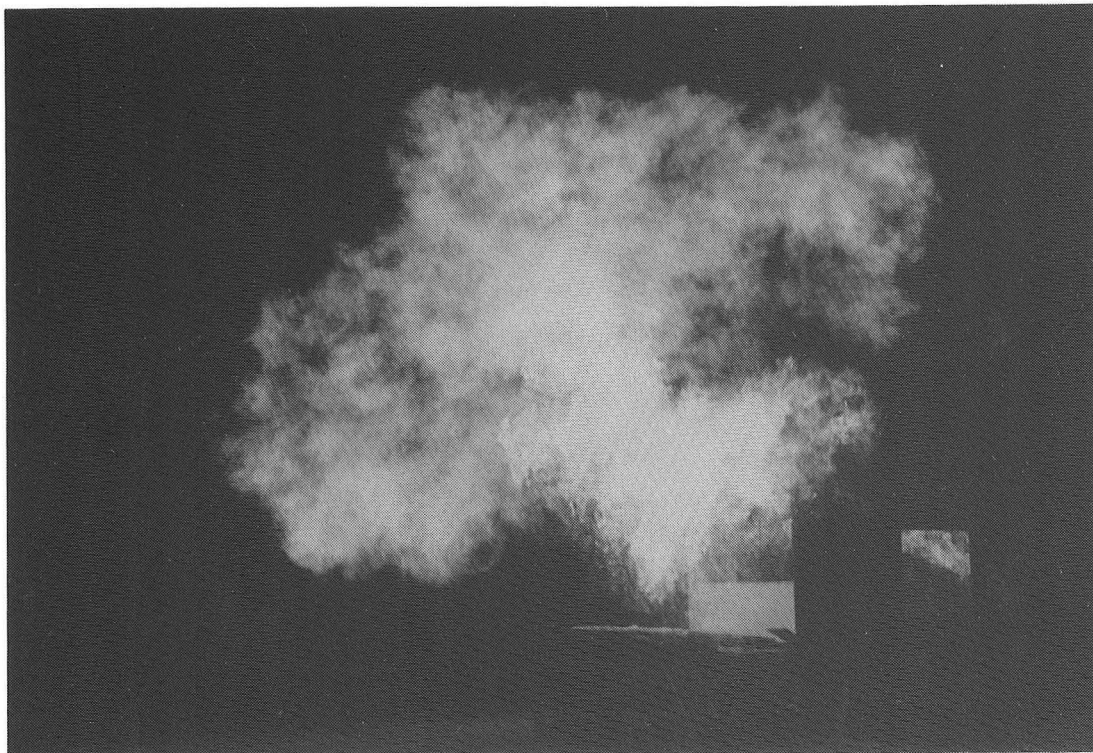


Photo 1.1 IFE backdraft demonstration

2. EXPERIMENTAL APPARATUS

2.1. CONTAINER

A shipping container (2.4m x 2.4m x 6m) was modified in order to design an apparatus in which to safely simulate the backdraft scenario. This size is similar to what may be expected for an office room or small bedroom. Modifications to the container include the installation of;

1. gypsum plasterboard and calcium silicate board,
2. a large window,
3. a pressure relief panel,
4. a front opening hatch.

Figure 2.1 shows the final test container with internal dimensions

To allow for ease of work under the container it was placed on wooden supports 0.8m high.

The framing for the observation window (PYRAN fire resistant glazing) is constructed in accordance to manufactures specifications to produce a fire and pressure resistant window system (SCHOTT). The pressure panel was required to relieve any over pressure hazard, in accordance to specific design (FMS 1991). To simulate a window breaking or a door opening a vent approximately 2.2m wide by 0.75m high was placed in the centre of the front panel. This vent was in turn covered by a manually operated hatch, which could be opened at a predetermined time. A 15000 volt transformer was used to ignite the propane pilot flame, and as an ignition source for the backdraft.

*Note that within the rest of this document the wall modified for the window is referred to the right wall. The non-window wall is referred to as the left wall.

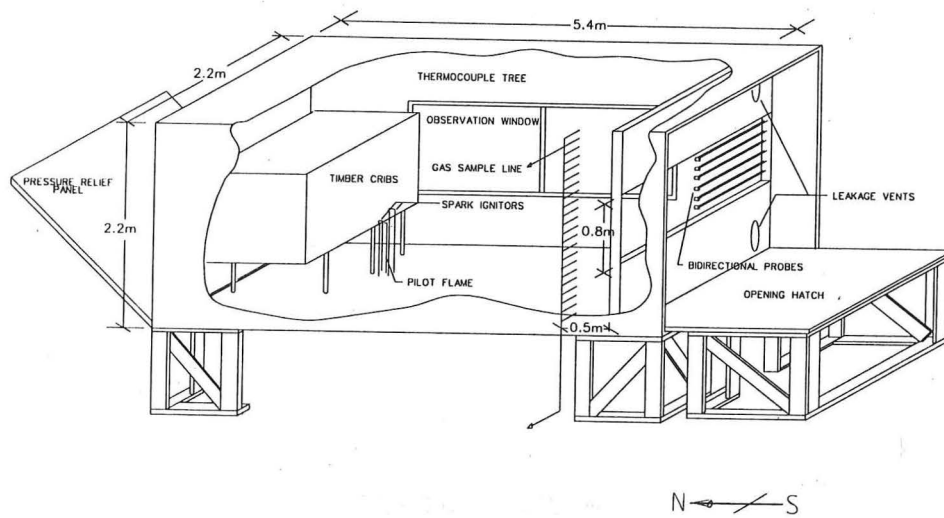


Figure 2.1 Schematic of the completed test container

Photo 2.1 shows the final compartment and test area. To the left is the experimental container, the container on the right was used to house the data acquisition system, oxygen analyser, gas flow regulators and for general storage.



Photo 2.1 Completed compartment

The container was constructed from steel sections, vertically corrugated steel side walls and end wall, flat plate steel roof and doors, assembled by means of automatic and semi-automatic MIG welding. The welding of all outside parts of the construction as well as the base structure is continuous and of full penetration to ensure strength and weatherproofness. A 30mm thick wooden floor is supported by 162 x 50 x 30 x 4.5mm thick steel press formed channel¹.

2.2. STRENGTH

Due to the explosive nature of backdraft, structural analysis of the container shell was required. Analysis determined the allowable internal pressure that the container could safely withstand. The surfaces considered in the analysis were the roof, side walls and the end wall. The floor was judged as sufficiently strong due to the load it is designed to carry.

A structural analysis of the container shell used material strength properties from Appendix A. The roof, side walls and end wall were analysed based on a tensile strength of 480 MPa and yield point of 343 MPa.

The container was analysed subject to an internal pressure of 10 kPa. The bending stresses in the plates were calculated and compared with the yield stress.

The analysis concluded that the container can withstand an internal over pressure of over 20kPa.

2.2.1. WALLS

A computer program for the finite element analysis of structures, was applied to each of the walls. The finite element analysis program, SAP90, consists of four elements, the most suitable for our situation being the three-dimensional SHELL element. SHELL simulates the behaviour of two-and three-dimensional plate bending systems:

¹ Appendix A contains a full description of all container components.

‘The plate bending behaviour includes two-way out-of-plane plate rotational stiffness components and a translational stiffness component in the direction normal to the plane of the element. The plate bending behaviour does not include any effects of shear deformation’ (Habibullah 1989).

The SAP90 analysis is based on members of uniform thickness. The corrugated profile of the container walls provide increased strength compared to that of a flat plate of equivalent thickness. In order to overcome this within SAP 90, the second moment of inertia for the actual profile was equated to that of a flat uniform plate. The thickness of corrugated plate and roof plate was 2mm. The equivalent thickness to account for the profile was ascertained to be 17mm.

The internal container pressure was simulated within SAP90 by applying self weight equivalent to 10kPa to the plates while under simply supported conditions.

Results indicated that the side walls could withstand an internal over pressure in excess of 20kPa.

2.2.2. ROOF

Due to its thickness, the roof was considered to be the major concern. Its small thickness led to the assumption that the resistance offered to bending was negligible hence the force in the plate was all tension. Subject to an assumed maximum deflection of 0.05m, the tensile stress in the plate was analysed as follows:

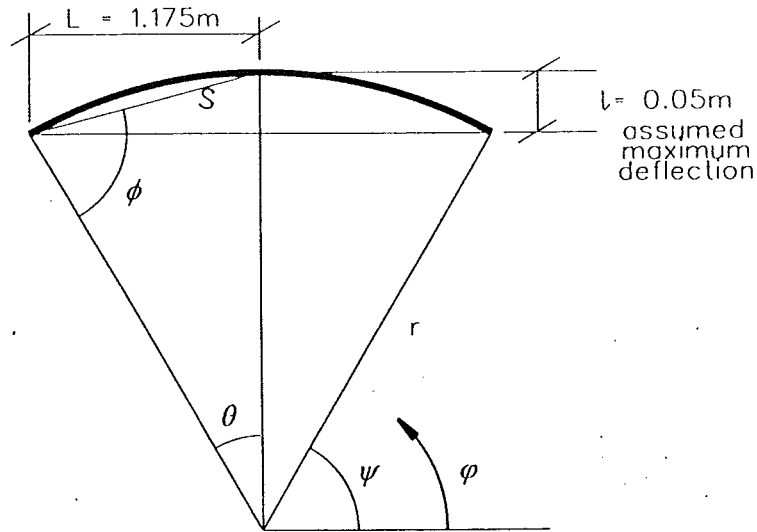


Figure 2.2 Roof element

Applying geometric relationships to the roof depicted in figure 2.2:

$$\phi = \left[\tan^{-1} \frac{L}{50} \right] \approx 87.5^\circ \quad (2.1)$$

$$\theta = 180 - 2\phi = 5^\circ \quad (2.2)$$

$$S = \frac{L}{\sin \phi} = 1176 \quad (2.3)$$

$$\therefore \text{from the sine rule } r = \left(\frac{S}{\sin \theta} \right) \sin[\phi] = 13.48m \quad (2.4)$$

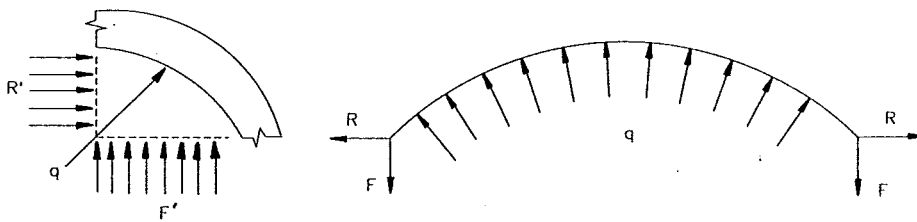


Figure 2.3 Free body of roof element

Taking a free body from the roof section (shown in figure 2.3), the forces in the x and y direction respectively are summed as follows

$$\sum F_x = R' = q \cos \varphi \quad (2.5)$$

$$\sum F_y = F' = q \sin \varphi \quad (2.6)$$

therefore solving over the entire plate

$$2R = 2 \int_{\psi}^{\psi+\theta} qr \cos \varphi d\varphi = 2qr(\sin(\psi + \theta) - \sin \psi) = 0.051q \text{ (kN)} \quad (2.7)$$

$$2F = 2 \int_{\psi}^{\psi+\theta} qr \sin \varphi d\varphi = -2qr(\cos(\psi + \theta) - \cos \psi) = 1.17q \text{ (kN)} \quad (2.8)$$

where q = force per metre width. The roof plate is continuously fixed along its length, 2x, at 0.6m centres. Hence an internal pressure of 20kPa equates to q=12kN/m.

The tensile force in the plate is found from geometry to be

$$\frac{1.17 \times (12 \times 10^3)}{\cos(90 - \theta)} = 160 \text{ kN} \quad (2.9)$$

$$\therefore \text{tensile stress} = \frac{160 \text{ kN}}{0.6 \text{ m} \times 0.002 \text{ m}} = 134 \text{ MPa} \ll 480 \text{ MPa} \quad (2.10)$$

\therefore roof element OK

In summary the analysis performed established that the steel container shell can withstand an internal pressure in excess of 20kPa.

2.3. PRESSURE RELIEF

2.3.1. PRESSURE RELIEF PANEL

Flammable gases represent explosion hazards if mixed with air in proportions between the upper and lower flammable limits (5 - 15% for methane) or more correctly the explosibility limits (5 - 17.5% for methane) (Hertzberg 1982). Ignition of a flammable gas-air mixture in a closed vessel will result in a deflagration, that is, flame propagation at subsonic speeds away from the ignition source. Along with the requirement of the gas being in the flammable region are two other prerequisites for a deflagration to occur. These are an oxidant in sufficient quantity to support the combustion process and an ignition source strong enough to initiate combustion.

Due to the possibility of the above three conditions being met in the test container, it was necessary to provide explosion venting. The aim of explosion venting is to limit pressure to an acceptable level, thus avoiding any damage to the container. This is achieved by the provision of a pressure relief vent through which the gases may expand and flow. The required pressure relief vent area depends on; the strength of the container, the rate of pressure rise, the maximum pressure developed for the fuel mixture, the presence or absence of a pressure relief panel and closure device, and the weight and location of the panel. (Zalosh 1988, NFPA 1988, FMS 1991)

2.3.2. SIZE OF THE PRESSURE RELIEF PANEL

The aim of the pressure relieving panel is to release at the lowest possible pressure, whilst providing adequate wind resistance. "Generally a static design pressure of 0.96 kPa is suggested and in no case should the relieving pressure exceed 1.92 kPa" (FMS 1991). In this instance it is desirable to have as large a relieving pressure as possible to resist the initial pressure build up from the ignition and secondly the effects of the backdraft. Therefore the upper limit of 1.92 kPa is used to determine the vent size. From FMS 1991 the recommended venting equation is;

$$A_v = \frac{C \times A_s}{\sqrt{P_{red}}} \quad (2.11)$$

where:

A_v = vent area (m^2)

C = fuel characteristic constant ($\text{kPa}^{1/2}$)

A_s = internal surface area of enclosure (m^2)

P_{red} = maximum internal over pressure that can be withstood by the weakest structural element (kPa)

However for elongated containers (length to width ratio less than 3) when the vent is restricted to one end, the venting equation is constrained by;

$$L_3 \leq \frac{12 \times A}{P} \quad (2.12)$$

where:

L_3 = longest dimension of the enclosure (m)

A = cross-sectional area (m^2)

P = perimeter of cross-section (m)

If this criterion is met, tables from (FMS 1991) are used to determine the vent area required for the given enclosure.

For ease of construction it was desirable for the vent to be in the end wall. Consequently for calculation of the required vent area, the container was analysed as being elongated, thus equation 2.12 and table 2.1 were used.

Pv kPa	As/Av																						
	3	4	5	6	7	8	9	10	11	12	13	14	15	16	17	18	19	20	21	22	23		
0.96*	3.36	3.55	3.84	4.18	4.46	4.80	5.09	5.42	5.71	6.00	6.29	6.62	6.96	7.25	7.58	7.87	8.16	8.45	8.78	9.12	9.41		
1.20	3.60	3.60	3.84	4.18	4.46	4.80	5.09	5.42	5.71	6.00	6.29	6.62	6.96	7.25	7.58	7.87	8.16	8.45	8.78	9.12	9.41		
1.44	3.84	3.84	3.84	4.18	4.46	4.80	5.09	5.42	5.71	6.00	6.29	6.62	6.96	7.25	7.58	7.87	8.16	8.45	8.78	9.12	9.41		
1.68	4.08	4.08	4.08	4.18	4.46	4.80	5.09	5.42	5.71	6.00	6.29	6.62	6.96	7.25	7.58	7.87	8.16	8.45	8.78	9.12	9.41		
1.92	4.32	4.32	4.32	4.32	4.46	4.80	5.09	5.42	5.71	6.00	6.29	6.62	6.96	7.25	7.58	7.87	8.16	8.45	8.78	9.12	9.41		

Table 2.1 FMS (Table 3) Table required to determine the minimum internal over pressure vent area.

Both equations 2.11 and 2.12 apply to only ‘low strength’ enclosures. The definition of a low strength enclosure is ‘the resistant design pressure (P_{red}) not

exceeding 10kPa". The strength of the walls has been determined to exceed this limit. The window however, could fail below this limit as shown in section 2.4.

The vent area was determined with respect to the weakest element of the containers construction, this being the windows. Conservative estimates (section 2.4.2) determined that the windows may withstand a pressure build up (P_{red}) of 7.37kPa. Thus the required vent size is 4.2m².

2.3.3. CONSTRUCTION

Due to the area required for venting, the whole rear wall was utilised for the pressure relief panel. To permit a seal around the panel the end wall was cut out and modified so when in a closed position Kaowool may be compressed around its perimeter, acting as a fire resistant gasket. The modifications included the welding of 75mm x 125mm x 6mm steel angle to the top and bottom of the panel and to the top of the container, plus the welding of steel flat plate (300mm x 6mm) to the sides of the panel so as to compress against the container sides (see figure 2.4).



Figure 2.4 Photo of pressure relief panel when closed

The panel was hinged along its bottom outer edge with three steel hinges. The interior of the panel was lined with refractory fibre blanket (Kaowool) and insulation board (Promatect H) to minimise heat loss.

2.3.4. OPENING FORCE

Plastic wire ties, each covering an equal area, were positioned along the top of the container to hold the panel closed (photo 2.2). These plastic wire ties were also used as a failure mechanism for the pressure panel, designed to fail at a predetermined internal pressure.



Photo 2.2 Pressure panel failure mechanism.

Tests were performed to determine the required number and location of ties to give a satisfactory opening pressure. To test the actual relieving pressure a large plastic bag was inflated inside the container. The bag was polythene plastic sheets joined with adhesive tape, to create a bag with dimensions greater than those of the interior of the container. Two vacuum-cleaners, as shown in photo 2.3, were used concurrently to pressurise the bag giving a uniform pressure on the container walls.



Photo 2.3 Testing of the Pressure relief panel.

A single pressure transducer was placed inside the bag to determine the maximum final pressure at which the relief panel opened. Tests showed that the panel will release at an over pressure of $1.2 \text{ kPa} \pm 0.1 \text{ kPa}$ when two wire ties (with dimensions $186\text{mm} \times 4.8\text{mm}$ and tensile strength of 22kg) were used. In this instance, the assumption of a uniform pressure is valid since the speed of the deflagration is less than the speed of sound thus the pressure increase occurs virtually uniformly throughout the container as the explosion evolves (Zalosh 1988).

The acceleration of the pressure relief panel is inversely proportional to its mass. That is the heavier the panel, the longer it will take to completely clear the vent opening. Conversely if the panel weighs less it will have a lower moment of inertia and move away from the vent opening quicker and venting is more effective. Thus it is recommended that the panel weight not exceed 19.5 kg/m^2 . The completed pressure panel weight was less than 40 kg/m^2 , the suggested maximum (FMS 1991) for a fire rated wall panel. It was decided to let the panel open to an angle exceeding 45 degrees but less than the horizontal. As shown in photo 2.4 chain was used to catch the door with a spring to minimise the horizontal force due to the rapid deceleration

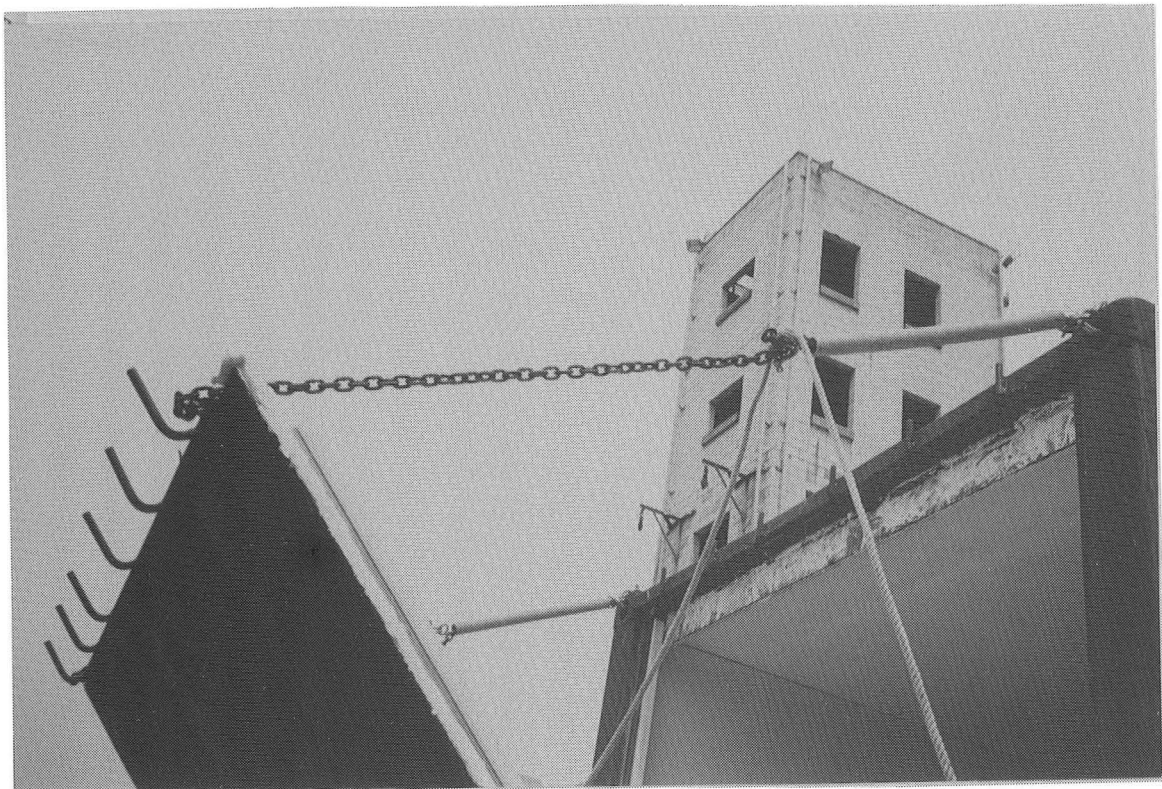


Photo 2.4 Pressure relief panel held open by the spring and chain system.

2.3.5. INTERIOR WALL VENTS

Additional vents were provided part way through the experimental programme, after an interior insulation board was dislodged. It is believed that this was due to an ignition of gases in the continuous void between the insulation linings and the steel shell of the container. It should be noted that during construction every effort was made to seal all leakage paths, however due to later modifications and thermal contraction, leakage of gases to the void became possible. Standard deflagration venting references were not applicable in this space due to the void volume to surface area ratio constraints. Thus engineering judgement was used to estimate the vent size required to alleviate any pressure build up. Two vents 0.31m^2 were placed in each of the long interior walls to allow controlled venting.

The pressure relief vents were friction fitted by compressing refractory fibre blanket between the vent itself and the wall. To inhibit any extra damage in the event of a panel releasing, the vents were joined to the container wall by steel wire.

2.4. WINDOW

For verification of the expected behaviour of backdraft along with estimation of gravity current travel speed, an observation window was installed. There were two requirements for the window;

1. to withstand high temperature (resist thermal stresses),
2. to withstand high pressure.

2.4.1. HIGH TEMPERATURE RESISTANCE

PYRAN® fire resistant borosilicate glass is manufactured in Germany. PYRAN has proven its capability of providing up to a 2hr fire rating, providing it is constructed in a tested and approved structure. The system of glass pane, frame, seal and fittings must be identical to that tested.

As the centre of the pane heats up and expands, it is resisted by the edges which are cooler and have not expanded, this results in the hot centre of the pane trying to force the cold edges apart creating tensile stresses along the edges of the pane. Tension is the most significant failure mode of glass. Therefore PYRAN is subjected to a special prestressing process to increase its mechanical strength by creating compressive stresses in its surfaces. These compression forces must therefore be overcome before any tension is experienced (this is analogous to a prestressed concrete beam). Three factors are required to reduce the tensile stress build up

1. using a glass with the lowest possible thermal expansion co-efficient ($\alpha_{\text{PYRAN}}=3.25 \times 10^{-6}/\text{K}$)
2. keeping the edge cover as small as possible by using specified frame construction

3. increasing the mechanical strength of the pane edges

Another problem associated with the use of glass subject to fire is the thermal gradient across the glass between inside and outside. Normally this would mean expansion of one face which would lead to internal stresses and the glass bowing inward. With Pyran glazing this problem is reduced by the low coefficient of thermal expansion. Internal stresses are also a function of the rate of temperature rise. Fire tests on glass are carried out subject to the international standard fire curve, which considers post flashover fires where the growth rate is well in excess of that expected in the experiments.

The frame system and low thermal expansion coefficients are only important below 800K (gas temperature subject to ISO fire). This is known as the transition temperature of the glass. At the transition temp no more stresses build up in the pane, the glass then becomes increasingly viscous and eventually will flow.

2.4.2. STRENGTH OF THE GLASS

The limiting factor in the design of the pressure relief panel was the strength of the weakest link (P_{red} (kPa)). As this design pressure increases the required vent area decreases. For construction purposes it was desirable to keep the pressure relief vent limited to the rear of the container. For a vent area of 4.2m^2 , the window had to be capable of withstanding 7.16kPa. (Table 3 FMS 1991)

No information is available on the bending strength of the glass. Hence, a specimen was obtained and tested in the laboratories. The set up is shown in figure 2.5. The specimen was tested as a simply supported element using an Instron test machine. The loading was applied at a constant rate of 1 mm/min under ambient conditions.

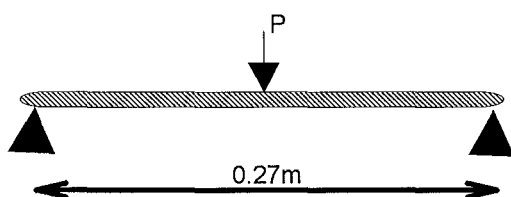


Figure 2.5 Glass specimen

The test specimen was 0.27m long, 0.2m wide and 0.0065m thick. The sample failed at a load of 2.0 kN, which equates to a moment, M , of 0.14kNm. The failure stress $\sigma_{failure}$ was calculated from

$$\sigma_{failure} = \frac{M}{Z} \quad (2.13)$$

where M = bending moment

$$Z = \frac{w \times t^2}{6}$$

w = glass width

t = glass thickness

The maximum bending stress at failure was found to be 96MPa.

For plate analysis however, results are given as moments per metre width. Hence the failure stress was converted to a moment per metre width. Thus, the corresponding uniform pressure that would cause a bending stress of 96Mpa could be determined. From simple algebra on equation 2.13

$$\frac{M}{w} = \sigma_{failure} \times \frac{t^2}{6} = 0.676 \text{ kNm/m}_{width}$$

Conservatively assuming the glass as simply supported on all four edges, the following plate formulae were applied (Szilardo) to give the maximum moments about the x and y axis, $M_{x \max}$ and $M_{y \max}$ respectively:

$$M_{x \max} = C2 \times P_o \times a^2$$

$$M_{y \max} = C3 \times P_o \times a^2$$

where $C2$ and $C3$ depend upon the ratio of the glass dimensions b/a (as seen in Table 2.2), where b is larger than a (Szilardo). P_o is the uniform pressure.

$$\epsilon = \frac{b}{a}$$

ϵ	c_1	c_2	c_3	c_4	c_5	c_6	c_7	c_8
1.0	0.0443	0.0479	0.0479	0.383	0.338	0.420	0.420	0.065
1.1	0.0530	0.0553	0.0494	0.360	0.315	0.440	0.400	0.064
1.2	0.0616	0.0626	0.0501	0.380	0.294	0.455	0.377	0.062
1.3	0.0697	0.0693	0.0504	0.397	0.275	0.468	0.357	0.061
1.4	0.0770	0.0753	0.0506	0.411	0.258	0.478	0.337	0.059
1.5	0.0843	0.0812	0.0500	0.424	0.242	0.486	0.323	0.057
1.6	0.0906	0.0862	0.0493	0.435	0.229	0.491	0.303	0.054
1.7	0.0964	0.0908	0.0486	0.444	0.216	0.496	0.287	0.052
1.8	0.1017	0.0948	0.0479	0.452	0.205	0.499	0.273	0.050
1.9	0.1064	0.0985	0.0471	0.459	0.194	0.502	0.260	0.048
2.0	0.1106	0.1017	0.0464	0.465	0.185	0.503	0.248	0.046
3.0	0.1336	0.1189	0.0404	0.493	0.124	0.505	0.166	0.031
4.0	0.1440	0.1235	0.0384	0.498	0.093	0.502	0.125	0.024
5.0	0.1416	0.1246	0.0375	0.500	0.074	0.500	0.100	0.019
∞	0.1422	0.1250	0.0375	0.500	—	0.500	—	—

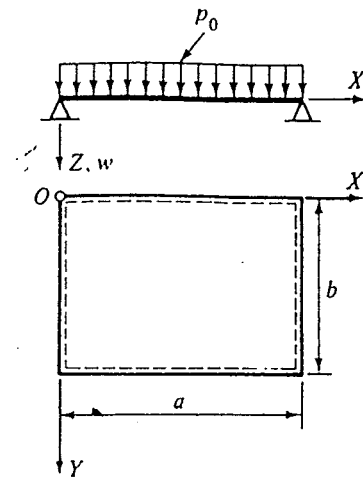


Table 2.2 Factors C_2 and C_3 for plate bending.

Analysis determined that a pane 1584mm x 1063mm could withstand 7.37kPa under ambient conditions.

2.4.3. CONSTRUCTION

Refer to figure 2.6 for frame layout. The frame system adopted has a 90 min fire rating. Sizes of the main members used in the frame are greater than those of the accepted frame systems. The variations limit the maximum deflection of any part of the frame to under 5mm (based upon calculations of a simply supported beam) when subject to an internal pressure of 10kPa. The internal area of the box beam is protected by two layers of Promatect H board to prevent any expansion and warping due to thermal gradients.

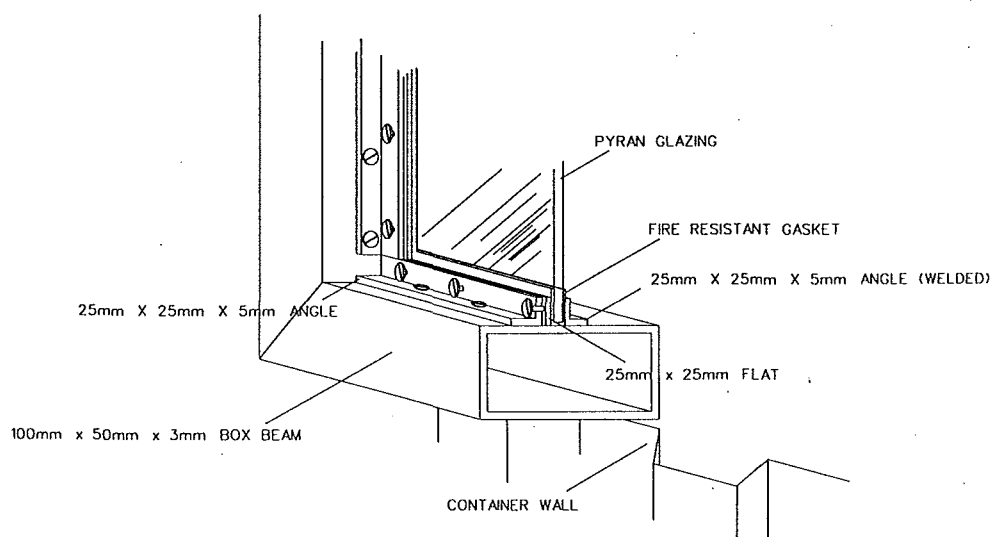


Figure 2.6 Window frame construction

2.5. FRONT OPENING

To simulate a ventilation source such as a window breaking due to fire induced thermal stresses, firefighter entry, or any other similar event, a horizontal vent was provided in the front end of the container. The vent was a third of the height of the front opening and the full width. The actual vent dimensions were 750mm high by 2250mm wide. The vent was located at the mid height of the front wall. Partitions above and below the vent were constructed with internal steel framing as the supporting structure and lined with 19.5mm thick Gib Fyrelite and two layers of 20mm thick Promatect H insulation board. The vent was then covered by a hatch the full size of the front opening, hinged along its bottom outer edge.

To allow the hatch to open as easily and freely as possible, its weight was kept at a minimum. The hatch was constructed using double steel studs covered by a single sheet of Promatect H insulation board over the vent area. Kaowool was sandwiched between the vent structure and the hatch to minimise leakage of heat and combustion gases. A single closure device was positioned at the top centre of the hatch. This was manually opened by a steel cable approximately five meters away from the container.

To keep vacuum effects and air disturbances to a minimum two springs were employed to slowly push the hatch past a point where gravity would takeover and open the hatch the remainder of the way. The hatch was prevented from travelling past the horizontal by a platform the same height as the container. Inflated rubber tyres were placed on the platform to cushion the impact.(See photo 2.5)



Photo 2.5 The hatch in the fully opened position.

2.6. INTERNAL INSULATION

2.6.1. LINING CONFIGURATION

Figure 2.7 shows the lining configuration used within the container. Screws at 0.2m centres fixed the linings to steel runners welded to the container as shown in photo 2.6.

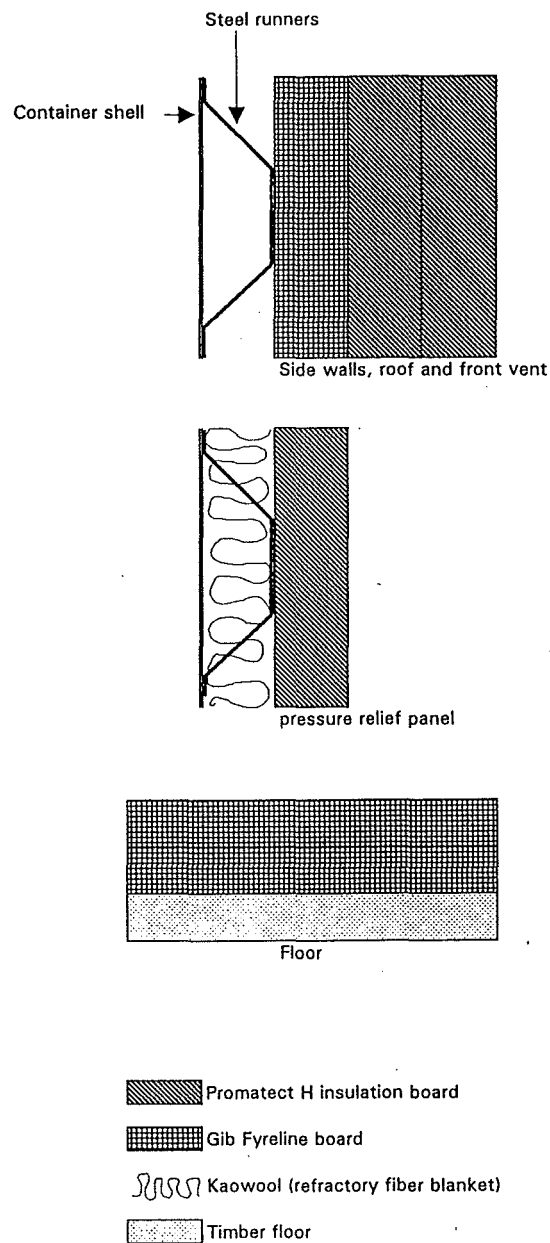


Figure 2.7 Lining configurations.



Photo 2.6 Steel runners for lining fixing. (At the top rear of the container)

2.6.2. LINING MATERIALS

2.6.2.1. GYPSUM PLASTER BOARD.

Once constructed, the container is to be used in a continual research program. With the container shell being constructed of steel it was important to protect it from the effects of the fire otherwise expansion leading to permanent deformation may occur. Concern was centred on expansion around the window frame and pressure relief panel which have been designed as tight seals allowing little room for movement. Of interest for the insulation of these was a lining product that did not degrade after continual use and was not strongly affected by water.

Fyreline is a Winstone Wallboards Ltd product that is formulated as a fire resistant panel. It contains a gypsum plaster core along with vermiculite and short fibreglass strands wrapped in combustible paper sheet producing a board that has a total thickness of 19.5mm. The chemical name for gypsum is calcium sulphate dihydrate, $\text{CaSO}_4 \cdot 2\text{H}_2\text{O}$. Upon heating the free water is driven off, being totally evaporated at 100°C . Once the board is heated between 100°C and 150°C calcination occurs. Calcium losing the chemically bound water, results in the loss of mechanical strength

and structural integrity. Due to the chemical reactions that occur as the board heats up it does not maintain constant values of thermal conductivity, k , or specific heat, c_p . Values from Mehaffey 1991 show that between 80°C and 120°C the conductivity actually decreases. The specific heat, energy required to raise 1kg of the material by 1°C, has a peak at 100°C, when the water evaporates. It is therefore important to keep the temperature of this board below 100°C, otherwise, its effectiveness and strength will decrease between tests.

2.6.2.2. CALCIUM SILICATE BOARD.

Promatect H is a calcium silicate board proven internationally as an effective and durable fire resistant lining material. Promatect H is often used for passive protection of steel structures.

2.6.3. TASEF ANALYSIS

In order to ascertain the degree of heat transfer through the interior lining, a two dimensional finite element analysis was performed.

TASEF, developed by the Swedish National Testing Institute, is a computer program that carries out a Temperature Analysis of Structures Exposed to Fire. The program applies a forward difference time integration scheme (Sternier 1990). The program was applied in order to predict the layers of insulation required to ensure endurance and the most appropriate method of fixing the lining material.

Figure 2.8 shows the two scenarios that were considered. Option A comprises of one layer of 19.5mm Fyreline and one layer of Promatect H board. Option B is simply the addition of another layer of Promatect H to option A.

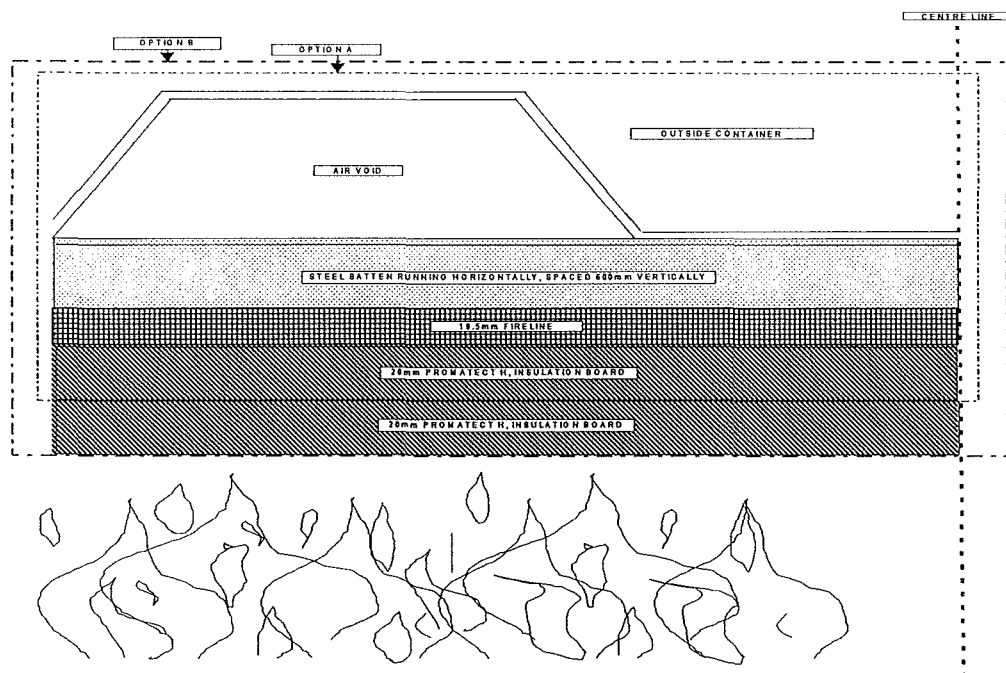


Figure 2.8 Lining systems A and B that were analysed using TASEF.

In order to further simplify the problem the following conservative geometry was used as input for TASEF (see figure 2.9):

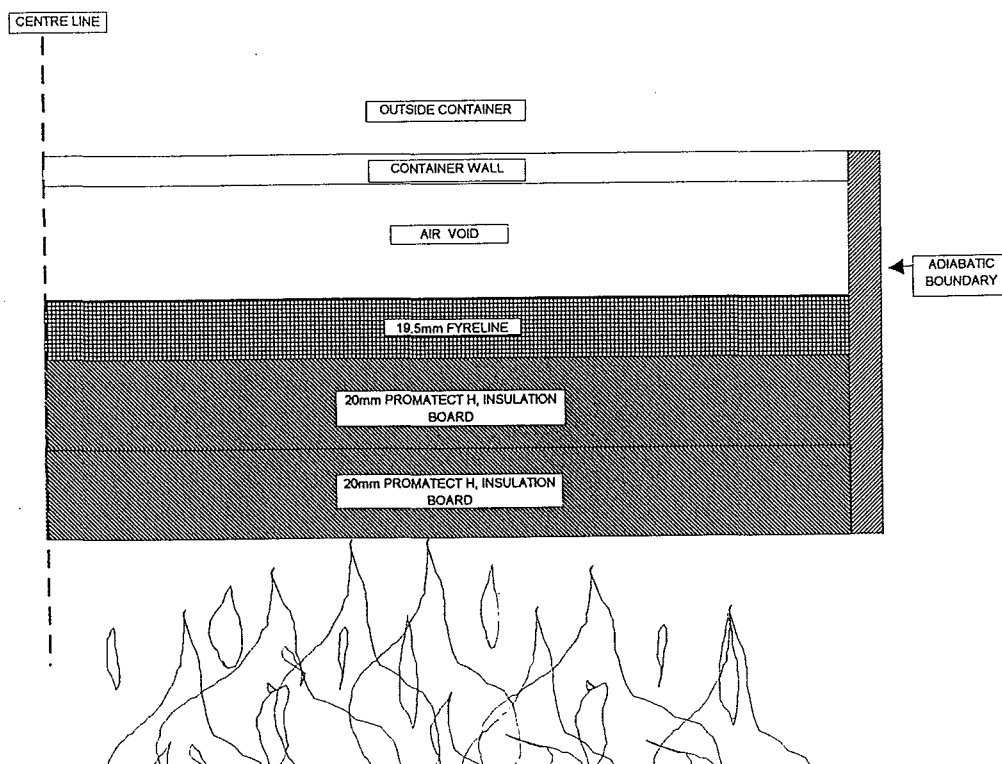


Figure 2.9 Simplified TASEF geometry

Input to the program is in three sections, geometry, thermal properties of the materials and the heat transfer co-efficients at the boundaries.

2.6.3.1. THERMAL PROPERTIES OF MATERIALS

TASEF requires the following thermal properties of all materials modelled

- conductivity,
- density,
- enthalpy.

all of which are a function of temperature.

Within TASEF is a list of standard materials (steel, concrete and mineral wool) and the required thermal properties. Thermal properties of 19.5mm Fyrelite were taken from Thomas 1994. As Promatect H is manufactured overseas, information on its properties were difficult to obtain. The conductivity, density (WORMALD 1993) and specific heat of Promatect H board were assumed to be constant with temperature. The following tables depict the values used for each material

TEMP C	DENSITY kg/m ³	CONDUCTIVITY W/m.C	ENTHALPY Wh/m ³
0	867	-	0
70	-	0.25	-
100	867	-	22879
110	858	-	86860
120	854	-	150359
140	846	-	154844
175	819	-	162533
200	818	-	167933
210	817	-	191093
220	817	-	214240
300	-	0.13	-
320	811	-	235712
350	815	-	242147
405	815	-	253975
540	811	-	282932
650	798	-	306274
1000	780	0.35	379145
4000	-	10	-

Table 2.3 Thermal properties of 16mm gypsum plasterboard

TEMP C	DENSITY kg/m ³	CONDUCTIVITY W/m.C	ENTHALPY Wh/m ³
0	1580	60	0
200	1580	-	216900
400	1580	-	466100
600	1580	-	758100
700	1580	-	926900
800	1580	27	1192000
1200	1580	-	1766000
2000	1580	27	-

Table 2.4 Thermal properties of steel

TEMP C	DENSITY kg/m ³	CONDUCTIVITY W/m.C	ENTHALPY Wh/m ³
0	780	0.23	0
100	780	0.23	-
1000	780	0.23	200000

Table 2.5 Thermal properties of Promatect H
- data not available.

2.6.3.2. HEAT TRANSFER CO-EFFICIENTS

TASEF requires the values of three heat transfer co-efficients, ε (emissivity), β (convection coefficient) and γ (convection power). All three parameters need to be defined at boundaries. A boundary is defined as the interface between gas and object. Heat transfer at these boundaries is governed by the following equation (Stern 1990)

$$\dot{q}'' = \varepsilon\sigma(T_g^4 - T_s^4) + \beta(T_g - T_s)^\gamma \quad (2.14)$$

The first term on the right hand side covers radiation and the second term convection.

\dot{q}'' = the rate of heat transfer (kW/m²)

ε = the resultant emissivity of the gas and the boundary (dimensionless)

σ = the Stefan-Boltzman constant (5.67×10^{-8} W/m² K⁴)

T_g = the gas temperature (K)

T_s = the surface temperature (K)

β = the convective heat transfer co-efficient (W/m² K)

γ = the convective heat transfer power (dimensionless).

Values used for ε , β and γ differ from those suggested in the TASEF users guide (Thomas 1994). The following table was applied to both simulations

Boundary condition	ε	β	γ
i) Fire side	1.0	5.0	1.33
ii) gypsum to void on the fire side of the cavity	0.6	1.0	1.33
iii) adiabatic boundary to air void	0.6	1.0	1.33
iv) container wall to air void	0.6	1.0	1.33
v) container wall to external ambient.	0.6	2.2	1.33

Table 2.6 Heat transfer co-efficients at the boundaries

The ISO834 fire history curve was used as the compartment fire history.

2.6.4. TASEF RESULTS

The results of the TASEF analysis favoured option B, one layer of 19.5mm Fyrelite and two layers of 20mm Promatect H (see figure 2.10). A similar analysis on the fixing

mechanism, concluded that the fasteners for the final layer had to be countersunk approximately 10mm and protected with Kaowool. Figure 2.7 shows a cross section of the lining arrangement for each wall. In order to keep the weight of the pressure relief panel within the acceptable limits (refer to section 2.3.4) only one layer of Promatect was attached. By sandwiching kaowool between the Promatect and panel, the heat loss through to the steel was minimalized.

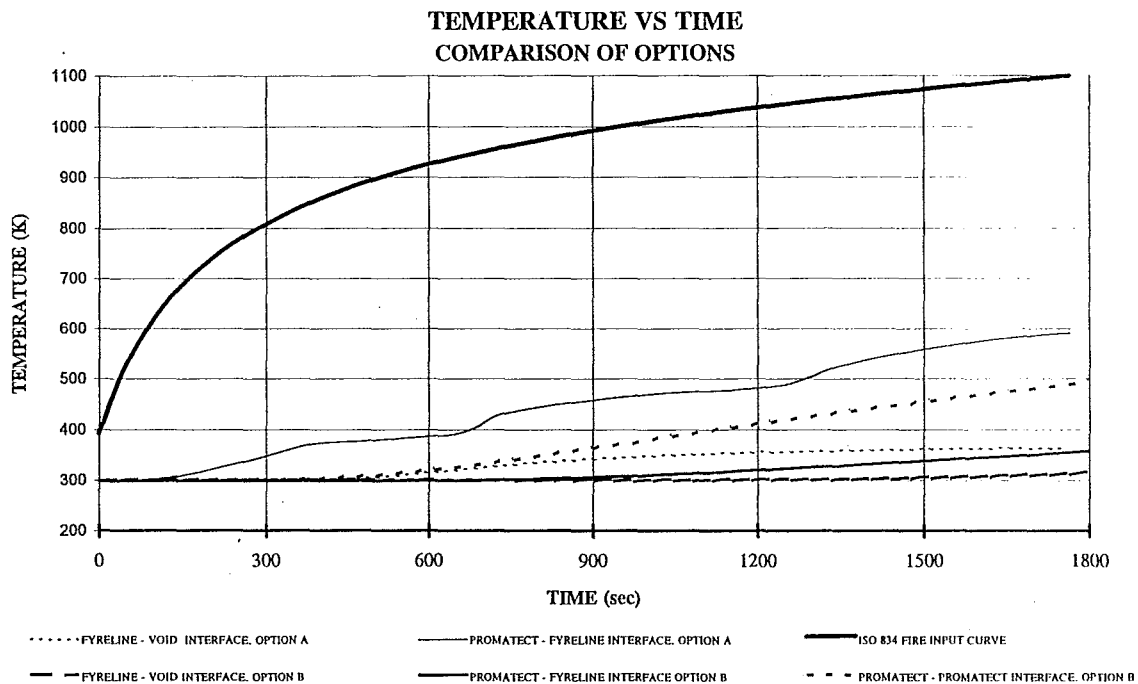


Figure 2.10 Comparison of lining options

2.7. IGNITER

Two 15 000 volt transformers were employed in order to ignite the propane pilot flame and to act as an ignition source for both a backdraft and smoke explosion upon the opening of the hatch. The transformers were attached to the underside of the container and joined to spark electrodes through high capacity wires. As shown in photo 2.8, the

3mm diameter 308 stainless steel electrodes were extended through the floor with the rear set positioned slightly above the pilot flame pipe and the front set at a height one third the height of the compartment. The tips of the electrodes were adjusted so as to Produce a spark between 5-10mm. Figure 2.11 indicates the position of the electrodes with respect to the timber cribs.

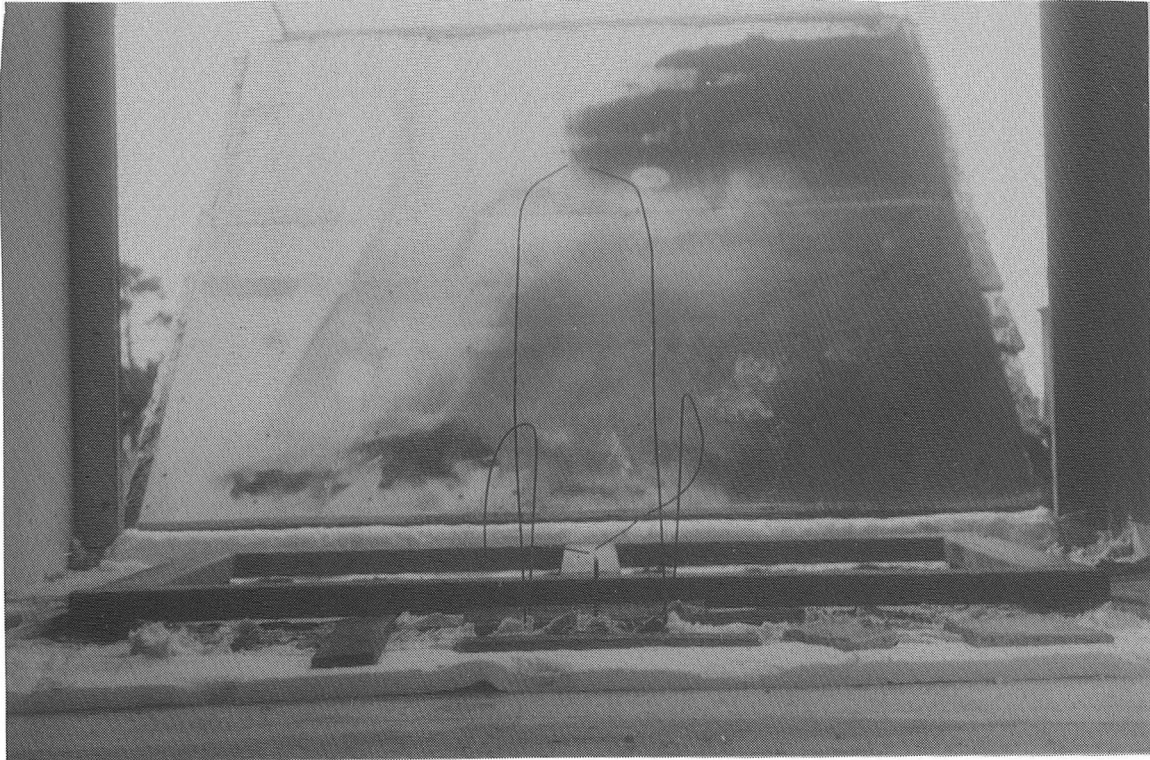


Photo 2.7 Location of the electrodes (in the background, the pressure relief vent open.and just above the ground is part of the load transfer frame.)

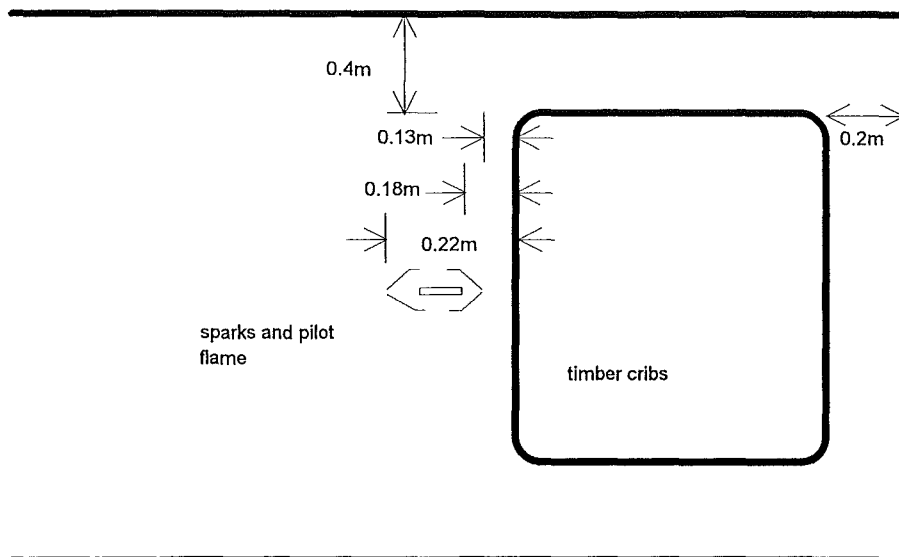


Figure 2.11 Location of the electrodes.

2.8. LEAKAGE VENTS

In order to control the degree of ventilation, two circular vents were installed as shown in figure 2.12., A full list of the sizes which varied between experiments may be found in section 4 . The vents were circular to provide a smooth elliptical velocity distribution with a definite max at the centre.

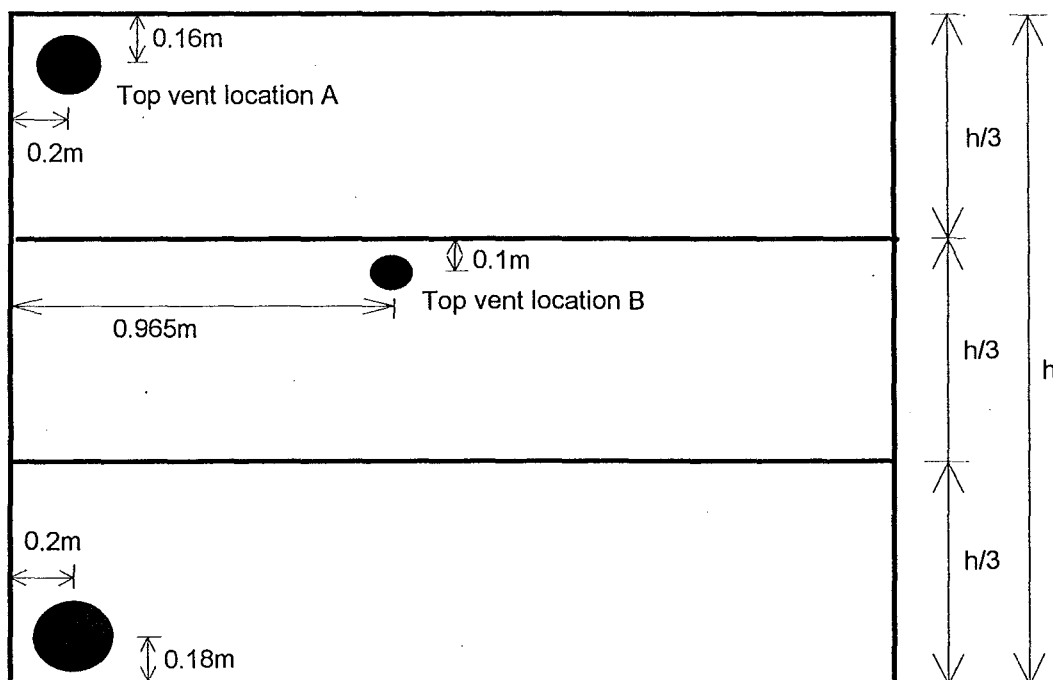


Figure 2.12 Location of vents looking from inside the container

3.1.2. WALL LINING TEMPERATURES

To ascertain the heat transfer through the various layers of insulation and gypsum board, type K bare bead 24 gauge with high temperature glass insulation thermocouples were placed throughout the compartment. Figure 3.1 indicates the position of each of these. At each of the points two thermocouples existed, one (A) at the Fyreline-Promatect interface, the other at Promatect-Promatect interface (B). These were installed to monitor the temperature of the wall lining materials. Due to the limited number of voltage channels available, they were not recorded within the experiments.

3.2. PRESSURE

Compartment pressure at the centre of the floor was monitored through all experiments. A probe resting at floor level was connected to two pressure transducers which provided a measuring range of -10Pa to +1250Pa. During the set of timber experiments a second compartment pressure probe was installed. To correspond with the centre of the top vent, the probe was located 0.16m down from the ceiling, protruding .22m out of the left wall, 1m away from the front internal face. The pressure range was 0Pa to +10Pa.

3.3. FRONT VENT FLOW VELOCITIES

The velocity of the vent flows (gravity current in, fire ball out) that occur upon the opening of the front hatch were measured using bidirectional probes (Emmons 1988). Photo 3.1 shows the six probes distributed evenly through the 0.75m slot height and positioned in the horizontal centre.

The velocity V can be determined from

$$V = \frac{1}{1.08} \sqrt{\frac{2\Delta P}{\rho}} \quad (3.1)$$

Where V = velocity (m/s)

ΔP = pressure difference measured with bi-directional probes (N/m²)

$$\rho = \frac{Mp}{RT}$$

= Density of the gas (a function of the local temperature),

M = Average molecular weight of the flowing gas (kg mol)

R = universal gas constant = 8314 ($\frac{J}{kg.mol.K}$)

T = temperature in Kelvin

p is the pressure within the compartment.

Incomplete knowledge of the composition of the gases from the fire leads to the assumption of the compartment gas having a molecular weight of air, hence application of the ideal gas law leads to

$$\rho = \frac{352.8}{T} \frac{kg}{m^3} \quad (3.2)$$

Thus it can be seen that the temperature at the position of each probe must be determined as a prerequisite to the determination of the velocity. Ideally for increased accuracy aspirated thermocouples would be used, however in this instance type K bare bead 24 gauge with high temperature glass insulation were installed. Therefore a correction for the effects of radiation should be applied. Due to the extremely rapid nature of backdrafts, the speed at which these thermocouples respond to the corresponding temperature change is too slow to warrant the accuracy of applying this correction. Consequently, these vent flow velocities should be considered to be a general evaluation rather than exact velocities.

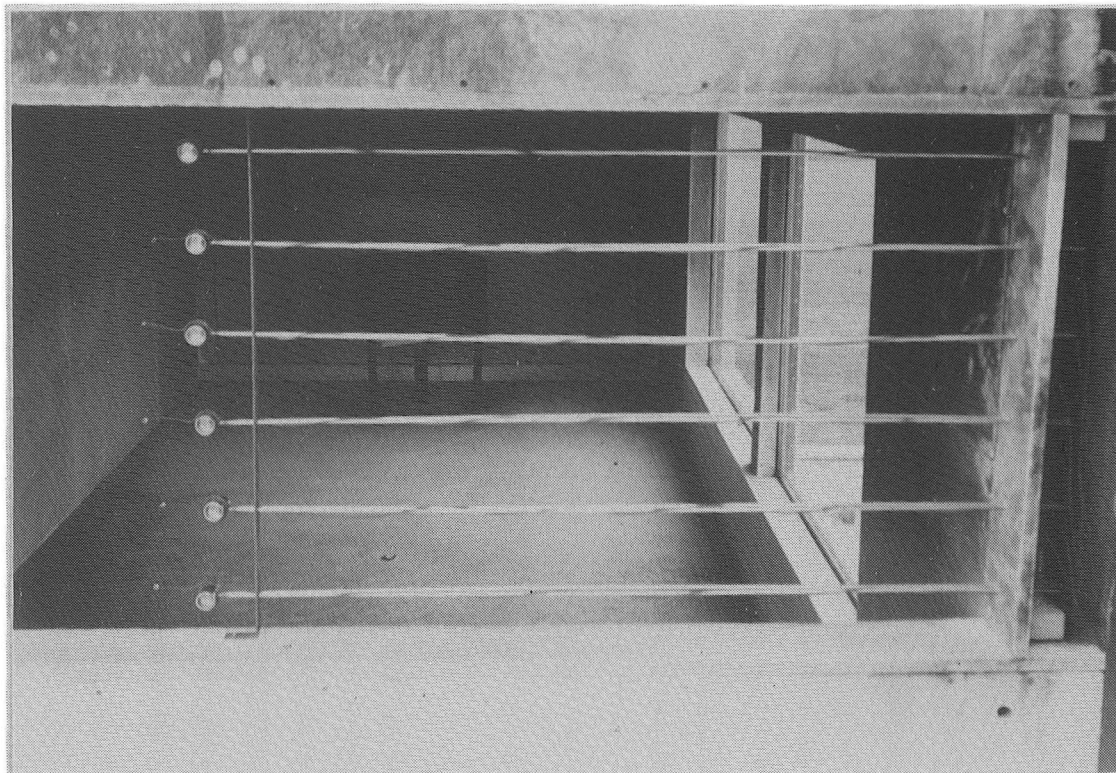


Photo 3.1 Installed bi-directional probes

3.4. GAS ANALYSIS

To determine the gas concentration history inside the fire compartment during the experiments, two methods of gas sampling were employed. The first was oxygen analysis which yielded continuous measurements. Secondly, grab-samples were taken at set times, which were analysed using gas liquid chromatography to give air, methane and carbon dioxide concentrations.

Five ports were placed down the left side of the compartment 0.51m from the front hatch (offset 0.01m from the thermocouple tree). These ports extended 0.2m into the container so as not to be in a quiescent zone. They were positioned at 0.2m, 0.6m, 1.0m, 1.4m and 1.8m down from the final ceiling height. A single sample tube ran from any one of these ports at any particular point of time to the oxygen analyser. The oxygen analyser required that all of the water and solid particles be removed from the sample, see figure 3.2.

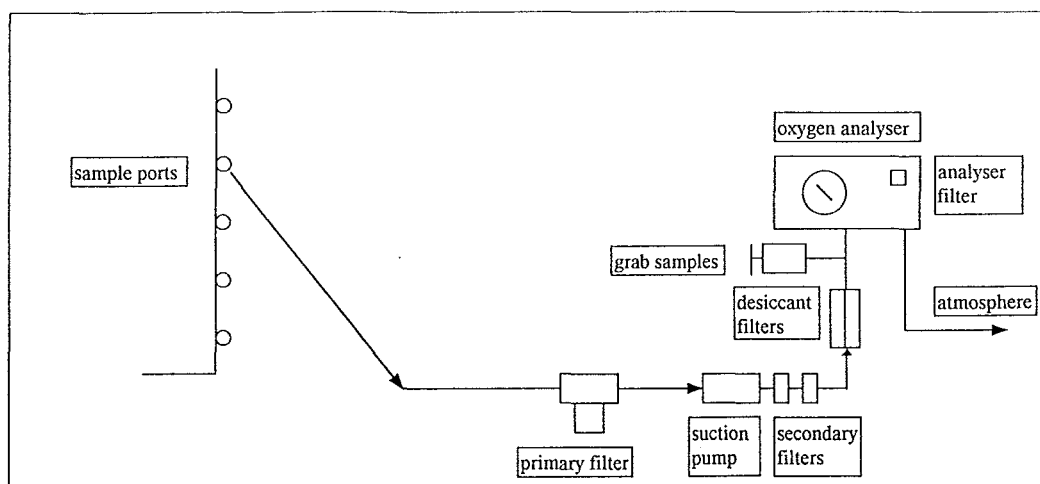


Figure 3.2 Gas sample line, from fire compartment to oxygen analyser.

The primary filter (glass fibre particle filter) was used to separate out the larger products, as low as $5\mu\text{m}$, and was emersed in an ice bath. This had two purposes, firstly to condensate out the products of combustion and secondly to cool the sample. The sample tube, a long copper pipe, lead from the sample ports to a GAST suction pump. This pump produced a suction flow rate of 0.5 l/sec. Following this pump was a secondary filter to extract any minute particles (as small as $0.3\mu\text{m}$) that may still be in the system. Prior to entering the oxygen analyser the sample was past through two desiccant filters. These filters contain calcium silicate crystals which removes moisture. As part of the oxygen analyser system was an internal filter, this was checked regularly but always remained clean.

3.4.1. OXYGEN ANALYSIS

The oxygen concentration was measured using a Servomex Model 540 paramagnetic oxygen analyser. The analyser is designed to continuously monitor the oxygen content of a sample, which is clean, dry, and non-corrosive. The oxygen content of a sample gas is determined by measuring its relative magnetic susceptibility. Using this method, the oxygen analysis is virtually unaffected by changes in the background gas composition, due to the high paramagnetism of O_2 compared to other gases (Servomex 1994). Since no heated filaments are in contact with the gas sample, the analyser is well suited for determining the oxygen content in flammable gases and vapours.

Output is in the form of volts, 0-10 volts DC for 0-100% oxygen. Variation in bypass flow has minimal to no effect, 500 cc/min to 8 litres/min will cause a variation of less than 0.01% oxygen. This is also true for changes in the ambient temperature, where a change of 10°C, in the ambient temperature range of -10°C to 50°C will cause the zero to change by less than 0.02% oxygen.

To estimate the lag time between the inlet port and the analyser a series of flow tests were performed. These were accomplished by sampling an inert gas (nitrogen) at the port end of the sample line at a specific time, then determining the response time of the analyser. It was ascertained that the lag time for the gases to flow from the container to the analyser was 15 seconds.

It is required that the oxygen analyser have at least 12 hours to warm up before introducing a gas. Therefore it the analyser left on during the period of testing (approximately 1 month) so that it was constantly ready. Prior to each days testing the oxygen analyser was zeroed by flowing oxygen free nitrogen through the system and spanned using clean dry air.

3.4.2. GAS CHROMATOGRAPHY

Gas chromatography was used to determine the total production of carbon dioxide and unburnt methane concentration that has accumulated in the container at a specific time. By taking a number of samples, the species concentration for each sample may be found. The more samples analysed the more accurate any interpolation between points will be. However any interpolation is obviously only conjecture and the exact result between successive samples are impossible to determine.

To determine the concentration of total production of methane and carbon dioxide at a particular point in time, a sample of the gas inside the container was obtained for that particular time. Plastic sealable syringes (50 ml) were used to obtain samples of the container gases. Samples were drawn from the exhaust tube before it enters the oxygen analyser. The flow through this tube being approximately 0.5mm/sec. Each sample was taken by drawing the syringe over a period of five seconds then allowing it to sit for a further five seconds so as not to be drawing a vacuum. After each sample has been

drawn it is sealed, labelled and stored. The samples were analysed as soon as possible after being drawn so as to minimise any corruption due to leakage. The average time between the sample being drawn and the analysis time was approximately 24 hours. The contamination within this time is considered to be minimal. It should be noted that leakage did occur in a small number of the samples due to their caps not being fitted sufficiently tight.

The GC-R1A gas chromatograph used was manufactured by Stimazdy and used a RPR-GI processor. The 2m column was made of stainless steel, having an inside dimension of 3mm. The column was filled with 100/120 mesh and heated to a temperature of 40°C. The carrier gas was helium flowing at 22mm/min. A sample of 0.5mls was drawn from the 50ml syringe and injected into the sample port which was at 150°C. The results obtained (air, CH₄ and CO₂) were presented in percent volume. These were converted to mass fractions by applying a calibration and determining the percent of each species with respect to the total calibrated volumes.

3.5. AMBIENT CONDITIONS

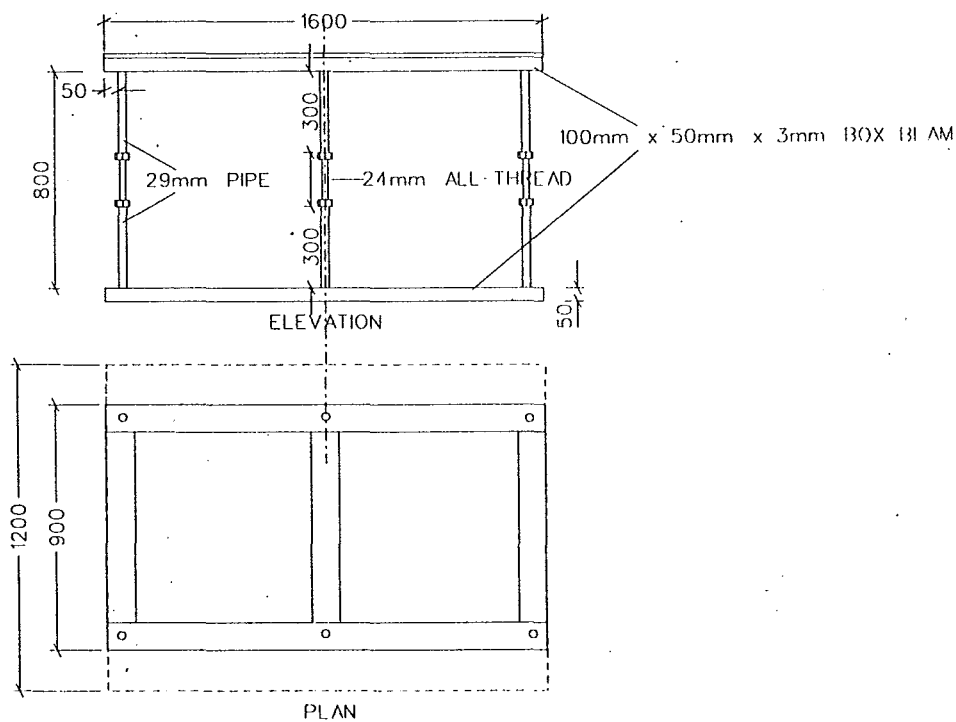
The ambient conditions monitored were, wind, temperature and relative humidity. It was found during the initial tests that the wind velocity and direction played a significant role in the outcome of each individual test. Changes in temperature and relative humidity had no obvious consequences.

The ambient temperature was measured using a digital thermometer with a thermocouple probe. Temperature is used to determine the ambient density. The ambient density is for vent flow calculations.

The relative humidity is measured and recorded for completeness, however is not considered further in this report.

3.6. LOAD CELL

A load scale (Toledo scale model 8510, 1000kg capacity with four strain gauges capable of 250kg each) was used to monitor the mass loss rate of the fuel. The load cell rested level on the ground under the container. Due to the elevation of the cribs a load transfer frame, as shown in fig 3.3 was designed to transfer the weight to the cell. The frame design allowed for height adjustment and a frictionless path through the container. The internal section of the frame was wrapped with kaowool. To provide a base for the cribs, a sheet of 19.5mm Fyrelite and Promatect H board were placed on top. This prevented any heating of the steel thus reducing distortion of the frame.



CRIB TO LOAD CELL SUPPORT

Figure 3.3. Load transfer frame.

3.7. DATA ACQUISITION METHOD

A 486DX/66 computer was used to continuously monitor and collect data during each experiment. To read and collect the data (as voltages and temperatures), two multiplexers, with 32 channel analog input were connected to the computer. Data collected included, 32 thermocouple and 10 voltage channels. Eighty scans were taken every second and then averaged over a two second period and stored on the hard disk.

4. EXPERIMENTAL PROGRAM

As discussed in section 1, the experiments were run to look at two issues subject to timber crib fires,

i) What conditions within the compartment are influenced most significantly from the variation in ventilation size and location, and fuel elevation. Potential conditions required for a backdraft.

ii) Under low ventilation is there enough production of pyrolyzates and incoming oxygen for an explosion within the container before any simulated opening

Shown in table 4.1 are the differences between each of the seven experiments conducted.

A total of eight parameters were varied in the experiments:

1. Top vent location
2. Top and bottom vent area
3. Fuel load
4. Elevation of the crib
5. Degree of ignition (pilot flame)
6. Time interval between attempted ignition from sparks
7. Duration of the spark
8. Opening time

Shown in section 2.8 are locations of vents A and B. By dropping the level of the top vent it was anticipated that instead of the upper layer gases having a residence time before leaving that a degree would be captured between the vent and ceiling, thus reducing movement in this area and hopefully reducing the level of oxygen entrained. Dropping the location also meant the pressure difference at the vent would be lower than previous thus the flow out would be reduced.

TEST	1	2	3	4	5	6	7
TOP VENT LOCATION	A	A	A	A	A	B	B
TOP VENT AREA (m²)	0.0660	0.0314	0.0154	0.0154	0.0079	0.0079	0.0079
BOTTOM VENT AREA (m²)	0.0660	0.0660	0.0314	0.0314	0.0154	0.0154	0.0154
FUEL LOAD (kJ)	3870	3816	3978	3960	2900	2900	2988
ELEVATION OF CRIB (m)	0.25	0.25	0.25	0.25	0.74	0.74	0.74
PILOT FLAME (s)	1860	15	15	15	40	15	240
SPARK INTERVALS (s)	0	600	600	600	300	300	480
SPARK DURATION (s)	0	10	10	10	10	10	120
OPENING TIME (s)	5400	3600	7200	2100	3600	3020	5400
SMOKE EXPLOSION	no	no	no	no	no	yes	no
BACKDRAFT	no	no	no	no	no	no	no

Table 4.1 Description of each experimental set up

Reducing the vent areas would reduce the mass flow of air in thus reducing the burning rate. If the burning rate is reduced but enough oxygen is supplied for smouldering then the production of unburnt pyrolozates will increase. However if the top vent is too small then it is anticipated that the layer will cover most of the fuel thus reducing the area available for pyrolysis.

The only reason for decreasing the fuel load was to extend the test series further. As shown in photo 4.1, by no means was all the fuel consumed during an experiment.

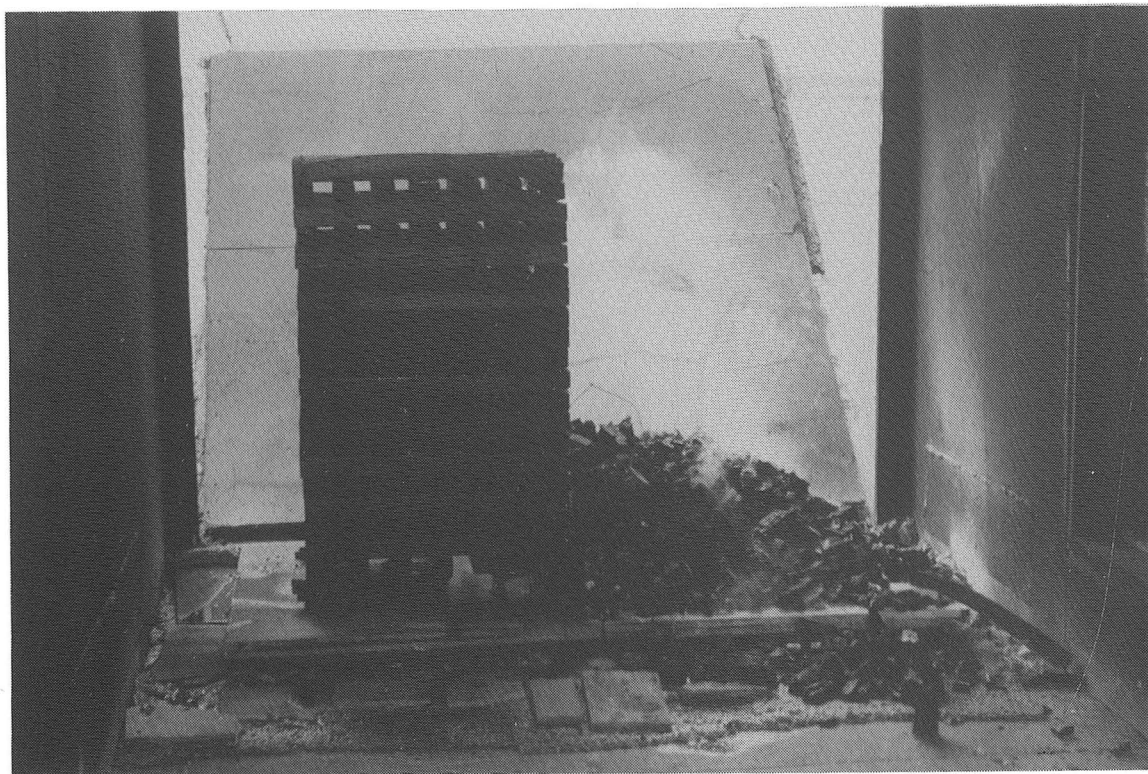


Photo 4.1 Partial involvement of the fuel

By the end of the fourth test more emphasis was put on obtaining a smoke explosion. Anticipating that the smoke layer would be at the same height as the base of the fuel, the base of the timber cribs were raised to $\frac{1}{3}$ the compartment height. If correct then the layer would coincide with the level of the sparks. At this interface it was hoped that the oxygen would mix with the upper layer gases and provide a mixture within the flammable limits, hence if the sparks are at the mixing interface then the potential for ignition has increased.

To allow pyrolozates to accumulate within the container, the times at which sparks were operated varied. If the sparks were left on continuously then ghosting flames, which remove the pyrolozates, could exist.

In order to administer the second objective, potential smoke explosion, sparks at both one third the compartment height and at the base of the cribs was produced during the

tests. At a predetermined time the front hatch was opened to simulate a new opening, allowing the entry of a gravity current. If the correct level of pyrolozates existed - a backdraft would result.

5. FUEL DESIGN, LAYOUT AND IGNITION.

5.1. INTRODUCTION

The only quantitative work on the phenomena of backdraft was carried out using methane as the fuel source (Fleischmann 1993). As the fuel for a backdraft is excess pyrolozates, it is therefore necessary for further understanding of the phenomena based on pyrolozates that exist in a real situation. In a review of ‘fires involving explosions’, Croft (1981) concluded that the majority of explosions were caused by cellulosic materials. Thus, timber² was chosen as being an appropriate fuel for the experiments. Experiments conducted over the years has proved timber cribs as reliable source for a reproducible fire of a predetermined magnitude (Heskestad 1973, Harmathy 1981, Harmathy 1972, Tewarson 1984). For example, if experimentation with a 200kW fire is required, a crib can be designed to provide that heat release rate. In experiments carried out by Butcher et al in which furniture was the fuel, the burning characteristics were practically unchanged if wood piles were replaced with furniture that represented the same fire load and same free surface.

5.2. CRIB DESIGN

In order to simulate a fire within a typical residential compartment, an estimation of the expected fuel load and heat release rate was required. A fuel load energy density of 500MJ/m²(FEDG) was used as a guide. The estimated peak heat release rate for typical contents of a residential room is 700kW per item (bed or wardrobe) when burnt in the open.

The heat release rate of timber cribs burning in a compartment, is controlled by one of three factors (Nilsson 1974):

1. surface area of the timber
2. porosity of the crib, or
3. ventilation within the compartment.

Note that when controlled by the surface area or porosity of the crib then it is a result of the fuel and if by ventilation, then it is a compartment effect. Equations 4.1 and 4.2 were

² Timber used was New Zealand Radiata Pine that was air dried and untreated.

applied to find a crib arrangement with a fuel load density and heat release rate similar to those discussed above

$$\dot{m} = \frac{4}{D} m_o v_p \left(1 - \frac{2v_p t}{D} \right) \quad (\text{fuel surface control}) \quad (4.1)$$

$$\dot{m} = 4.4 \times 10^{-4} \left(\frac{s}{h_c} \right) \left(\frac{m}{D} \right) \quad (\text{porosity controlled}) \quad (4.2)$$

where \dot{m} = mass loss rate (kg / s)

$$v_p = 2.2 \times 10^{-6} D^{-0.6}$$

m_o = initial mass (kg)

D = thickness of sticks (m)

s = spacing of sticks (m)

h_c = height of the crib (m)

t = time (sec)

It was estimated that the density of the wood, which is at 15% moisture content, was 500kg/m³. Using two timber cribs, separated by 0.05m, each 1m high with 0.05m x 0.05m x 0.65m long sticks spaced 0.05m, was adequate. This arrangement equates to a fuel load density of 340 MJ/m² (assuming ΔH_c of 18MJ/kg) and a steady heat release rate controlled by porosity of 870 kW per crib.

5.3. LAYOUT AND IGNITION SOURCE

As shown in figure 4.1, the cribs were placed at the rear of the container.

The timber cribs were elevated above a base. Between the base and the cribs, shredded paper covered in methylated spirits formed an ignition source to ensure even burning. To ignite the paper an LPG pilot flame was installed. Ignition of the pilot flame came from a 15 000 volt transformer that created an arc across two electrodes 10mm apart.

In order to ignite the cribs uniformly, shredded paper sprayed with methanol was spread underneath the cribs. (Shown in photo 5.1 is the typical layout before addition of the timber cribs)

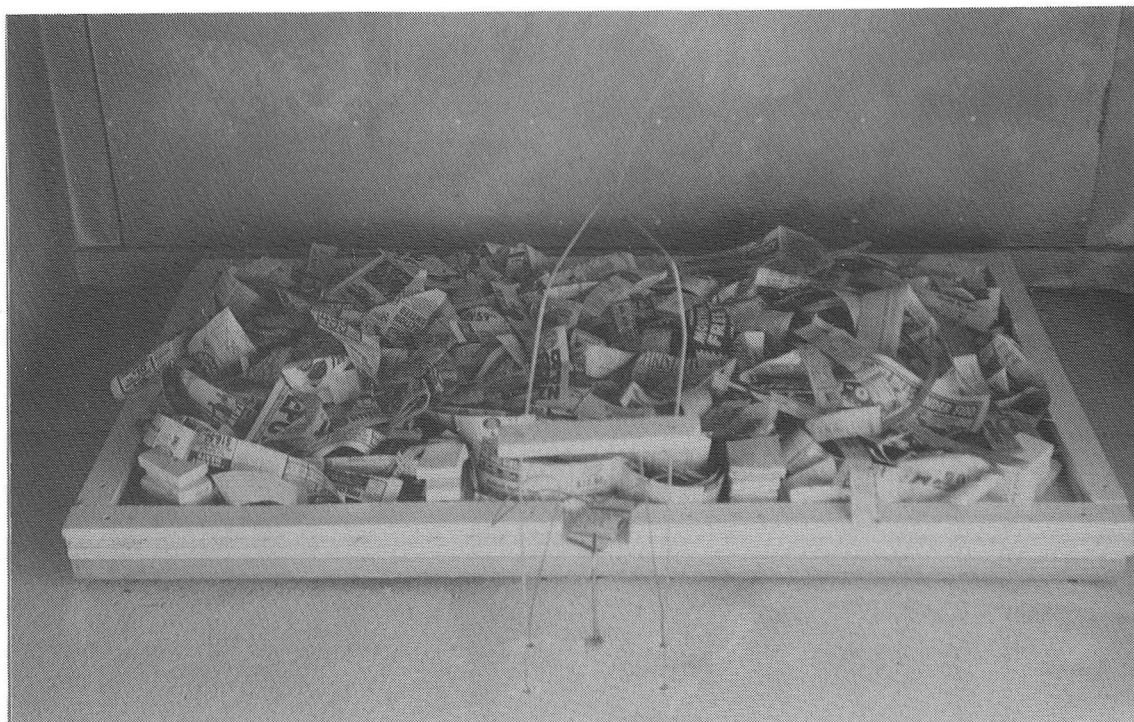


Photo 5.1 Shredded paper to provide an even ignition source

The spacing of the ignition and fuel set up can be seen in figures 4.1 and 4.2

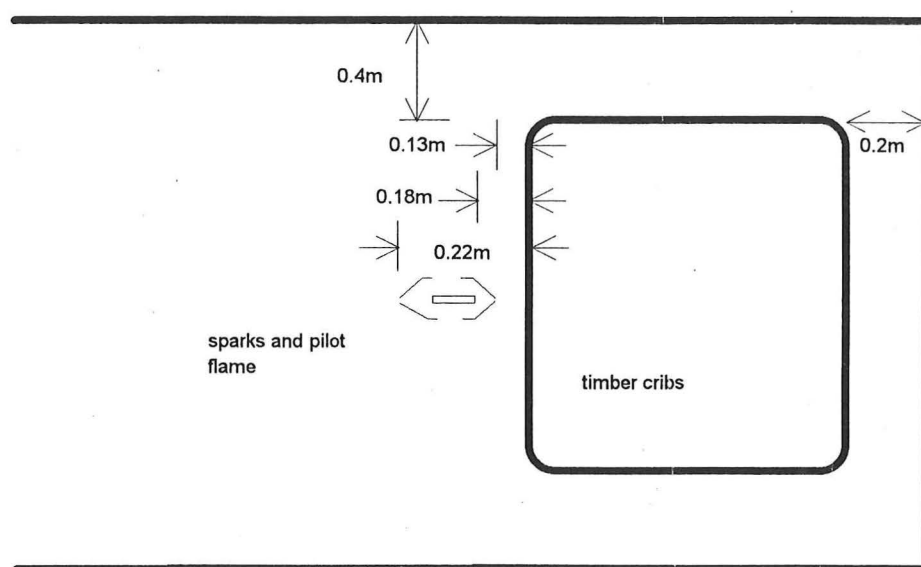


Figure 4.1 Plan view of crib layout

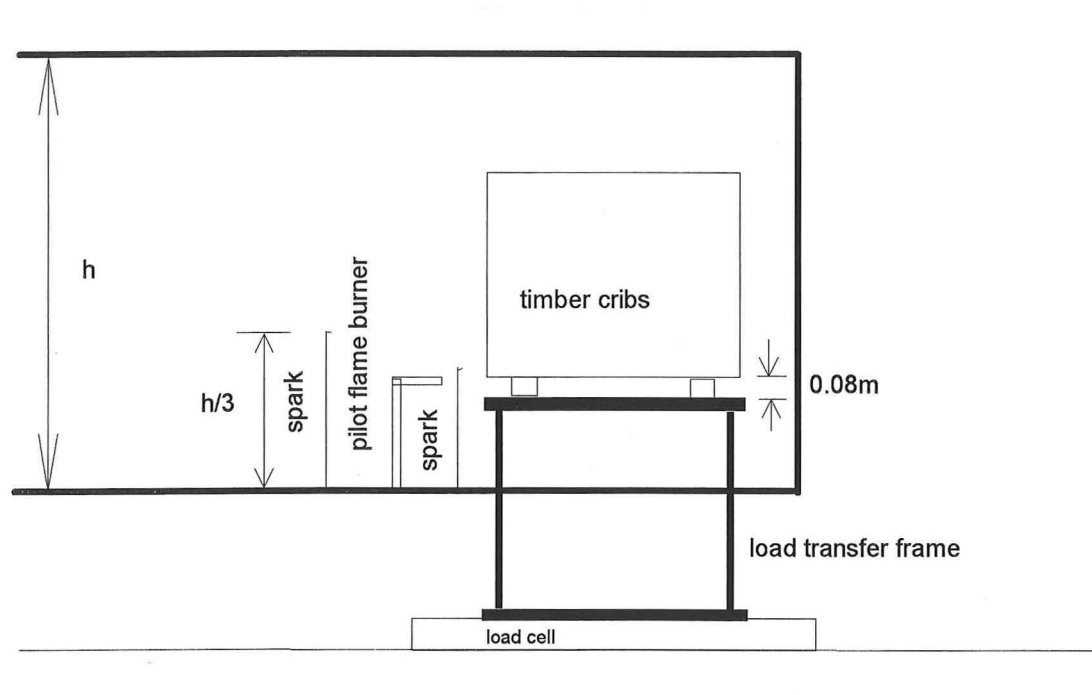


Figure 4.2. Elevation of the set up.

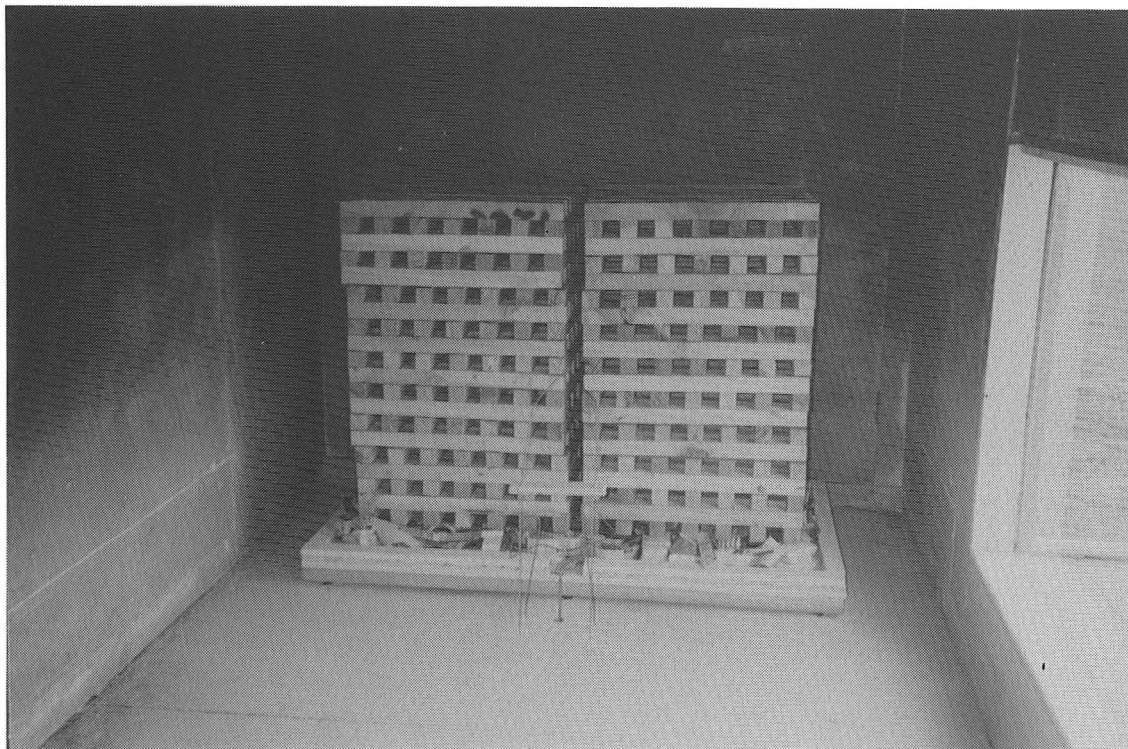


Photo 5.2 Layout of timber cribs

6. METHOD OF RESULTS ANALYSIS

6.1. ANALYSIS

The following compartment conditions were monitored during testing:

- compartment temperatures
- pressures at the floor and ceiling
- heat loss through the walls
- mass loss rate of fuel
- pressure difference profile at vent
- O₂ concentration history

Along with these, the mass flow in and out of the compartment was estimated from Emmons 1988 .

Applying a two zone approximation, as used within the computer model, the compartment temperature profile was converted into two zones. See section 6.3 for a description of the technique.

6.2. MASS FLOW RATES

In order to quantify the level of flow it is necessary to evaluate the pressure difference across the vents. Once a base point has been established, then applying hydrostatic analysis the pressure difference at different heights y can be determined from the following

$$\Delta p = p_1 - p_2 = (p_f - p_a) - \int_0^y (\rho_2 - \rho_1) g dy \quad (6.1)$$

$$\text{where} \quad p_1 = p_f - \int_0^y \rho_1 g dy \quad (6.2)$$

$$p_2 = p_a - \int_0^y \rho_2 g dy \quad (6.3)$$

p_f = pressure at the floor inside the compartment (Pa)

p_a = pressure at the floor level outside the compartment (Pa)

ρ_1 = inside density (kg/m^3)

ρ_2 = outside density (kg/m^3)

$\rho = 352.8/T$

T = temperature in Kelvin

= f(y).

Assuming

$$\rho_2 = 1.17$$

$$g = 9.81 \text{ (m/s}^2\text{)}$$

Equation 6.1 was rearranged to

$$\Delta p = \Delta p_f - 15.92 + 3461 \int_0^h \frac{1}{T_1(y)} dy \quad (6.4)$$

where h = height from the floor to the centre of the vent

= 1.39m for top vent location B.

Hence pressure differences at all vent locations can be determined.

Application of equation 6.1 was required for experiments two (pressure probe was installed after this) six and seven (when the vent was relocated). Otherwise ΔP^3 was taken directly from the results.

³ ΔP for the bottom vent was monitored during the tests.

The volume flow can be calculated from (Emmons 1988)

$$Q = CA\sqrt{\frac{2\Delta p}{\rho_h}} \quad (\text{m}^3/\text{s}) \quad (6.5)$$

where C = flow co-efficient (assume equal to 0.68)

A = the area of the vent (m^2)

ρ_h = the density of the flowing gas at vent height h . (kg/m^3)

In order to normalise this value with respect to the size of the container the flow was converted to room air changes per hour. Due to the noise in the readings, the plotted values are ten minute averages.

6.3. LAYER HEIGHT AND TWO ZONE TEMPERATURES

The vertical compartment temperature distribution at a particular time can be approximated as two thermal layers of uniform temperature (upper and lower zone) from a theoretical two zone model. Quintiere et al 1984 provide a method which allows the determination of the thermal interface height and the unsteady upper and lower average temperatures. The fundamental process is discretionary but the general principal is as follows;

1. An arithmetic mean is used to fit the upper temperatures. The temperature data includes points from the top down until the data significantly departed from the average fit.
2. Two integral identities are then used to compute the interface height (x_1) and the lower layer temperature (T_l). These integrals are

$$\int_0^H \left(\frac{1}{T} \right) dx = \frac{(H - x_1)}{T_u} + \frac{x_1}{T_l} \quad (6.6)$$

$$\int_0^H T dx = (H - x_1)T_u + x_1T_l \quad (6.7)$$

where T_u and T_l are the upper and lower temperatures and H and x_i are the compartment and layer interface heights respectively. Equation 6.6 constitutes a mass balance and equation 6.7 retains the same mean temperature as in the data. In this analysis T_l was assumed equal to the average of the three lowest thermocouple probes.

7. EXPERIMENTAL RESULTS AND DISCUSSION

A total of seven different experiments were run. Due to the duration of the pilot flame, experiment one has not been discussed. The influence of four test variables has been considered in the analysis.

1. Reduced vent areas
2. Change in vent location
3. Elevation of the fuel
4. Pilot flame duration

Each comparison made considered the events over the same duration of time. Because of the varying mass of fuel (paper) used to ignite the cribs and the variance in the ignition phase, the first five minutes of each experiment has been ignored

For each of the comparisons a total of five aspects of the fire were compared.

1. Temperatures
2. Mass loss
3. Layer depth
4. Vent flow
5. Global equivalence ratio

Temperature comparisons (both the upper and lower layer, U.L.T and L.L.T) are from the two zone approximation described above and are taken after 1800 seconds. The figures shown also give the experimental data from which the estimation was made. The layer depth is also estimated from the two zone approximation. Mass loss comparisons are given at the time of shortest test duration. Vent flows at ten minute averages were averaged between in and out over the shortest test duration to give one value for the test (values in brackets show the range from which the average came). The equivalence ratio (ϕ) (defined in section 8.2.2.1.1) was also averaged over the shortest test duration.

Graphs of the temperature, mass loss, pressure and compartment flow histories, and a full list of observations including a description of the weather conditions, can be found in Appendix B.

For ease of reference table 7.0 gives a description of each test that has been discussed:

TEST	2	3	4	5	6	7
TOP VENT LOCATION	A	A	A	A	B	B
TOP VENT AREA (m²)	0.0314	0.0154	0.0154	0.0079	0.0079	0.0079
BOTTOM VENT AREA (m²)	0.0660	0.0314	0.0314	0.0154	0.0154	0.0154
FUEL LOAD (kJ)	3816	3978	3960	2900	2900	2988
ELEVATION OF CRIB (m)	0.25	0.25	0.25	0.74	0.74	0.74
PILOT FLAME (s)	15	15	15	40	15	240
SPARK INTERVALS (s)	600	600	600	300	300	480
SPARK DURATION (s)	10	10	10	10	10	120
OPENING TIME (s)	3600	7200	2100	3600	3020	5400

Table 7.0 Experimental conditions.

7.1. CONSISTENCY

Table 7.1 shows the consistency that existed within the set up. The experiments were the same, the only difference being the duration of the test.

Experiment	U.L.T (K)	L.L.T (K)	Mass Loss (kg)	Layer height (m)	Air flow (AC/hr)	Equivalence ratio
3	478	351	53	0.55	5.5 (3.5-7.5)	5.3
4	484	348	52	0.55	4.7 (4-7.5)	3.6

Figure 7.1 Comparison of experiments 3 and 4.

7.2. REDUCED VENT AREAS.

To show the influence of reduced vent areas, experiments 2 and 3 were compared. The difference between the areas was a factor of two at both the top and bottom.

Experiment	U.L.T (K)	L.L.T (K)	Mass Loss (kg)	Layer height (m)	Air flow (AC/hr)	Equivalence ratio
2	523	389	130	0.76	12.4 (9-17)	2.4
3	478	351	80	0.55	5.5 (3.5-8.5)	5.2

Table 7.2 Effect of reduced vent areas

7.3. CHANGE IN ELEVATION OF THE TOP VENT.

As discussed in section 2.8, the top vent location was changed between experiments 5 and 6. In experiment 6 the vent elevation was lowered and its lateral position centralised, the results of which, can be seen in Table 7.3.

Experiment	U.L.T (K)	L.L.T (K)	Mass Loss (kg)	Layer height (m)	Air flow (AC/hr)	Equivalence ratio
5	417	311	27	0.91	1.8 (1.5-2.4)	2.9
6	320	314	12	0.96	2 (1.75-2.5)	1.05

Table 7.3 Change in location of top vent.

7.4. ELEVATION OF THE FUEL

In order to compare the effects of elevation of the fuel, experiments 4 and 5 were reviewed.

Experiment	U.L.T (K)	L.L.T (K)	Mass Loss (kg)	Layer height (m)	Air flow (AC/hr)	Equivalence ratio
4	484	348	50	0.55	4.7 (4-7)	2.4
5	417	311	21	0.91	1.8 (1.5-2)	2.9

Table 7.4 Elevation of the fuel.

7.5. PILOT FLAME DURATION.

Experiment 6 and 7 were only varied in the ignition phase. The latter had a pilot flame consistently on the fuel for 240 seconds as opposed to 15. As is seen in table 7.5, the temperatures in the upper layer increase but the lower layer stays relatively the same. However the time at which the comparison is made is during the trough in the temperature history of experiment 6.

Experiment	U.L.T (K)	L.L.T (K)	Mass Loss (kg)	Layer height (m)	Air flow (AC/hr)	Equivalence ratio
6	374	314	12	0.96	2 (1.75-2.5)	1.05
7	428	320	18	0.95	1.3 (.75-2)	4.7

Table 7.5 Effect of pilot flame duration.

7.6. DISCUSSION OF RESULTS

Although only one experiment per variation was carried out, the comparison of tests three and four show the consistency that existed. The level of similarity is shown in figure 7.1

The weather conditions played a significant role in the progress of the fire. The conditions have only been considered when looking at irregular and unexpected results. A full analysis incorporating the wind conditions is not within the scope of this report.

It was anticipated that both timber cribs, which were separated by 0.05m, would be involved in the burning. However, as shown in photo 7.1, one crib dominated burning in every experiment and was not consistent to any location.

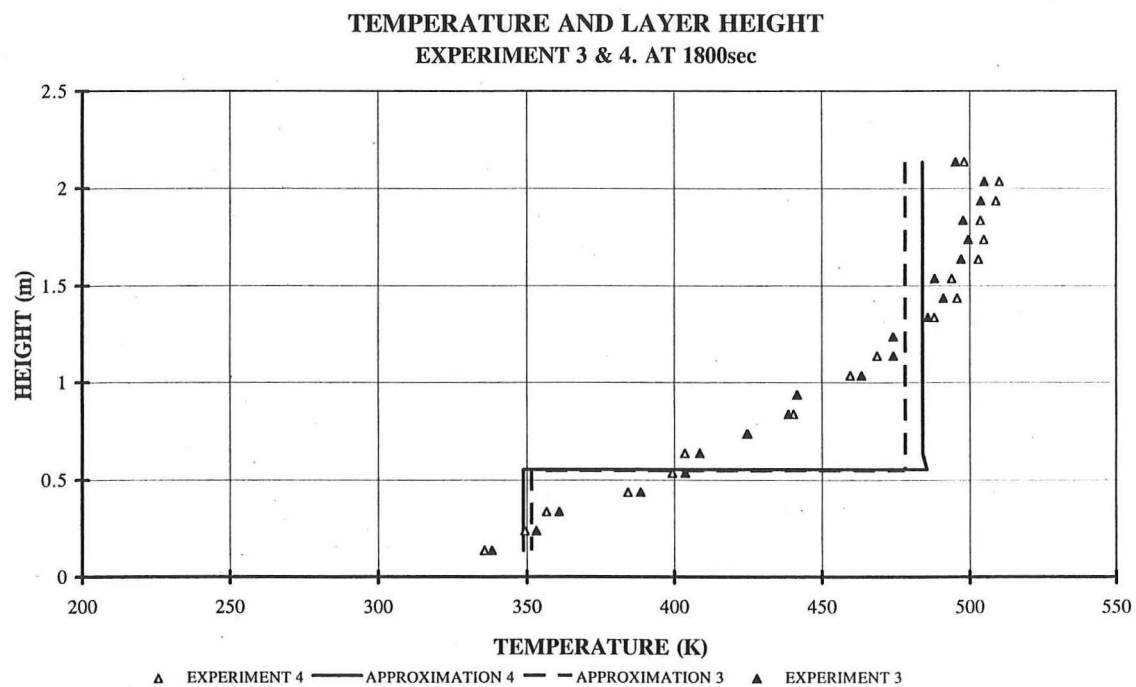


Figure 7.1. Consistency between temperatures and layer height.

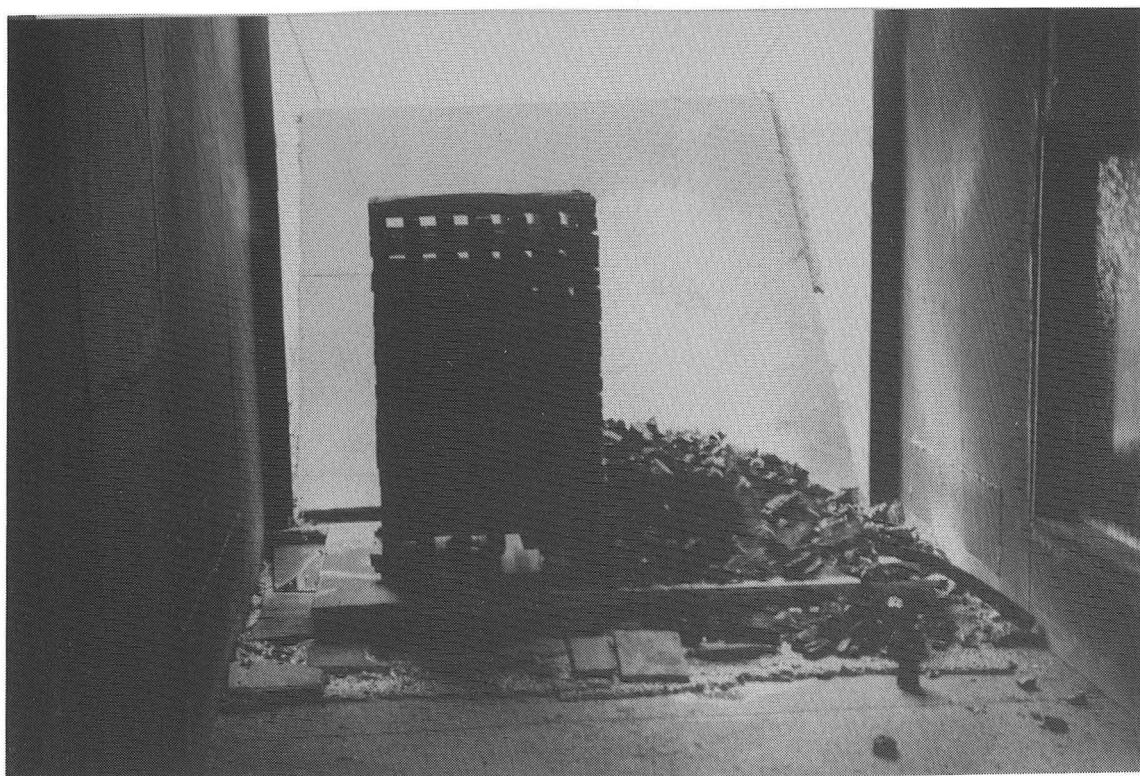


Photo 7.1 Partial involvement of the fuel.

As shown in figure 7.2 the temperature history in experiment 6 was very erratic. Analysis of the mass loss history do not show any abnormalities (eg crib dropping to floor). It may have been due to the compartment ventilation conditions not allowing enough air in during the ignition phase while the fuel was elevated or the ignition was inconsistent. Either way it raises many questions.

Shown in figure 7.3 and 7.4 the flow in appears to be larger than that out of the container for experiments 5 and 6. Due to mass equilibrium these raise questions. Unfortunately flows depend upon the results of both temperature and compartment pressure. If either is inaccurate then the flow estimation will be affected. Another possibility is unaccounted for leakage areas will increase area for flow out.

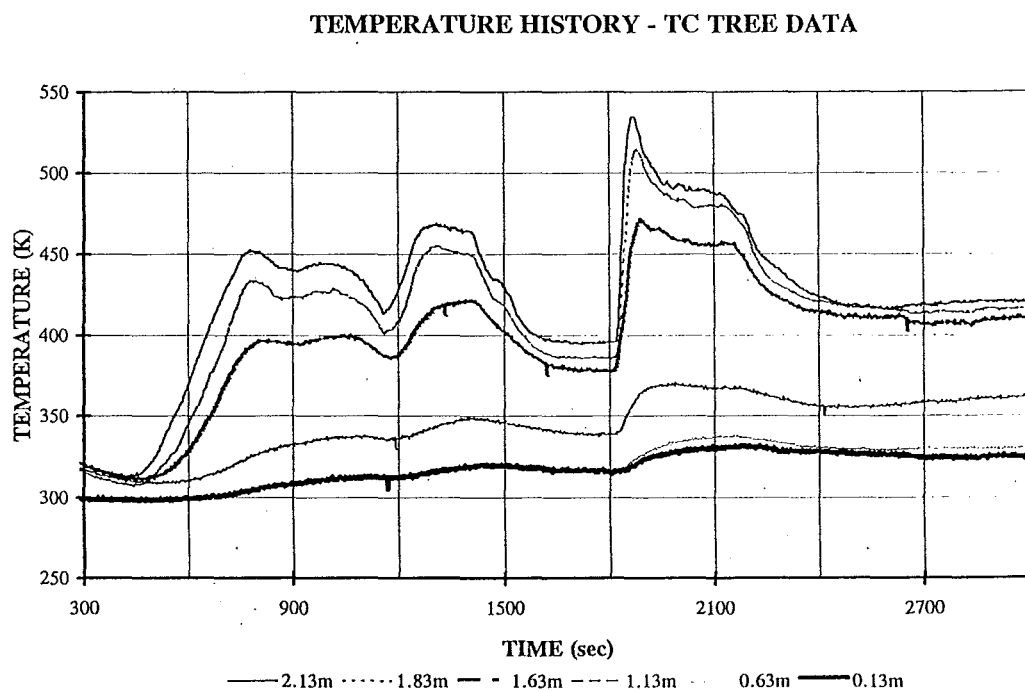


Figure 7.2 Temperature history of experiment 6.

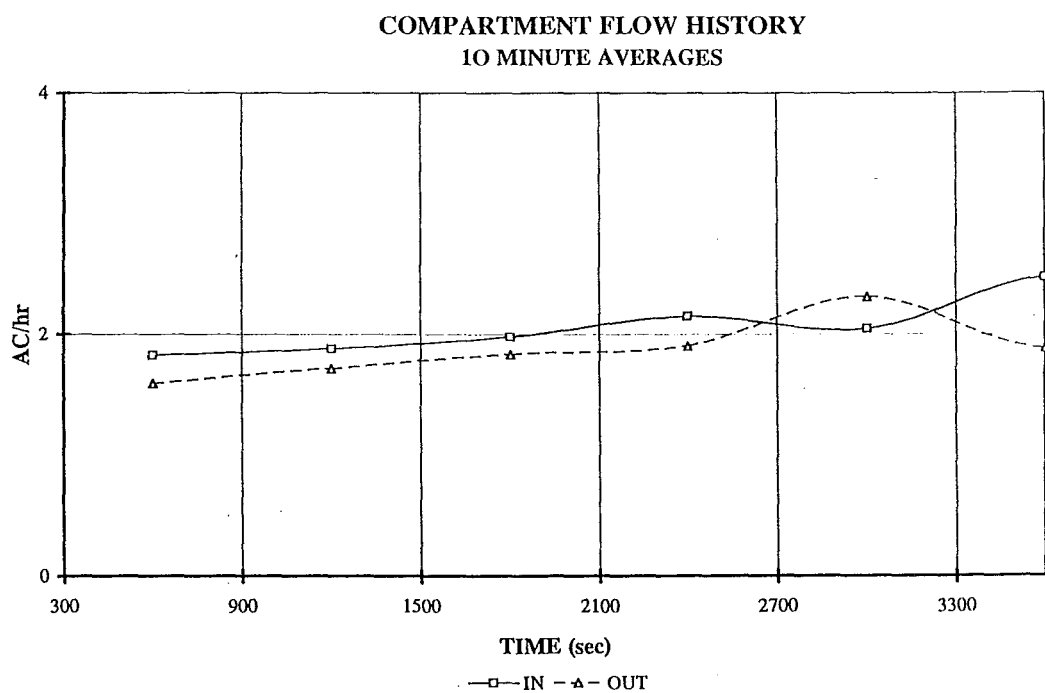


Figure 7.3 Compartment flow history for experiment 5

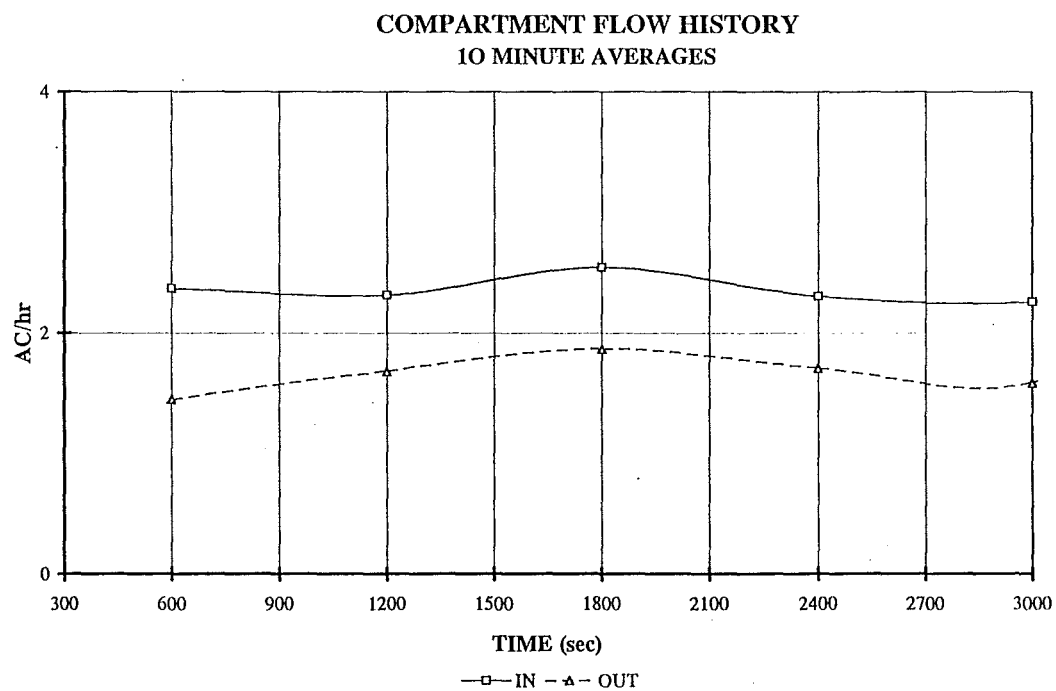


Figure 7.4 Compartment flow history for experiment 6

7.6.1. REDUCED VENT AREA

As expected, reducing the vent areas reduced the flow, mass loss and temperatures within the compartment. The latter two are a direct result of reduced flow into the compartment. Also expected was an increase in the equivalence ratio, ϕ . When ϕ is equal to one, theoretically there is enough air to burn all the pyrolozates. When ϕ is above one, there is not enough air compared to the rate at which pyrolysis products are released, hence excess pyrolozates are produced. An assumption in determining ϕ , (all of the incoming oxygen goes to the reaction zone), produces values within this report that are underestimated.

As shown in figure 7.5 the layer height decreased. Since the flow out has been restricted the expanded hot gases forced an increase in depth of the layer.

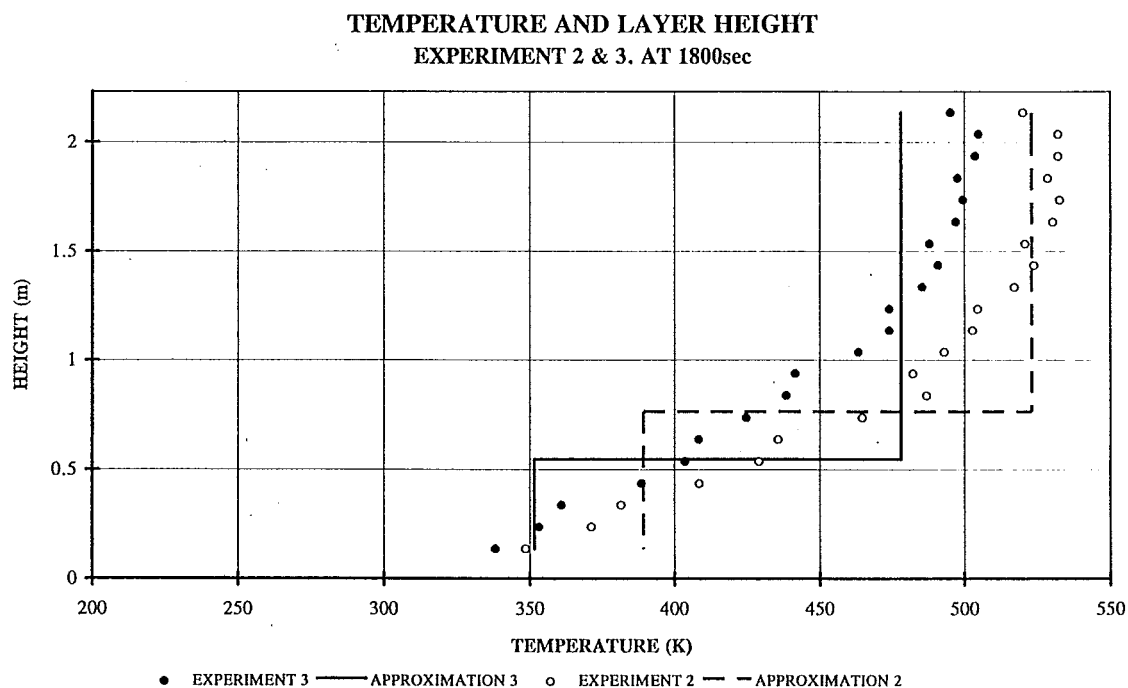


Figure 7.5 Temperature and layer height for experiments 2 and 3.

7.6.2. LOWERED ELEVATION OF THE TOP VENT.

In reducing the elevation of the top vent the upper layer temperatures decreased. However, as shown in figure 7.2 the point in time (1800 sec) that values were taken from experiment six, temperatures were at a low. During a steady period of high temperature (800 - 1500 sec) the upper layer temperature was approximately 415°K but the layer

height never went below 1 metre. Hence, decreasing the height of the top vent does increase the height to the layer. (Shown in figure 7.6)

Comparison of air flows shown in table 7.3 indicate little difference. Comparisons of the mass loss histories given in table 7.3 show a large decrease has resulted from the change. Both of these results provide data for determining ϕ . It is difficult to rely upon any of these results as the out flow of gas was higher than that of inflow for both experiments 5 and 6. It may be possible that the different lateral position of the vents has caused pressure variations in the lower layer resulting in poor representation of the situation.

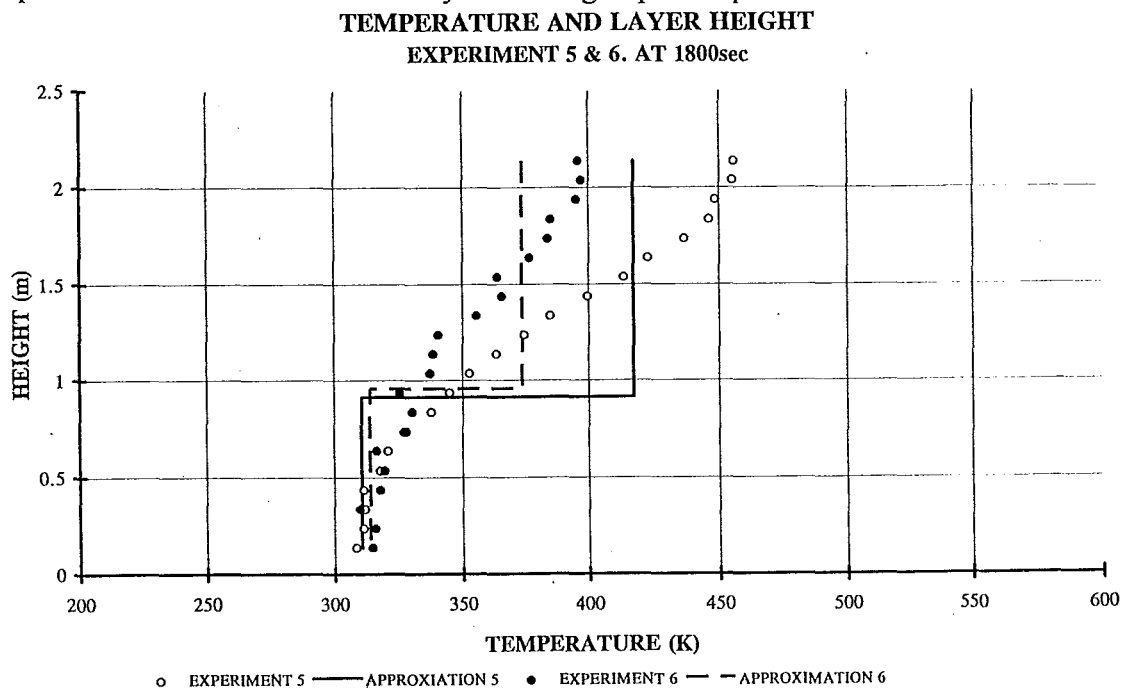


Figure 7.6 Temperature and layer height for experiments 5 and 6.

7.6.3. ELEVATION OF THE FUEL.

Comparison of experiments 4 and 5 involve both elevation of the fuel and vent areas were also decreased by a factor of two. However, as can be seen in table 7.2 it is expected that the temperatures, mass loss, layer height, air flow and equivalence ratio will all decrease due to vent area reduction. As shown in table 7.4 and figures 7.7 and 7.8 all of these expectations occur except for the layer height and the equivalence ratio. It

can only be concluded that elevation of the fuel increases the layer height. (see photos 7.2 and 7.3)

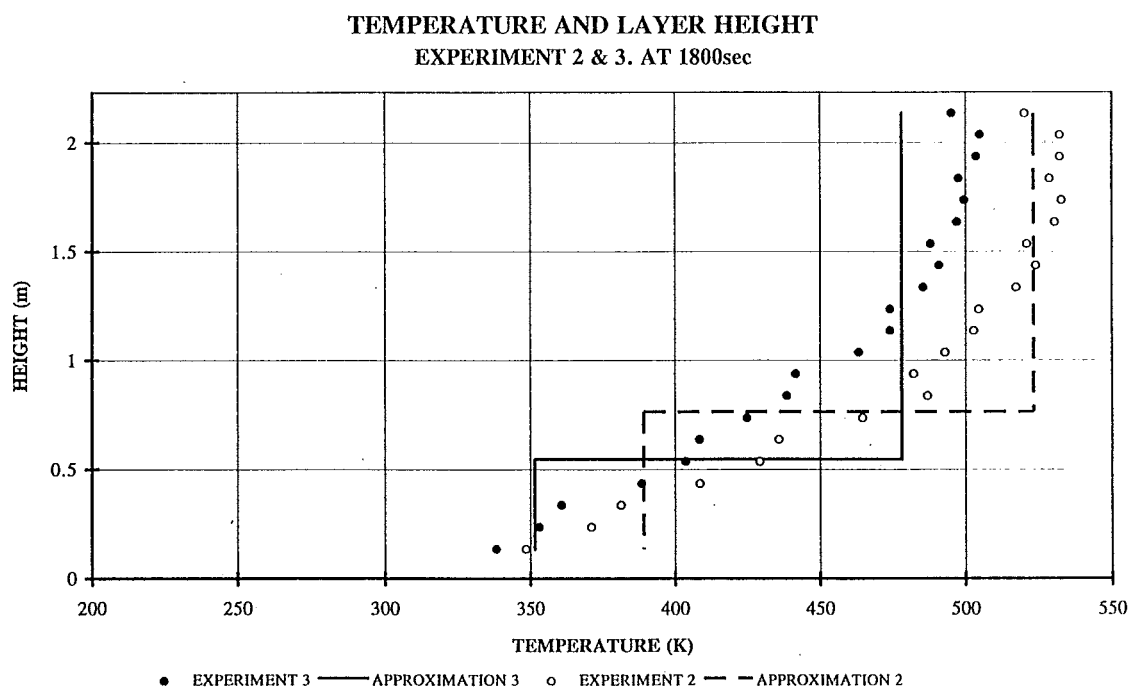


Figure 7.7 Temperature and layer height of experiments 2 and 3.

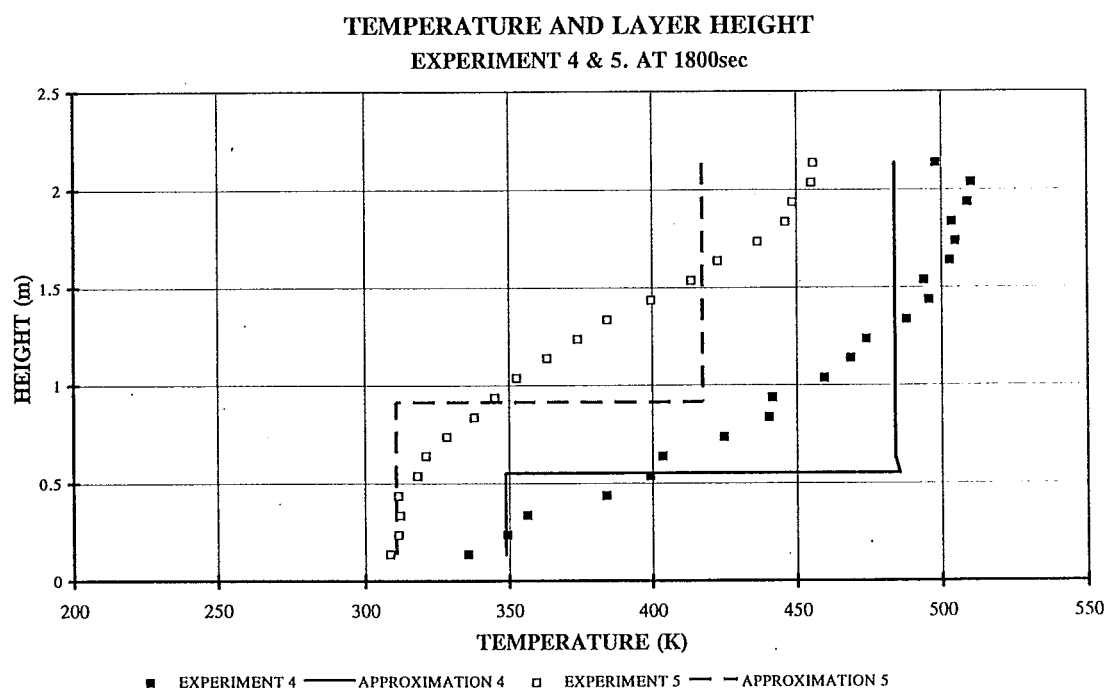


Figure 7.8 Temperature and layer height of experiments 4 and 5.

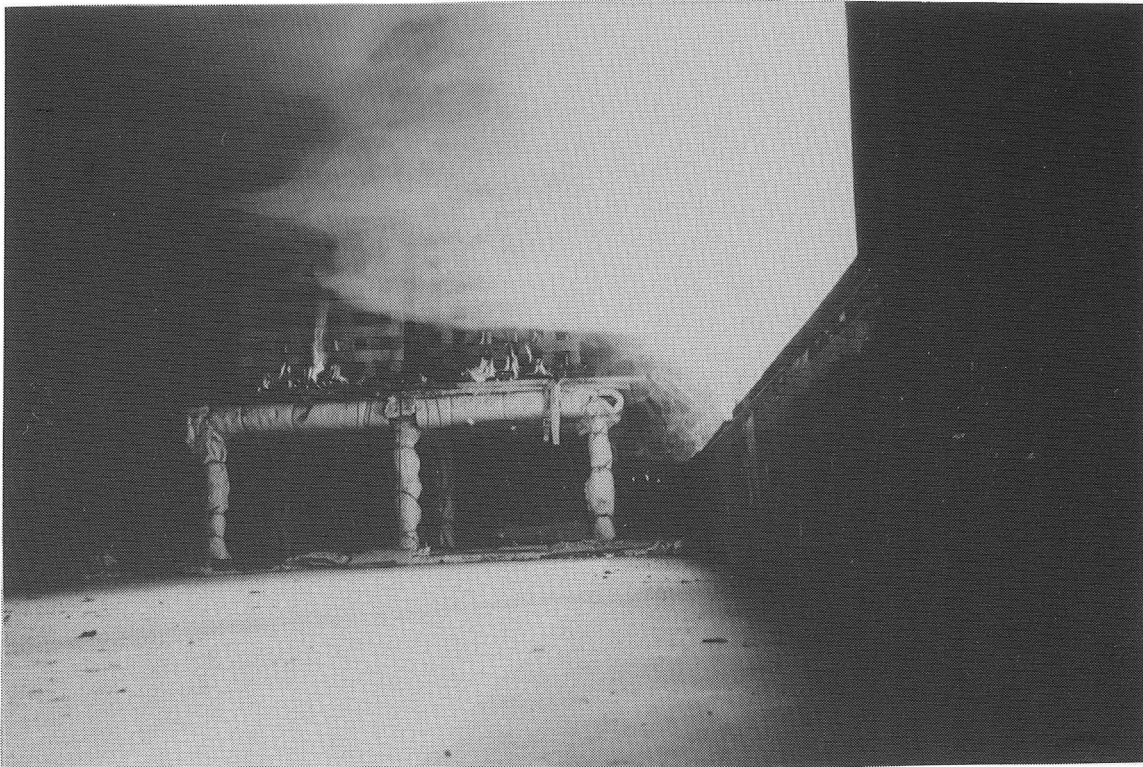


Photo 7.2 Early development of a layer

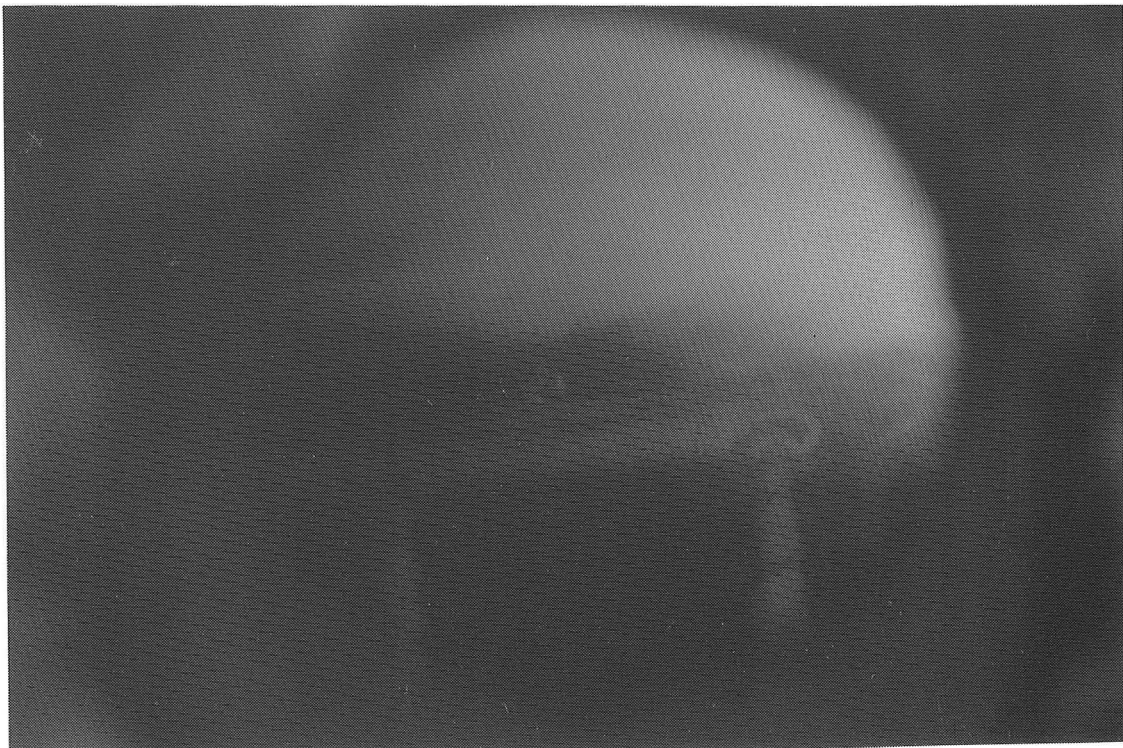


Photo 7.3 Taken through the bottom vent, consistent smoke layer level.

7.6.4. EXTENDING THE DURATION OF THE PILOT FLAME.

By extending the duration of the pilot flame, the cribs in experiment 7 became more involved, however once the pilot flame was turned off, crib burning was still controlled by available oxygen. As mentioned above the temperatures compared from experiment six are at a low (see fig 7.2). As shown in figure 7.9 the layer height appears unaffected. The air flow for each was similar but the equivalence ratio quite different which is due to the difference in mass loss.

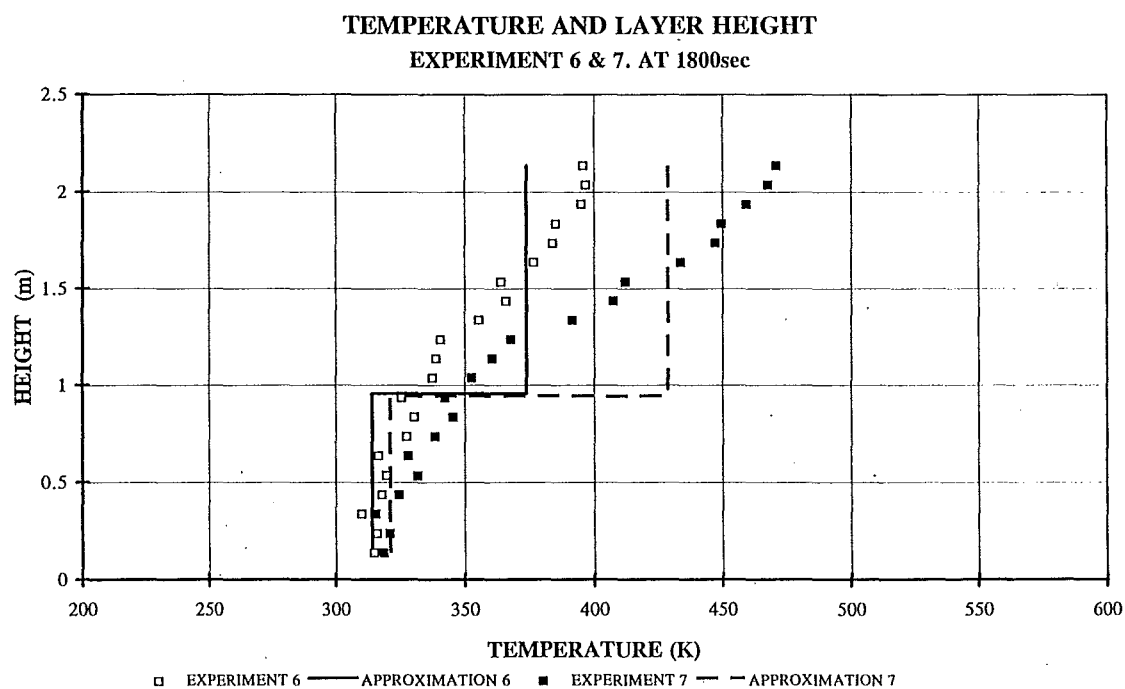


Figure 7.9 Temperature and layer height for experiments 6 and 7.

7.6.5. SMOKE EXPLOSION.

In experiment 6 several variances from the expected occurred. Firstly, the growth of the fire was much slower and appeared to have self extinguished but after 600 seconds its mass loss showed major increase. As shown in figure 7.2 the temperatures within the compartment began to decrease, however the mass loss rate had not varied prior to this. At 1824 seconds an instantaneous temperature increase of $140\text{ }^{\circ}\text{K}^4$ occurred along with a 30Pa pressure rise and 50% oxygen decrease (at the top of the compartment) (see figures 7.10, 7.11 and 7.12). Prior to this occurrence, both the temperatures and CO_2 mass fraction decreased. Following the event, the CO_2 and O_2 mass fractions increased. All of these circumstances hint at the occurrence of a smoke explosion. Also of interest is that no externally applied ignition existed at this time. The hypothesised occurrence was that the pyrolozates accumulated in the upper layer to the point at which the gas composition was in the flammable range. Ignition then came from a floating ember or sudden flaming of the crib. Ignition of all the flammable gases released sufficient energy to cause a sudden rise in pressure and temperature. Further experimentation is required to fully understand this phenomena.

No backdrafts were witnessed during any of the experiments. As with the smoke explosion, there is more questions than answers as to why not. It is suggested that conditions studied and the fuel used may have not been adequate to cause the pyrolysis accumulation.

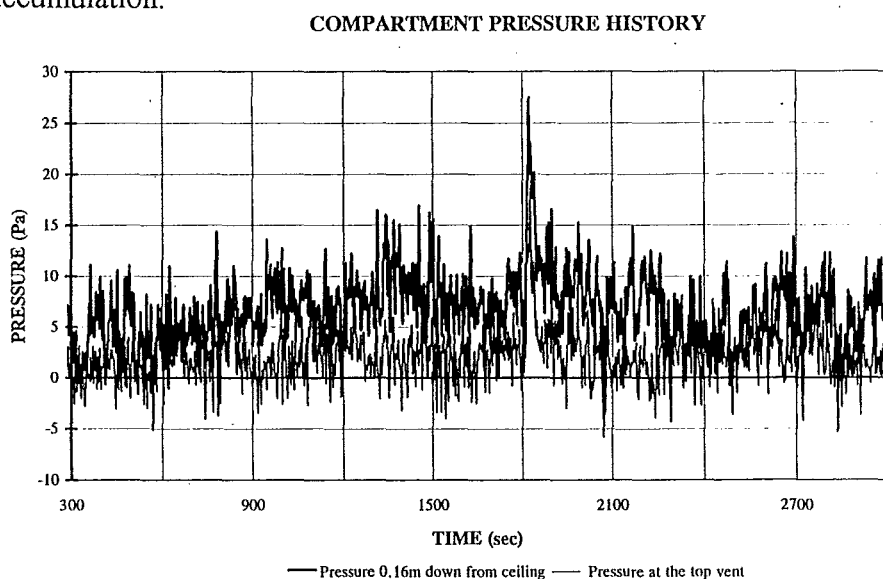


Figure 7.10 Compartment pressure history of experiment 6

⁴ Recorded at the top thermocouple probe.

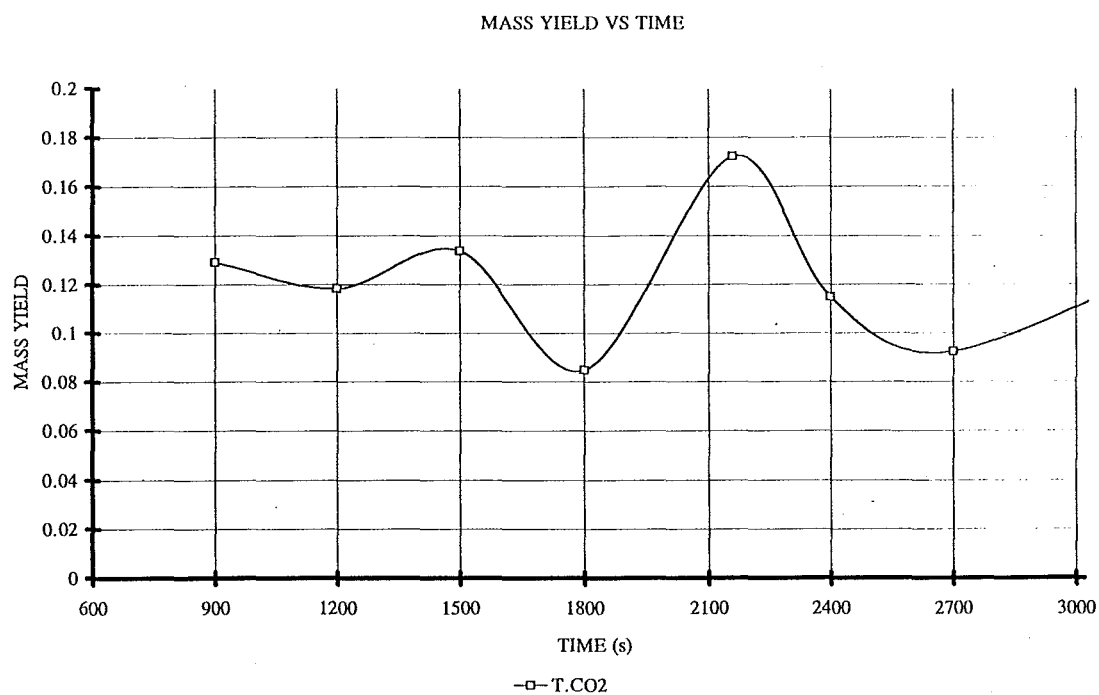


Figure 7.11 Mass yield of CO_2 at the top port during experiment 6

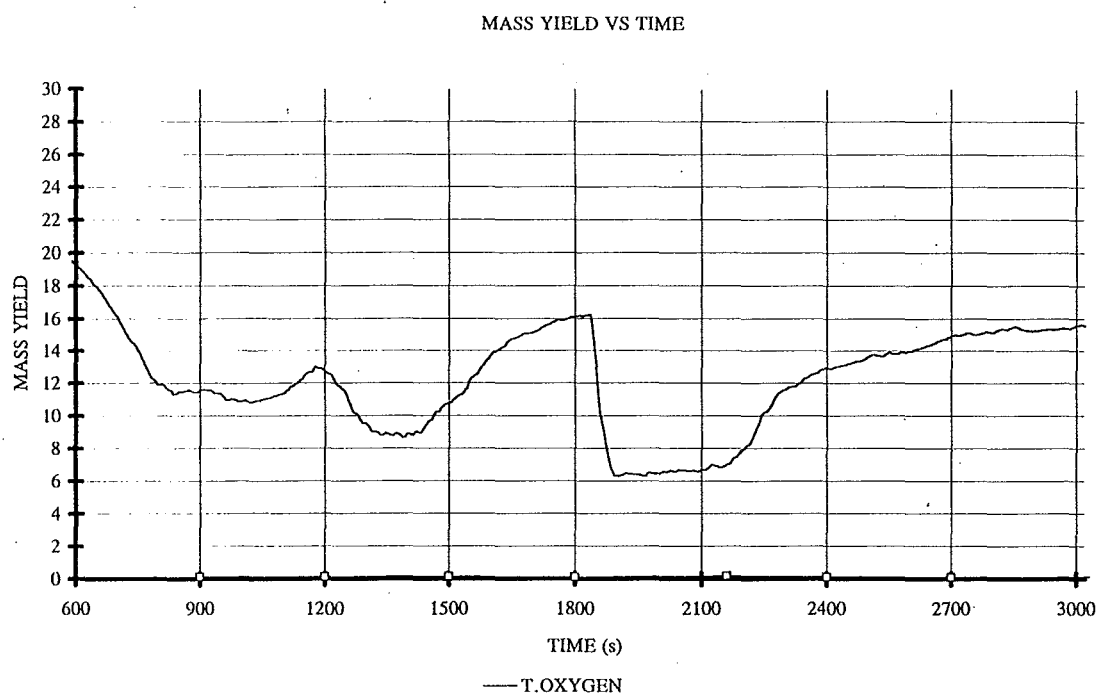


Figure 7.12 Mass yield of O_2 at the top port during experiment 6.

8. COMPUTER MODELS

8.1. INTRODUCTION

Deterministic⁵ models exist in three different levels:

1. experimentation,
2. field modelling,
3. zone modelling.

Experimentation is not financially viable for many and field modelling requires an enormous amount of computer time. For these reasons the low ventilation results were compared with those of a zone model.

Zone models break the compartment of origin into three zones which represent the fire plume, upper and lower layers. Each layer is assumed to be homogenous and the plume behaviour is described by algebraic expressions (Savilonis 1988). The environment is constantly changing through the fire so any equations are usually in the differential form.

The model chosen for comparison was CFAST (Consolidated Model of Fire growth And Smoke Transport). The decision was based on the ease of access to CFAST, its already proven record for large ventilation compartments and the input data available (pyrolysis rate).

8.2. CFAST

“CFAST is based on solving a set of equations that predict state variables based on the enthalpy and mass flux over small increments in time. These equations are derived from the conservation equations (mass , energy and momentum) - which are always correct thus any errors come from simplifying assumptions made”(NIST⁶ 1993).

⁵ Stochastic models have been ignored as they do not quantify any physical aspect of the fire.

⁶ National Institute of Standards and Technology.

8.2.1. PREVIOUS COMPARISONS

In order to validate the computer model, NIST published a series of comparisons with experimental data (NIST 1993). Selected parameters for comparison were as follows

1. upper and lower layer gas temperature
2. layer interface position
3. gas species concentration
4. vent flow
5. heat release rate
6. room pressure

This report has reviewed all of the above except for heat release rate. Unfortunately all of the published comparisons made to date are with experiments where the room of origin had an opening equivalent to either a door or window which would represent good ventilation (generally reached flashover temperatures of 600° C).

An independent survey of smoke movement models by Savilonis 1988 looked at FAST, the older version of CFAST. As with NIST, comparisons were only made with well ventilated rooms of origin. Savilonis concluded that FAST compared well although its temperature rose too quickly and under predicted the layer depth as the fire progressed. CFAST was only introduced in 1993. Unfortunately no indepent published work could be found on the model.

8.2.2. ESTIMATIONS OF UNKNOWNNS

‘How to best quantify the comparisons between model predictions and experiments is not obvious. The necessary and perceived level of agreement for any variable is dependent upon both the typical use of the variable in a given situation , the nature of the experiment, and the context of the comparison in relation to other comparisons being made

(a true validation of a model would involve proper statistical treatment of many compared variables)” (NIST 1993)

The areas of concern in comparison was the pyrolysis rate, temperature of the gases and mass flow rate. Everything is cyclic and influences itself progression. The pyrolysis rate will be governed by the vent flows which are governed by temperatures. Temperatures depend on heat release rate, and so on.... It is expected therefore, if one component is inaccurate in its estimation then it strongly effects the rest of the comparisons.

The comparisons for mass flows shall only be looked at in terms of their order of magnitude. This is primarily due to the large spread of values that were used to obtain the averaged experimental results.

8.2.2.1. GAS COMPOSITION

Heat transfer occurs between the fire , gases and compartment surfaces. The radiative transfer is highly dependent upon temperature differences and the emissivity of the compartment gases and lining material. The range of emissivity values for the wall surfaces is small so most of the attention has been directed at the gases.

‘Errors in species concentration can give rise to errors in the distribution of enthalpy among the layers which results in errors in temperature.’(CFAST 1993)

The species of most concern are predominantly CO₂ and H₂O (CFAST 1993, DRYSDALE 1986).

Figure 2.32 of Drysdale 1986 indicate that H₂O has a higher gas emissivity than CO₂ for the equivalent conditions (pressure of the emitter times mean equivalent beam length). Hence CFAST comparison will be subject to the extreme conditions both high and low levels of H₂O production.

To estimate c/co_2 , values were varied with time based on the mass yield history that came from the gas chromatography results.

Gas chromatography results could only provide the mass yield of CO_2 , hence values for the yields of CO to CO_2 (Y_{co}/Y_{co2}), as required for CFAST, were estimated from Tewarson 1988. Tewarson developed the following ratio for wood crib fires

$$\frac{Y_{co}}{Y_{co_2}} \approx 0.87 \exp(-3.2(1/\phi)) \quad 8.1$$

where Y_{co} = mass yield of carbon monoxide (g/g).

Y_{co_2} = mass yield of carbon dioxide (g/g).

ϕ = equivalence ratio⁷

Assuming all incoming air goes directly to reaction zone then

$$\Phi = \frac{\left(\frac{\dot{m}_{fuel}}{\dot{m}_{air}} \right)_{actual}}{\left(\frac{\dot{m}_{fuel}}{\dot{m}_{air}} \right)_{stoichiometry}}$$

where $\dot{m}_{fuel actual}$ = pyrolysis rate during experiment.

$\dot{m}_{air actual}$ = mass flow of air into the compartment.

$$\left(\frac{\dot{m}_{fuel}}{\dot{m}_{air}} \right)_{stoichiometry} \quad \text{for timber was assumed to be 0.175 (Brabaskis 1986).}$$

As discussed above, H_2O also plays a significant role in the heat transfer. Beyler also compared production species as a function of the mass fuel to oxygen

$$\text{ratio} \left(\frac{\dot{m}_{fuel}}{0.233 \dot{m}_{air}} \right)_{actual} \quad \text{) providing estimates of mass yield values for } H_2O \text{ and } CO_2.^8$$

⁷ Tewarson refers to an air to fuel stoichiometric fraction which the recipricol of the equivalence ratio.

⁸ Based on experiments using panderosa pine.

Good first estimation of the production rate of CO₂, and H₂O come from the following

$$f_{CO_2} = f_{H_2O} = \frac{1}{\Phi} \quad 8.2$$

where f_i = the normalised yield of species i

$$= \frac{Y_i}{k_i}$$

Y_i is the mass production rate of a species i per unit mass of fuel volatilised

k_i is the maximum possible mass production rate of species i per unit mass of fuel volatiles.

$$k_{CO_2} = 1.4$$

$$k_{H_2O} = 0.72^9$$

Therefore, from equation 8.2

$$Y_i = \frac{k_i}{\Phi}$$

The estimates of species yields obtained from the two methods just mentioned, formed the base for ratios required for CFAST input. The CFAST input varied during the course of the fire and the input of the necessary fractions altered for each experiment but ensuring that all are within steady mass loss phase.

8.2.3. CFAST CALIBRATION.

Within CFAST several assumptions (square vent, flow coefficient of 0.7, uniform temperatures in each layer etc) are made and various input parameters need to be estimated (limiting O₂ concentration, gas species concentration, base of burning etc). For this reason a series of CFAST runs were undertaken to determine the sensitivity of these

⁹ all fractions are g/g

parameters. In order to calibrate the experimental and CFAST results, experiment number 3 was compared with all runs involving parameter variation. From these comparisons, a calibration of the input could be made for the rest of the tests. Table 8.1 shows the variations from a base line, run A, and their influence. The baseline run concluded that with all the jets off and a limiting oxygen concentration of 10%, CFAST pyrolysis rate is identical however it highly overestimates the temperatures in the first 5 minutes and then underestimated for the next 90 minutes. Pressures and mass flows are also underestimated, the later by over 100%.

RUN	CHANGES	COMPARISON WITH BASE FILE
B	Limiting $O_2 = 2\%$	In early stages the temperature increased. Slight increase in mass flow in and out. O_2 drops quicker. Pressure at floor marginally more negative.
C	Fire in the middle of the room	No difference.
D	Drop the size of both vents	Decreases temperature, mass flow in and out and layer depth drops.
E	Increase base of burning height	Decreases temperatures, mass flow in and out, O_2 depleted quicker. Increase in layer height.
F	Increased H/C and C/ CO_2 ratios	No influence.
G	Ceiling jet on	Slight decrease in upper layer temperatures, mass flow in and pressure (less negative).
H	Only one layer of Gib3/4 as insulation	Major decrease in temperatures.
I	Both vents increased in size.	Major decrease in temperatures, mass flow in and out, layer goes to floor, approximately zero pressure at floor, O_2 concentration higher.
J	Increased size of top vent only.	Large increase in temperatures, mass flow in and out, pressure more negative. O_2 drops quicker.
K	All jets on	Slight decrease in upper layer temperatures, mass flow in and pressure (less negative).
L	Fire in middle of room and all jets on	Very slight decrease in temperatures.

Table 8.1 CFAST sensitivity to variables

The result of the calibration series, a limiting O₂ concentration of 2 % and all of the jets turned on, was applied to all the tests. Otherwise input was as expected with the correct insulation, base of burning equivalent to base of cribs, and the same vent areas applied. However gas species were those used for run 3, except for (Y_{co}/Y_{co2}) which were determined for each as described in section 8.2.4 (Run F indicated variation in H/C and C/CO₂ ratios had little effect).

Pyrolysis rates from each experiment were averaged between each time step. Any abnormalities, for example timber falling off the scales during testing, were eliminated.

Note that CFAST contains an option to set the ambient conditions. Due to the crudeness of measurement during the tests, they were left as default.

9. COMPARISON BETWEEN EXPERIMENTS AND CFAST

Within Appendix C are graphs of all comparisons made with CFAST and experiments two to seven. Note however that due to different run times the comparisons for each test do not use the same scale on the axis. Table 9.1 summarises the comparisons made between experimental results and CFAST predictions for scenarios 2,3,4,5,6 and 7. Any reference is to how CFAST performed with respect to experimental results.

Appendix D contains data and result files of the CFAST scenarios.

VARIABLE	ASPECT	2	3	4	5	6	7
Mass loss	magnitude	identical	identical	identical	identical	identical	identical
	shape	good	good	good	good	good	good
U.L.Temp	magnitude	high	high & low	high & low	high & low	high & very low	high & very low
	shape	poor	poor	poor	poor	poor	poor
L.L.Temp	magnitude	high	high & low	high	high	high and low	high & low
	shape	good	average	good	good	good	average
Layer hgt	magnitude	identical	identical	identical	high	high	high
	shape	good	good	good	good	average	good
Mass in	magnitude	low	low	very low	very low	low	very low
	shape	good	good	poor	average	poor	average
Mass out	magnitude	high	Very low	slightly high	high	low	very low
	shape	good	good	good	average	poor	poor
Oxygen	magnitude	low	low	low	low	very low	very low
	shape	average	average	average	average	average	average

Table 9.1 Comparisons of CFAST estimations and experimental results.

Ratings in table 9.1 were judged as follows.

- “very high” is larger than a 20% increase in magnitude
- “high” is between 10% and 20% increase in magnitude
- “very low” is larger than a 20% decrease in magnitude
- “low” is between 10% and 20% decrease in magnitude
- “average” means it does not progress opposite to that of experiments (“poor” comparison) but does not follow same shape exactly (“good” comparison).

9.1. DISCUSSION

9.1.1. MASS LOSS WITH TIME

The mass loss history were identical in all of the comparisons. This shows that when experimental results are imputed for the pyrolysis rate then CFAST portrays the fire accurately. That is not to say that any of the latter results should be accurate. Estimation of the heat of combustion was required. The value for wood was applied but as discussed by Harmathy (ref) the heat of combustion for timber varies depending upon whether the wood is burning or charring. This information was not monitored during the experiments and hence the approximation of $\Delta H_c = 18\text{MJ/kg}$ was made within CFAST ($\Delta H_c = 33\text{MJ/kg}$ for char) (Harmathy 1972).

9.1.2. COMPARTMENT TEMPERATURE

As seen in figure 9.1, CFAST overestimated both the upper and lower layers during scenario 2. In experiments 3,4 and 5 the general trend within the first 10 minutes was the upper layer temperatures were highly overestimated and then global CFAST temperatures fluctuated between under and over estimating (figure 9.2). Shown in figure 9.3 CFAST results for scenarios 6 and 7 were overestimated in the first 5 min then the compartment temperatures became uniform and were below that of the true lower layer. In all of the experiments CFAST over predicts the temperatures in the early stages. It is not possible to quantify the other temperatures but only to state that under conditions of experiment six and seven CFAST consistently underestimates the upper layer temperatures.

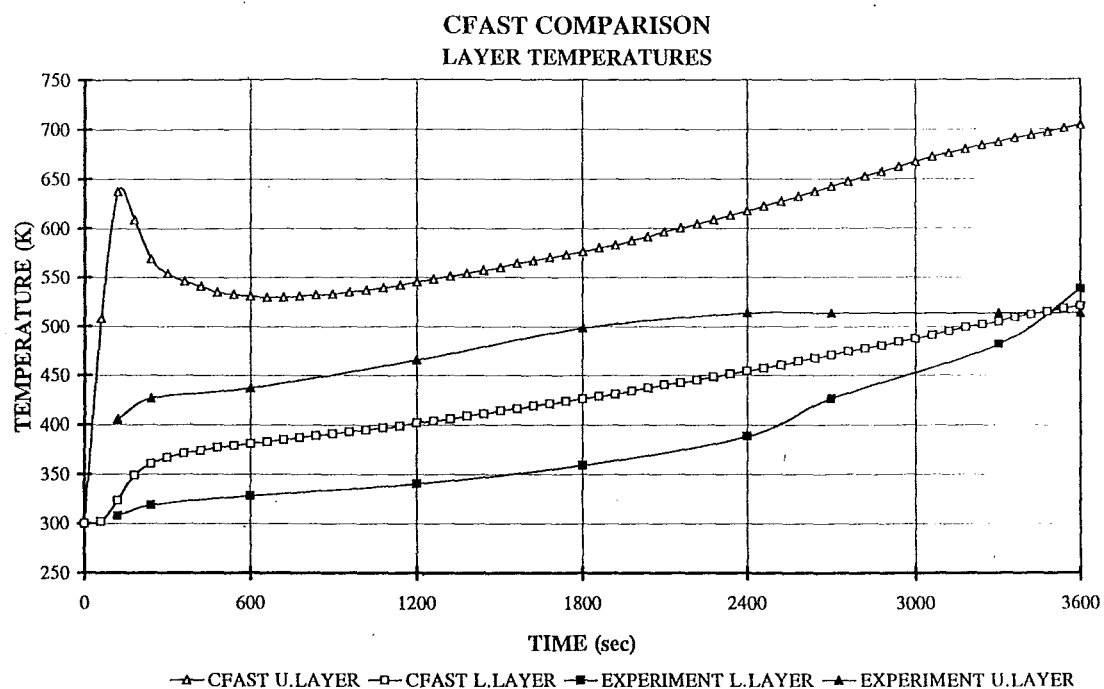


Figure 9.1 Comparison of layer temperatures in scenario 2.

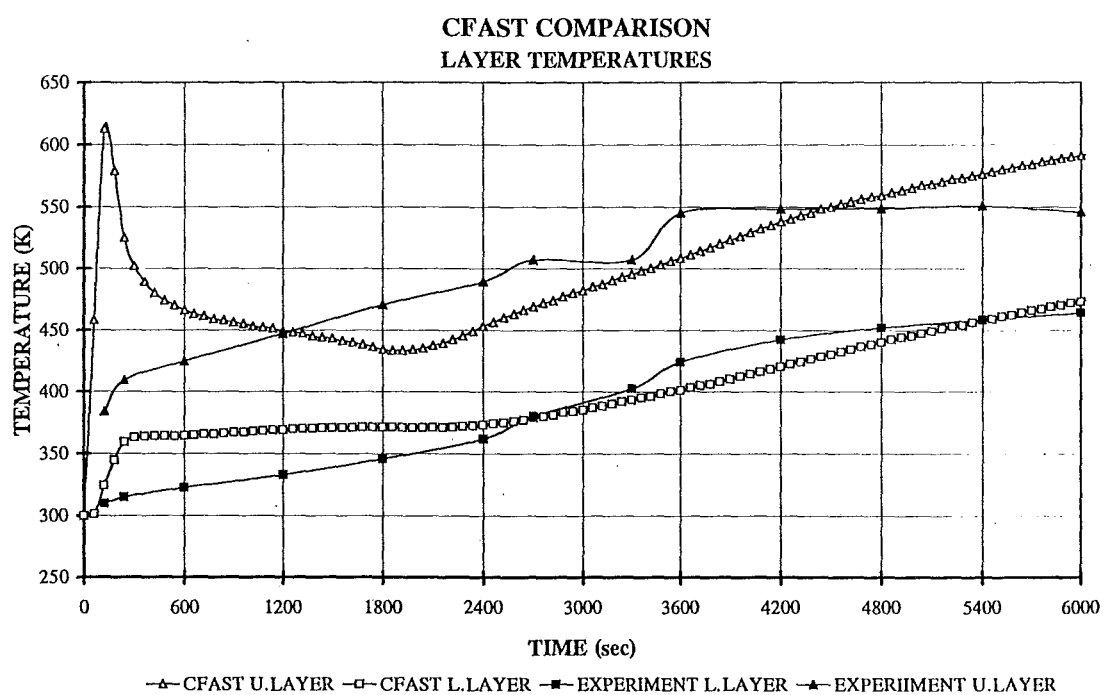


Figure 9.2 Comparison of layer temperatures in scenario 3.

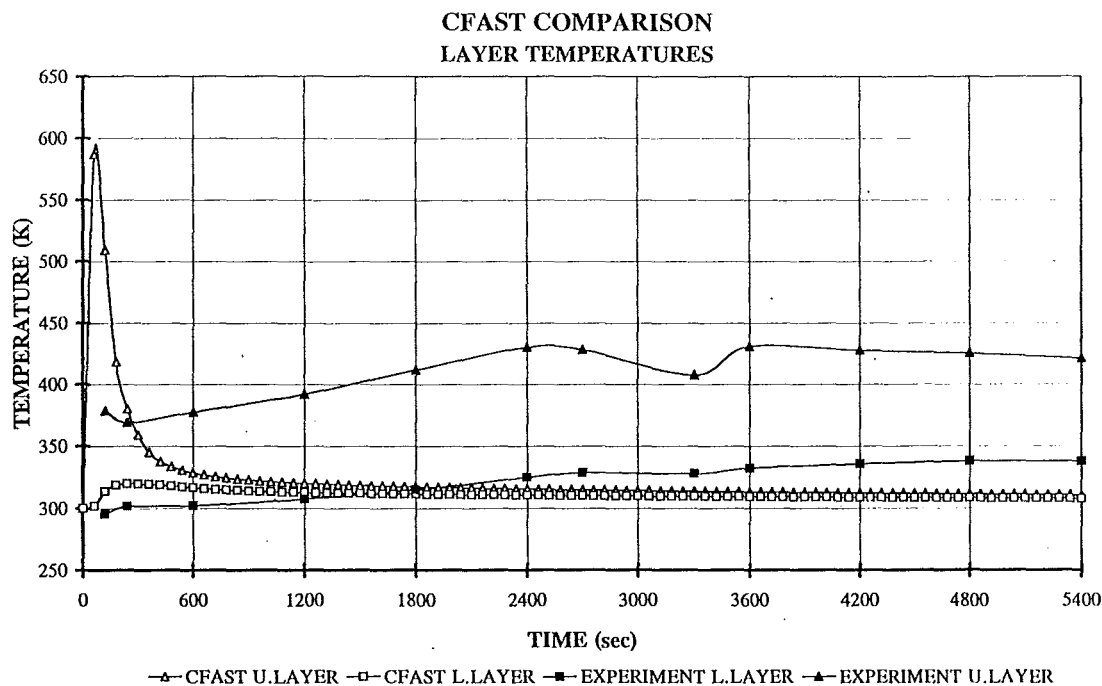


Figure 9.3 Comparison of layer temperatures in scenario 7.

9.1.3. INTERFACE HEIGHTS

CFAST layer prediction for scenarios 2,3 and 4 were identical to the two zone approximation of Quintiere et al. CFAST estimates of scenarios 5,6 and 7 were too high by roughly 0.5m. This suggests that CFAST layer estimation is not accurate under low ventilation when the fuel source is raised significantly off the ground.

9.1.4. MASS FLOWS

CFAST estimates for the mass flow in to the container follow the same shape but the magnitudes are significantly less than those calculated from the experiments.

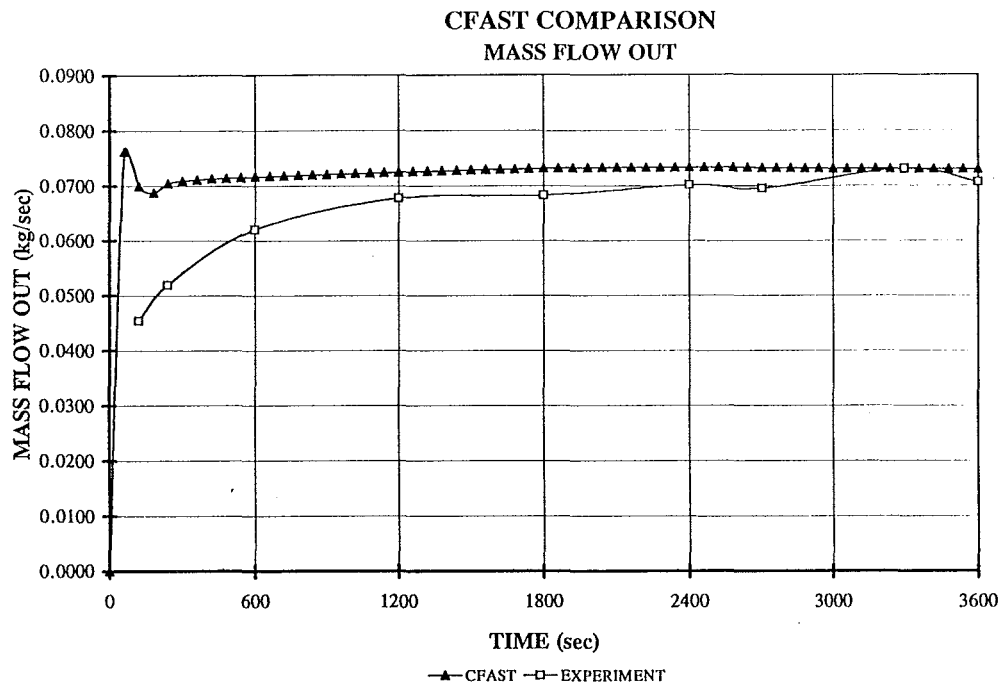


Figure 9.4 Comparison of mass flow out in scenario 2.

Mass flows out in scenarios 2,3,4 and 5 fluctuated between over and underestimating with the first 5min always overestimating. The magnitude of difference was not high. Figure 11.5 shows the typical level of accuracy.

Mass flows out of scenarios 6 and 7 were in poor comparison. They followed the same shape but the magnitude was a significant underestimate of the calculated experimental result. This may stem from the inaccurate prediction of the upper layer temperature. The reduced upper layer temperature would affect the gas density and thus the pressure difference, finally resulting in an underestimated mass flow. In the early stages of comparisons 6 and 7 CFAST predicted that the layer is above the top vent thus no flow out occurs (during this time the mass flow in as at a peak).

9.1.5. OXYGEN CONCENTRATION HISTORY

In every simulation CFAST underestimated the oxygen in the upper layer. Figure 9.5 shows the typical correlation

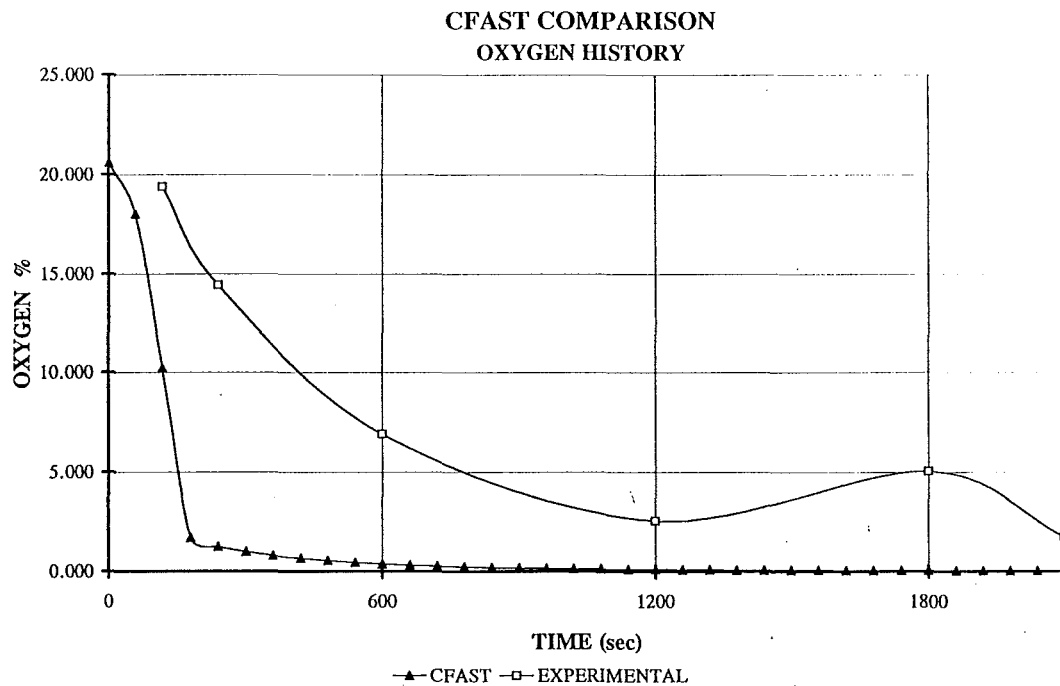


Figure 9.5 Oxygen history for scenario 4.

10. CONCLUSIONS.

The experimental program carried out in this report highlights the difficulty in analysis of full scale low ventilation experiments. To obtain a more comprehensive understanding of the behaviour in a low ventilated compartment fire, a full gas analysis is required. As seen by the build up on the window, droplet form of pyrolozates are lost in the container during experiments which makes an accurate gas analysis difficult to complete.

Subject to the conditions of experiment 6 and without the addition of any externally applied energy, a smoke explosion occurred. Further research is required to gain a quantitative understanding of the phenomena.

The comparisons made with CFAST, (upper and lower layer temperatures, layer height, oxygen concentration and mass flows) indicate that it is inadequate in coping with limited ventilation in single compartment simulations.

11. FUTURE RESEARCH

The experiments undertaken were limited in analysis of the gaseous products within the compartment. As mentioned within this report, these results will be difficult to ascertain. Further investigation into the phenomena of smoke explosions is necessary. The suggested conditions in developing an experimental set up should contain a pressure monitoring system that gives a more global result. Pressures at one location of the floor is inadequate. Future work should concentrate on incorporating instruments to measure the pressure difference at the vent directly.

Future research needs to look at the limitations of commonly used computer models such as CFAST. Due to the expense of full scale experiments it is recommended that prior investigation is carried out in a smaller scale.

12. REFERENCES

- Babrauskas, V. 1986 *Free Burning Fires*. Fire Safety Journal, 11 (1986) 33-51.
- Beyler, C. L. 1986 *Fire Plumes and Ceiling Jets*. Fire Safety Journal, Vol 11, 1986, pp 53-75
- Beyler, C L. *Major Species Production by Solid Fuels in a Two Layer Compartment Fire Environment*. Fire Safety Science, Proceedings of the First International Symposium. pp 431-441
- Butcher E. G., Clark J. J., Bedford, G. K. 1968 “*A fire test in which Furniture Was the Fuel,*” JFRO, Fire Research Note No 695, 1968.
- Chitty, R. 1993 *A Survey of Backdraft*. Fire Research and Development Group, FRDG Publication Number 5/94.
- Croft, M. 1980 *Fires involving explosions - a literature review*. The Journal of Fire Safety, 1980 3 (1) 3-24
- Drysdale, D. 1986 *An Introduction to Fire Dynamics*. A Wiley-Interscience publication. U.K 1986
- Emmons, H. W. 1988 *Vent Flows*. The SFPE Handbook of Fire Protection Engineering. Chapter 1-8.
- FEDG. 1994 *Fire Engineering Design Guide*. Centre for Advanced Engineering, University of Canterbury, April 1994.
- Fleischmann 1993. *Backdraft Phenomena*. NIST-GCR-94-646.
- FMS 1991 *Loss Prevention Data*. Factory Mutual System 1991. Damage Limiting Construction 1-44

- Habibullah, A. Wilson, E.L. *SAP90 Users Manual*. Computer & Structures Inc. 1989.
- Harmathy, T Z. 1981 *Some Overlooked Aspects of The Severity of Compartment Fires*. Fire Safety Journal, Vol 3, 1981, pp 261-273.
- Harmathy, T Z 1972 *A New Look at Compartment Fires. Part I*, Fire Technology Vol 8, No3 Aug 1972, pp 196-217.
- Hertzberg, M 1982. *The flammability limits of gases, vapors and dusts: Theory and experiments*. Fuel-air explosions. University of Waterloo Press, 3
- McHaffey, J. R. 1991. Development of Fire Endurance Models for Wood Stud Walls - Progress Report. Forintek Canada Corporation.
- NFPA 68 1988, *Guide for Venting of Deflagrations*, National Fire Protection Association.
- Nilsson, L. 1974. *Time curve of Heat Release for Compartment Fires with Fuel of Wooden Cribs*. Lund Institute of Technology, Lund, Sweden. Bulletin 36.
- NIST 1993. *CFAST, the Consolidated Model of Fire Growth and Smoke Transport*. NIST Technical Note 1299.
- Quintiere, J G. Steckler, K. Corley, D 1984. *An Assessment of Fire Induced Flows in Compartments*. Fire Science & Technology, Vol 4, no1, 1-14, 1984.
- Savilonis, B. Richards, R 1988. *Survey and Evaluation of Existing Smoke Movement Models*. Fire Safety Journal, 13 (1988) 87-97.
- SCHOTT. *PYRAN Fire-resisting Glass*. SCHOTT Product Information Handbook.
- Servomex 1994. *540A Oxygen Analyser Instruction manual*.

Sterner, E. Wickstrom, U 1990. *TASEF Temperature Analysis of Structures Exposed to Fire - User's Manual*. Fire Technology SR Report

Szilardo, R. *Theory of plates, elastic and numerical methods*.

Tewarson, A 1988. *Generation of Heat and Chemical Compounds in Fires*. Section 1/Chapter 13. SFPE Handbook.

Tewarson, A. 1984 *Fully developed Enclosure Fires of wood cribs*. Twentieth Symposium (International) on Combustion/ The Combustion Institute, 1984/ pp 1555-1566.

Thomas 1994. *Light Timber Framed Walls Exposed To Compartment Fires*. University of Canterbury, Christchurch, New Zealand. To be published

Vogel's 1978. *Textbook of Quantitative Inorganic Analysis*. Fourth Edition

Wormald 1993. *Passive Fire Protection*. Handbook

Zalosh R.G., 1988, *Explosion Protection* The SFPE Handbook of Fire Protection Engineering. Section 2/Chapter 5

13. BIBLIOGRAPHY

Backdraft: *A horrible Reality that Kills or Maims in Seconds*, Fire Fighting in Canada, 4-5, April-May, 1980

Craig, J. M. 1988 *Fire Ventilation, Where do we go from here ?* Fire Command, 12-15, December 1988.

Ohlemiller, T J. *Smoldering Combustion Propagation on Solid Wood*. Fire Safety Science, Proceedings of the Third International Symposium. pp 565-575

Quintiere, J G. Steckler, K. Corley, D. *An Assessment of Fire Induced Flows in Compartments*. Fire Science & Technology, Vol 4, no1, 1-14, 1984.

Rocket, R A. *Fire Induced Gas Flow in an Enclosure*. Combustion Science and Technology 12, (1976) 165-175.

Russel, D 1983. *Seven Fire Fighters Caught In Explosion*, Fire Engineering, 22-23, April, 1983.

Steckler, K D . Quintiere, J G . Rinkinen, W J . *Flow Induced by Fire in a Compartment*. National Bureau of Standards. NBSIR 82-2520. September 1982.

Takeda, H. *A Trial of Flashover Prediction in Compartment Fire Modelling*. Fire Science & Technology, Vol 7, No 1, 1987, pp 15-23

Tewarson, A. Steciak, J. *Fire Ventilation*. Combustion & Flame, Vol 53, pp 123-134, Nov 1983.

Thomas, P H. *Two-Dimensional Smoke Flows from Fires in Compartments: Some Engineering Relationships*. Fire Safety Journal 18 (1992) No2 125-137.

Thomas, P H . *On Fire Flames out of Vertical Openings*. Lund Institute. 1986.

APPENDIX A

CONTAINER SPECIFICATIONS

3 MATERIALS

All materials used in construction of the containers will be of the best quality and conform to British Standards (BS).

Certification to be produced as requested.

Material List of Main Components

Parts		Materials	
1	Bottom side rail	BS 4360 50B	
2	Cross member	Structure steel;	
3	Top Plate, forkpocket	Tensile strength	50kg/sq mm
4	Bottom plate, forkpocket	Yield point	29kg/sq mm
5	Front Header		
6	Header extension plates		
7	Front sill		
8	Front corner post		
9	Rear header		
10	Rear sill		
11	Rear (door) corner post, outer		
12	Floor Support Strip	BS 4360 43A	
13	Floor top-hat section	Structure steel;	
14	Gusset plate, base	Tensile strength	41kg/sq mm
15	Top side rail	Yield point;	25kg/sq mm
16	Roof protection plates		
17	Roof panels	CORTEN A	
18	Side-end panels	Superior atmospheric corrosion resisting rolled steel	
19	End-wall panels	Tensile strength	49kg/sq mm
20	Door panels	Yield point	35kg/sq mm
21	Door horizontal edge member		
22	Door centreline edge vertical member		
23	Gasket retainer	BS 304 Stainless steel: 2 mm thickness	
24	Rear (door) corner post, inner	BS 436050B High-tensile steel:	
		Tensile strength	50kg/sq mm
		Yield point	37kg/sq mm

Parts	Materials
25 Door hinge edge vertical member	ASTM A500-80 Carbon steel tube: Tensile strength: 41kg/sq mm Yield point: 21kg/sq mm
26 Door hinge	BS 060A25 Carbon steel forging Tensile strength: 45kg/sq mm Yield point: 27kg/sq mm
27 Door looking bar	Carbon steel pipe
28 Corner fittings	BS 592 Grade B Carbon steel casting: Tensile Strength: 49kg/sq mm Yield point: 28kg/sq mm
29 Flooring	Apitong or Keruing Plywood Specific gravity: 0.65-0.85 Thickness: 28 mm Plies: 18 minimum Moisture content: 12%-14%
30 Door gasket	Double lip seal type Material EPDM
31 Hinge pin	BS 304 S15 18-8 stainless steel Tensile strength: 52kg/sq mm
32 Marking plate	BS 304 Stainless Steel: 0.8 mm thick
33 Marking decals	Film: Cast vinyl Adhesive: Pressure sensitive low-temperature
34 Ventilator	ABS Resin: Two ventilators per container
35 Door locking gear	Bloxwich "BS-2555 Modified" bolt-on

4 CONSTRUCTION

4.1 General

The container frame will be constructed from steel sections, vertically corrugated steel side walls and end wall, corrugated steel roof and doors, assembled by means of automatic and semi-automatic MIG welding.

The welding of all outside parts of the construction as well as the base structure will be continuous and of full penetration to ensure strength and weatherproofness. All welding processes must be approved by the authorised Classification Society.

One pair of forkpockets is provided.

A wooden floor is laid on the crossmembers of the base structure.

Double wing type doors each fitted with four (4) hinges are installed at the rear end of the container.

4.2 Corner Fittings

Corner fittings are welded at the top and bottom of each corner of the container.

Corner fittings will be designed in accordance with ISO 1161 and UIC standards: The manufacturer must be approved by the authorised Classification Society.

The lower faces of the bottom side rails will be 12 mm above the plane of the lower faces of the bottom corner fittings. All the transverse members in the base of the container will be 17 mm above the plane of the lower faces of the bottom corner fittings. The highest point of the roof will be 6 mm below the plane of the upper face of the top corner fittings.

The side and end faces of the top and bottom corner fittings will protrude beyond vertical outer surfaces of the corner posts by 3 mm.

4.3 Base Structure

Base structure will be an all-welded construction, consisting of two bottom side rails, cross members and one pair of forkpockets.

- 4.3.1 Each bottom side rail will be constructed from 162 x 50 x 30 x 4.5 mm thick steel press-formed channel. The bottom flange will face outward and is reinforced underneath at both ends with a 3.0 mm thick angled steel plate. Additionally, a 4.5 mm thick gusset plate will be welded at each end of bottom side rails to the vertical webs, horizontal flanges and corner fitting. A doubler of 4 mm steel angle will be fully welded to the bottom side-rail above the mouth of each fork pocket and extend 50 mm on either side of the pocket mouth.

4.3.2 Cross members will be made of 4.0 mm steel press - formed channel. The edges of the channel will face towards the door end of the container. (See also Section 4.9.3).

4.3.3 Each forkpocket will be formed as a welded assembly of:

- Two (2) 4.0 mm steel side channels (cross members),
- Four (4) 6.0 mm bottom plates
- One (1) 4.0 mm top plate

4.4 **Front End Structure**

The front end structure will consist of front sill, front header, two front corner posts, four corner fittings and one end wall.

4.4.1 The front sill will be a 4.0 mm steel open-section pressing with 3 mm ribs for reinforcement. Cut-outs of 60 x 200 mm will be made in the lower flange of the sill adjacent to the corner castings at the edge of the cut-out will be reinforced with 10 mm plate.

4.4.2 The front header will be formed by a 4 mm steel open - section pressing. A 4.0 mm steel, header extension plate will be welded to the front header. It will measure approximately 450 mm from the front face of the container and extend across the full roof width.

Corner protection plates of 3 mm steel, approximately 350 x 350 mm will closely surround each corner casting on two sides and be fully welded to the header extension plate and the corner casting.

4.4.3 Each front corner post will be a 6.0 mm steel pressing to ensure suitable strength, light weight and easy maintenance.

4.4.4 The inside corner of the top front corner fittings will be rounded off with a radius of approximately 20 mm.

4.4.5 The front end wall be composed of two (2) or three (3) 2.0 mm Corten A steel panels vertically corrugated to trapezium sections of the standard pattern shown on the attached General Arrangement Drawing. Individual panels will be butt-welded together by automatic MIG welding to form the end wall. The end wall will be attached to the header and will by fillet welding, and to the corner posts by seam welding on the outer face and by stitch welding on the inner face. The panel edge between the stitch welds will be sealed to the structure, after painting, with a bead of grey butyl sealant.

4.5 **Rear (Door) End Structure**

The rear end frame will consist of a door sill, door header, rear corner posts and four corner fittings.

- 4.5.1 The door sill will be constructed from 4.5 mm open-section steel pressing, with 3 mm ribs for reinforcement behind cam keepers. The top face of the door will be at the same level as the upper face of the wooden floor and will slant downward for easy drainage. Cut-outs of 60 x 200 mm will be made in the lower flange of the sill adjacent to the corner castings; the edge of the cut-out will be reinforced with 10 mm plate.
- 4.5.2 The door header will be constructed of a 4.0 mm U-section steel pressing and a 4.0 mm steel plate which are welded together to form a box member with reinforcing webs positioned behind each cam-keeper. The upper section will extend by approximately 450 mm from the extreme rear end as part of the roof. Corner protection plates of 3 mm steel, approximately 350 x 350 mm, will closely surround each corner casting on two sides and be fully welded to the header extension plate and the corner casting.
- 4.5.3 Each corner post will be constructed from a 6.0 mm steel outer pressing, and a rolled 40 x 113 x 10 mm thick inner steel channel to ensure maximum width of the door opening and suitable strength for stacking and racking forces. Eight (8) hinge pin lugs will be welded to the outer section of each corner post.

4.6 **Top Side Rails**

Each top side-rail will be a 50 x 12 mm solid rectangular steel bar.

4.7 **Side Walls**

The side walls be composed of five (5) or six (6) 1.6 mm Corten A steel panels vertically corrugated to trapezium sections. Individual panels will be butt welded together by automatic MIG welding to form one wall. One recessed area of 450 mm width will be provided at each end of each side wall for decal application. This area is formed as a shallow chevron corrugation for strength, and will have two standard corrugations between it and the end of the side-wall.

The side walls will be attached to the top rails and bottom side rails by continuous fillet welding, and to the corner posts by seam welding on the outer face and by stitch welding on the inner face. The panel edge between the stitch welds will be sealed to the structure, after painting, with a bead of grey butyl sealant.

4.8 **Roof**

- 4.8.1 The roof will be composed of five (5) 2.00 mm die-stamped corrugated Corten A steel panels 2.0 mm. Individual panels will be butt welded together by automatic MIG welding. There will be at least three corrugations on each panel, and each corrugation will not exceed 200 mm in width. After completion of the container the roof will show a positive camber of 8 mm measured at the container half-width in each trough of the corrugation.

- 4.8.2 The roof panel will be continuously welded to the top side rails and headers.
- 4.8.3 The peripheral clearance on the inside of the container, between roof sheet, and top rails and headers, will be caulked, with grey Butyl sealing compound, after completion of painting.

4.9 **Floor**

- 4.9.1 The wooden floor be made of 35 mm thick timber supported by one (1) hat-section centre spacer and steel floor support strips along the bottom side rails and sills. The flooring will be treated - as specified by the Australian Quarantine and Inspection Service - before assembly into the container.

The edges of each board will be sealed to prevent moisture entering the end grain.

- 4.9.2 All joints between each board and the perimeter of the floor will be sealed with Butyl sealant, but Neoprene will be used at the visual seam of the floor top surface, to give protection against water entry.
- 4.9.3 Individual panels will not exceed 2,430 mm in length and will cover at least six (6) spans, ie, seven (7) bearers.

Note Well

Where the joint between two floor panels fall on a crossbearer, that crossbearer will be modified C-section with return angle on the top flange.

- 4.9.4 The floor will be secured with zinc plated and passivated steel countersunk self-tapping screws of 8.0 mm dia. to the cross members and sills.
- 4.9.5 The heads of the floor screws will be countersunk below the level of the upper surface of the floor by 1.5 mm to 2.5 mm.

4.10 **Doors**

- 4.10.1 Each door will consist of a 2.0 mm corrugated Corten A steel panel welded to steel edge members. Weld joints will be caulked on the interior of the doors, with grey Butyl sealing compound, after completion of painting. The top and bottom edge members of the doors will be 4.5 mm Corten A steel C-section. The vertical edge member nearest the container centre line will be 4.0 mm Corten A steel rectangular hollow tube. The vertical edge member carrying the door hinges will be 4.0 mm steel rectangular hollow section. The lower position of each vertical edge member will be drilled with an 8 mm diameter drain hole.

- (a) Lashing points on the front and rear corner post - 1,000 kg each.

4.11 **Threshold Plate**

The flooring of the container will be protected by a threshold plate at the door end of the container. The plate will extend from the inner edge of the door sill to the first crossmember over the full width of the floor. The threshold plate will be 2 mm steel plate hot-dip galvanised and will be secured through the floor to sill and crossmember by M8 counter-sunk self tapping screws.

If an extended sill is offered in place of a threshold plate it shall extend at least 210 mm into the container and the edge of the floor shall be protected by a full-width 2 mm thick hot-dipped galvanised steel angle laid over the end of the flooring and secured through the flooring to the sill with M8 counter-sunk self tapping screws.

The galvanising thickness will be 50 microns minimum.

APPENDIX B

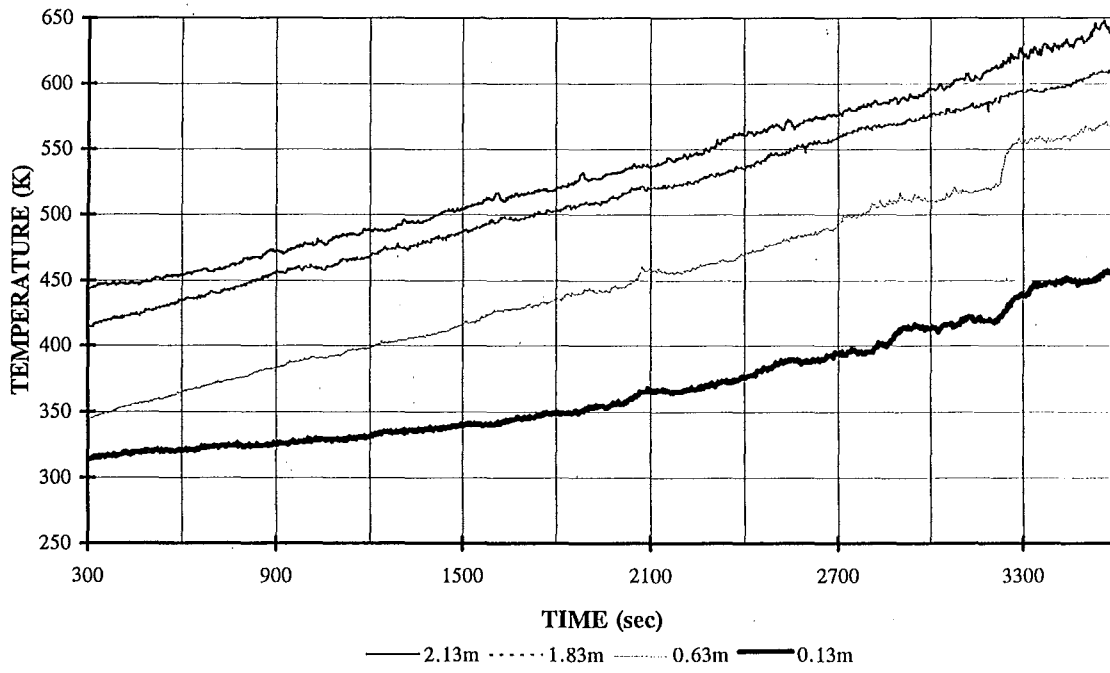
GRAPHS OF THE RESULTS FROM EXPERIMENTS 2 - 7

<u>EXPERIMENT</u>		NZP2E02
Vents (m ²)	top	0.0314
	bottom	0.0660
<u>WEATHER CONDITIONS</u>		
Relative Humidity (%)		80
Ambient Temperature (K)		288
Conditions		50 MPH, North Easterly, Overcast.
<u>WOOD</u>		
Moisture Content (%)		14
Weight of paper used for ignition (kg)		0.5
Weight of timber cribs (kg)		211.8
<u>EVENTS</u>		
Start Computer (s)		-60
Sparks on (s)		-5
LPG on (s)		0
LPG off (s)		15
Sparks off (s)		20
Sparkling procedure during test ¹ (time starts from when LPG on)		at 600s intervals for 10s duration
<u>OPENING</u> ²		3600s and again at 5400s

OBSERVATIONS AND IRREGULARITIES

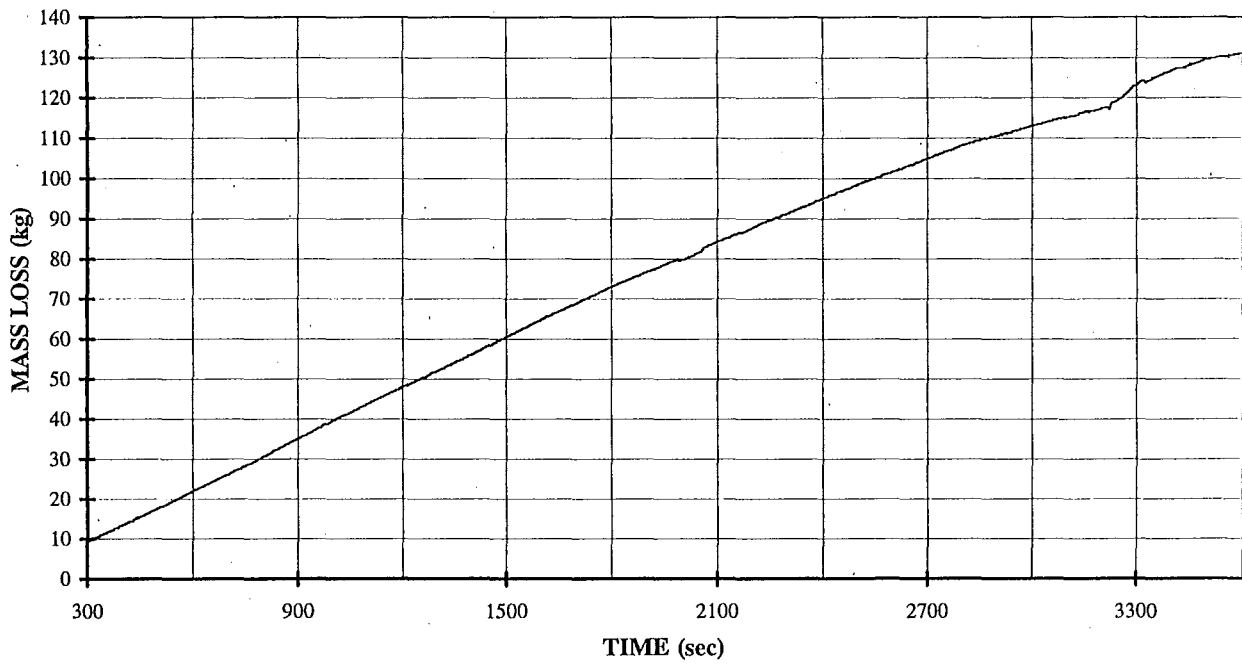
- Had leakage at top of pressure relief panel, right hand side of front vent(where Bi-Di probes are).
- Bottom vent had smoke pulsating,varying with wind intensity.
- At around the 1500s no water could be seen running down the window.
- ²Took approximately 60s to close hatch after first phase
- ²Second phase appeared to be producing cleaner smoke.
- ¹Sparked at 4260s not 4200s.

TEMPERATURE HISTORY - TC TREE DATA



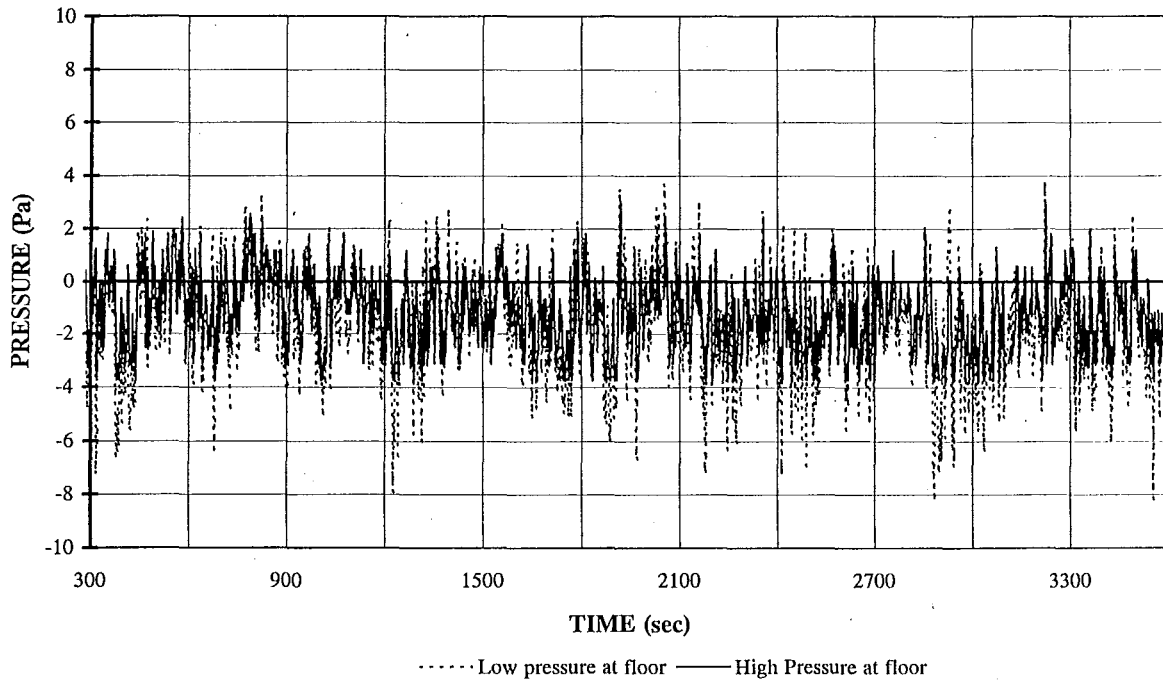
NZP2E02

MASS LOSS HISTORY



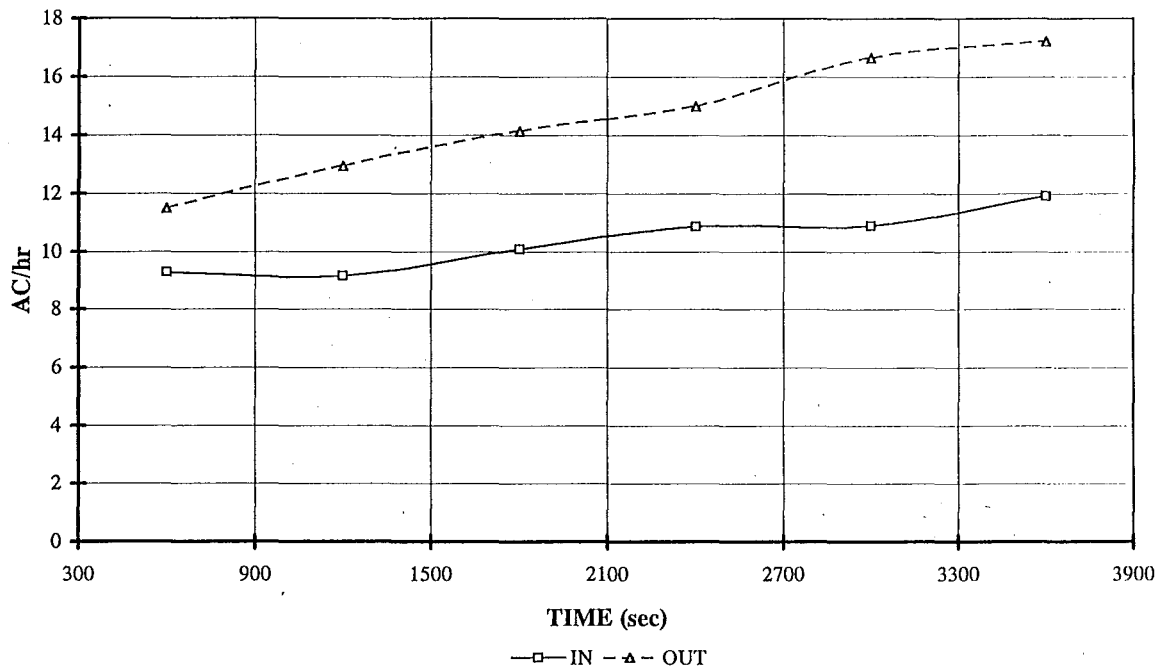
NZP2E02

COMPARTMENT PRESSURE HISTORY



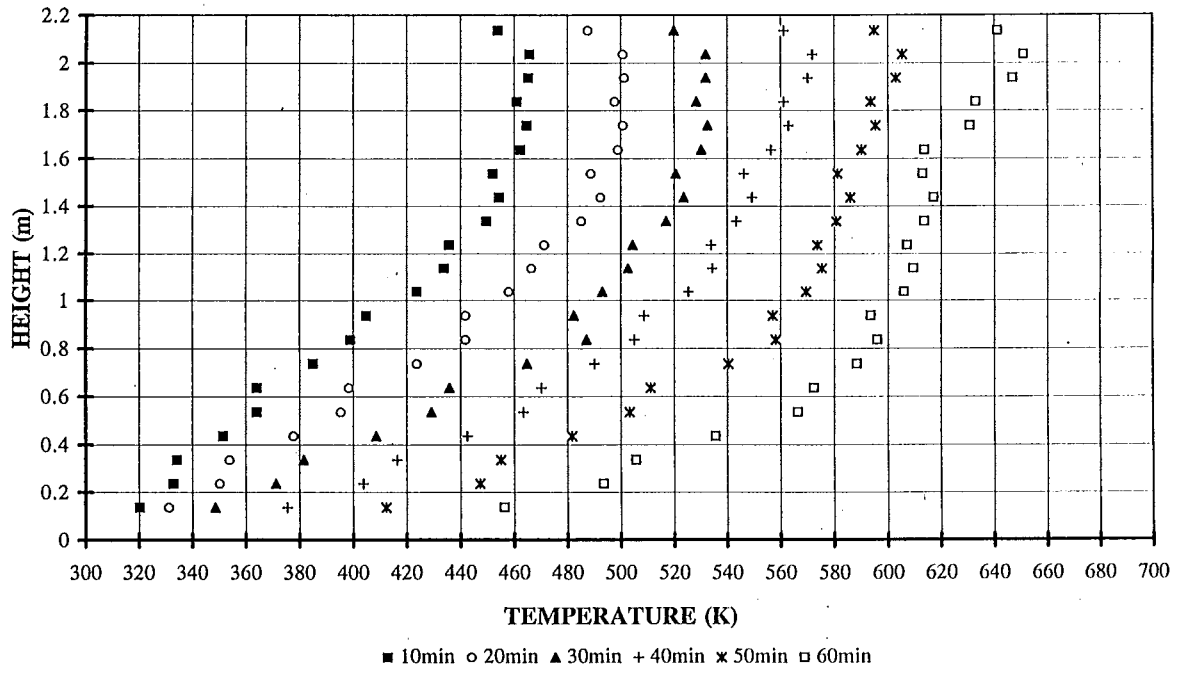
NZP2E02

COMPARTMENT FLOW HISTORY 10 MINUTE AVERAGES



NZP2E02

TEMPERATURE PROFILES

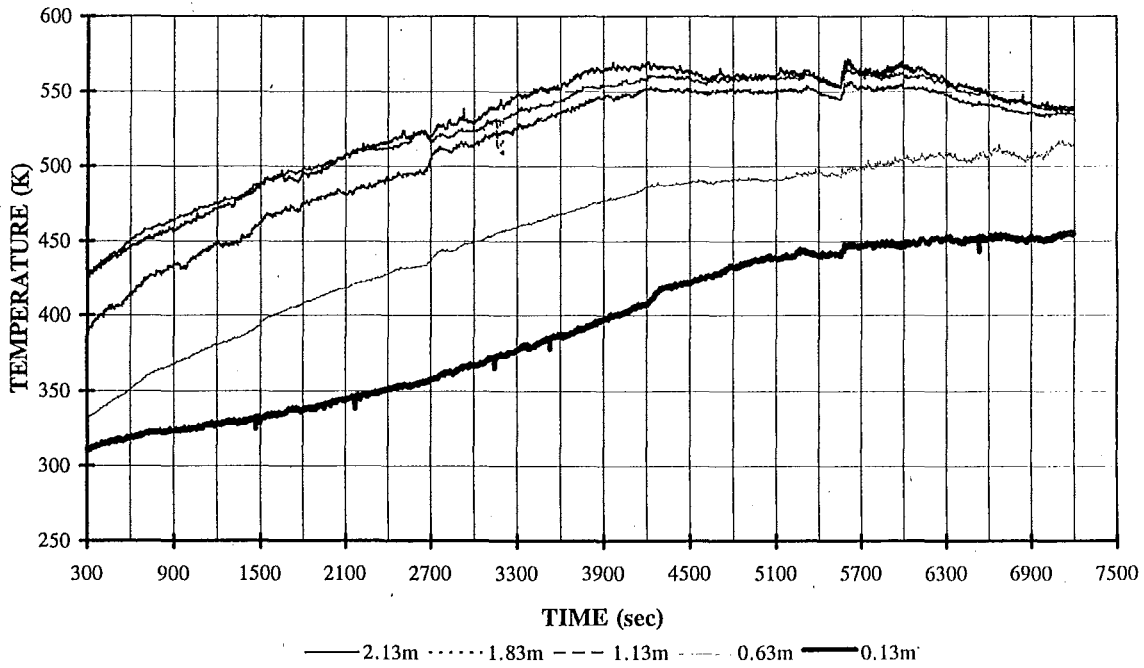


<u>EXPERIMENT</u>		NZP2E03
Vents (m ²)	top	0.0154
	bottom	0.0314
<u>WEATHER CONDITIONS</u>		
Relative Humidity (%)		50
Ambient Temperature (K)		293
Conditions ¹		5 MPH, Southerly.
<u>WOOD</u>		
Moisture Content (%)		15
Weight of paper used for ignition (kg)		2.1
Weight of timber cribs ²		221
<u>EVENTS</u>		
Start Computer (s)		-60
Sparks on (s)		-5
LPG on (s)		0
LPG off (s)		15
Sparks off (s)		20
Sparkling procedure during test ³ (time starts from when LPG on)		at 600s intervals for 10s duration
<u>OPENING</u>		7200s

OBSERVATIONS AND IRREGULARITIES

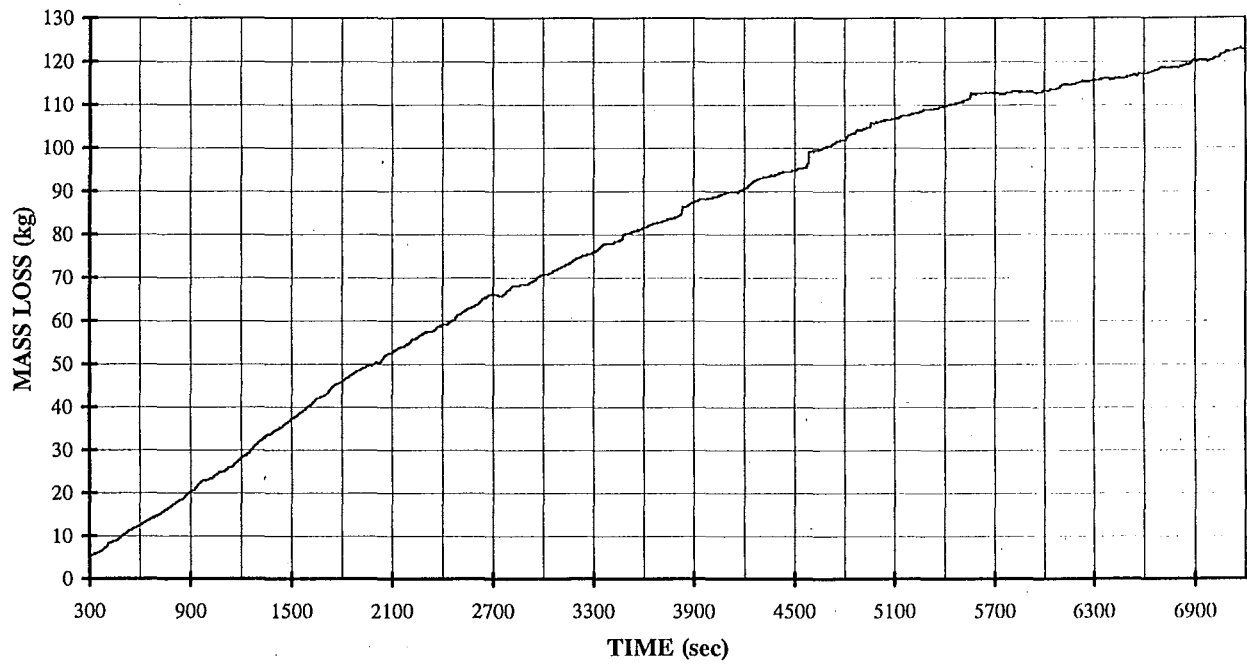
- Appeared that leakage was more severe.
- Had leakage at top of pressure relief panel, right hand side of front vent(where Bi-Di probes are).
- Bottom vent had smoke pulsating, varying with wind intensity.
- ¹At 4380s the wind direction changed to a North Easterly.
- ²At 4560s it sounded as if a crib dropped.
- ³Sparked for 10s after 360s.
- ³Missed 3600s spark, but sparked at 3900s.

TEMPERATURE HISTORY - TC TREE DATA



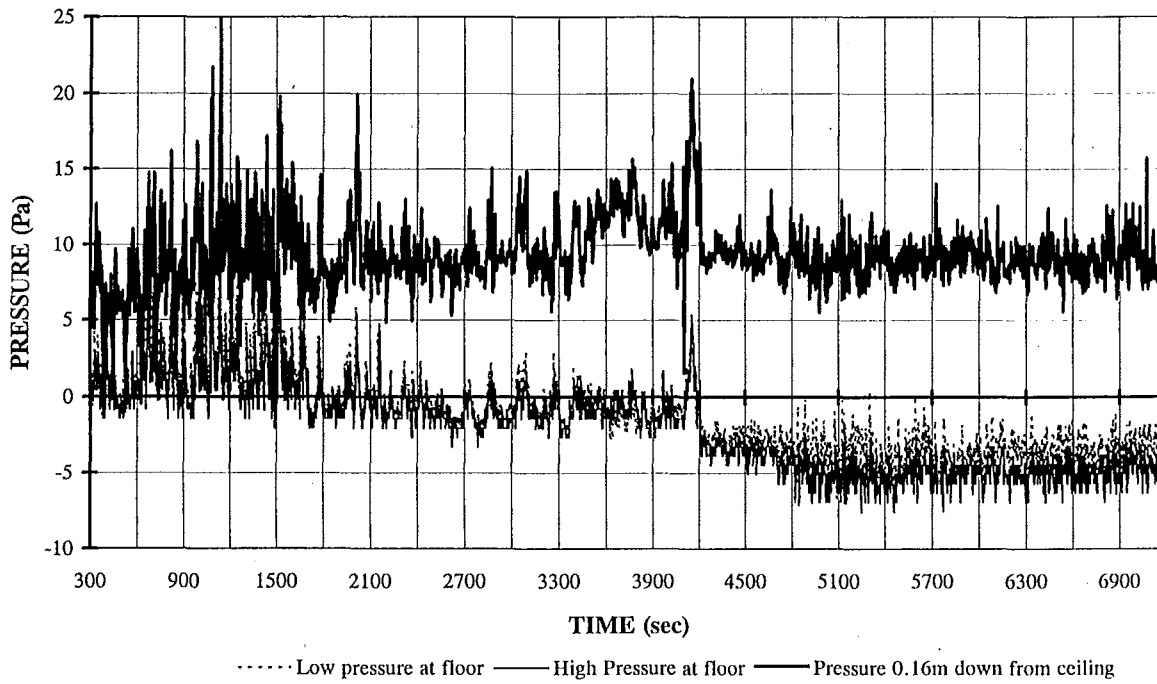
NZP2E03

MASS LOSS HISTORY



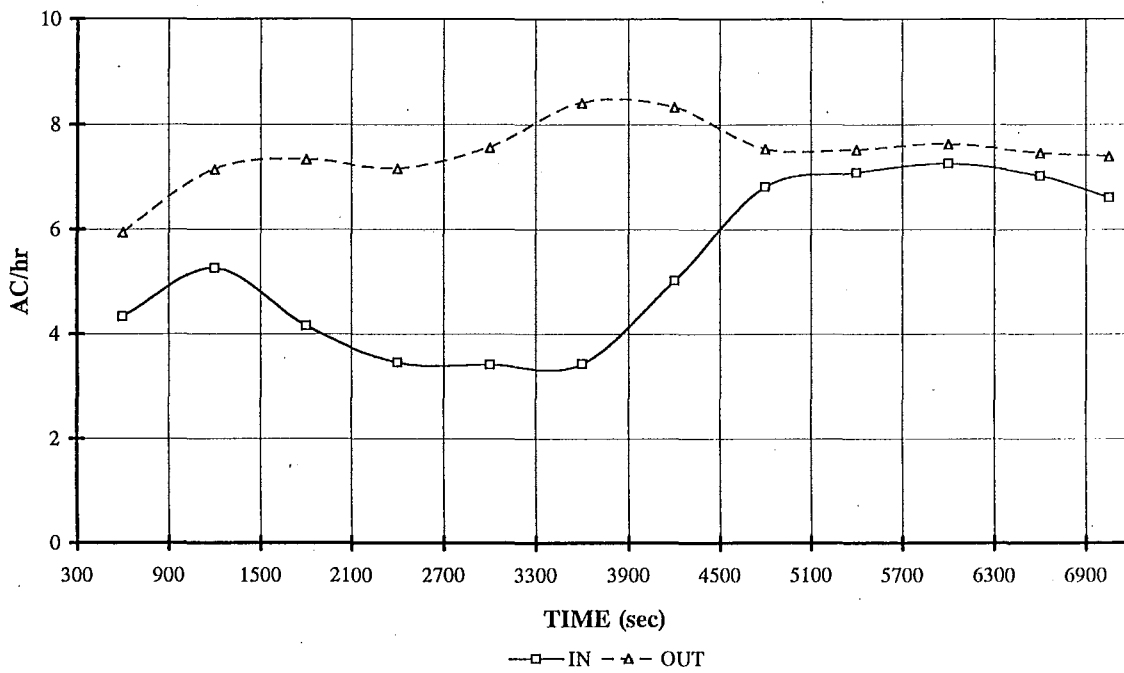
NZP2E03

COMPARTMENT PRESSURE HISTORY



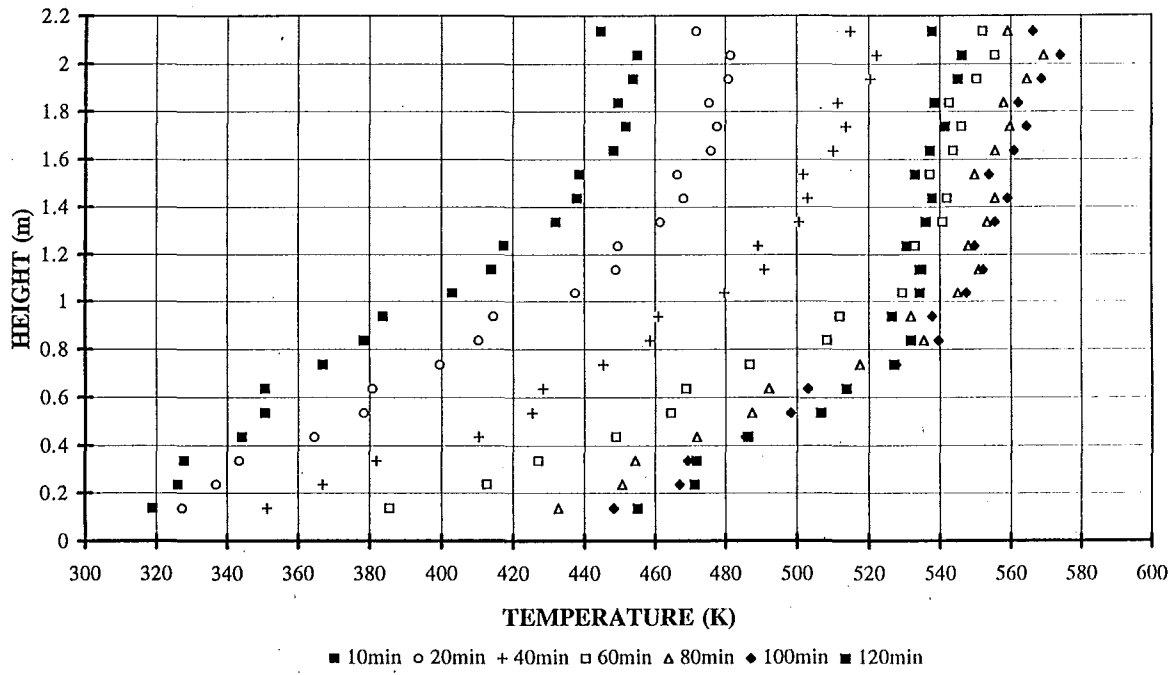
NZP2E03

COMPARTMENT FLOW HISTORY 10 MINUTE AVERAGES



NZP2E03

TEMPERATURE PROFILES

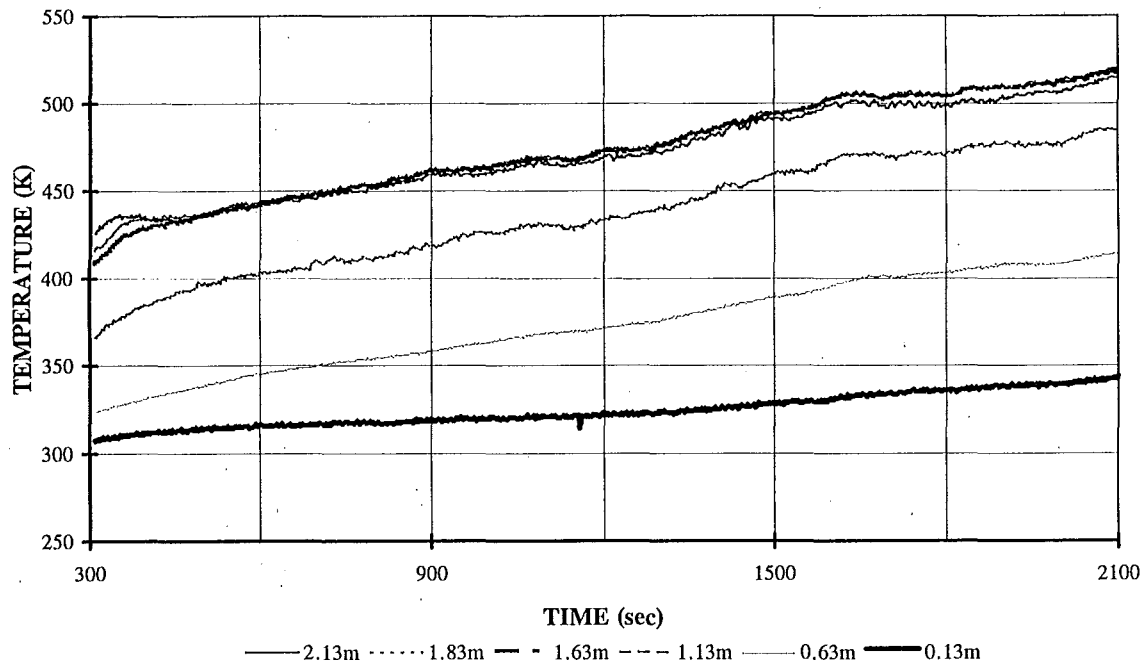


<u>EXPERIMENT</u>		NZP2E04
Vents (m ²)	top	0.0154
	bottom	0.0314
<u>WEATHER CONDITIONS</u>		
Relative Humidity (%)		72
Ambient Temperature (K)		291
Conditions ¹		5 MPH, South Westerly.
<u>WOOD</u>		
Moisture Content (%)		15
Weight of paper used for ignition (kg)		0.9
Weight of timber cribs (kg)		219.5
<u>EVENTS</u>		
Start Computer (s)		-60
Sparks on (s)		-5
LPG on (s)		0
LPG off (s)		30
Sparks off (s)		35
Sparking procedure during test (time starts from when LPG on)		at 600s intervals for 10s duration
<u>OPENING</u>		2100s, 3600s

OBSERVATIONS AND IRREGULARITIES

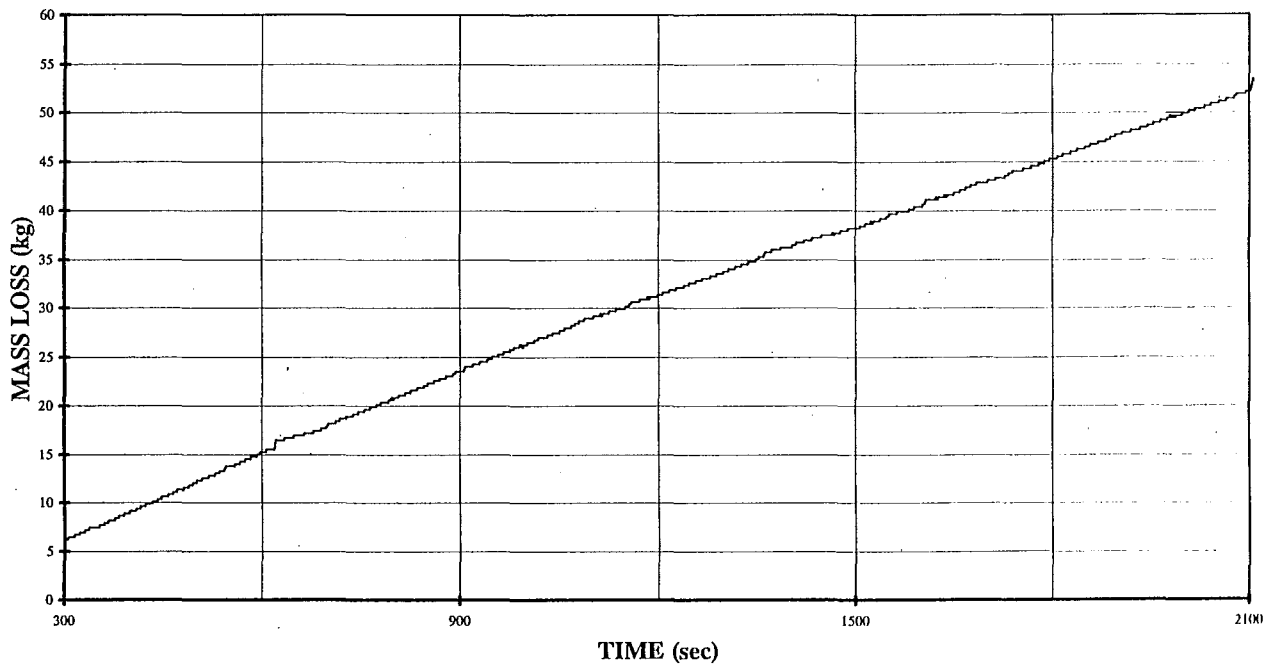
- ¹Wind direction was directly into the front end of the container
- Had leakage at top of pressure relief panel.
- ¹Wind started to increase after 1500s.
- Smoke possibly clearer, hard to be sure as wind may be diffusing it.
- Right hand crib burnt, left virtually untouched.

TEMPERATURE HISTORY - TC TREE DATA



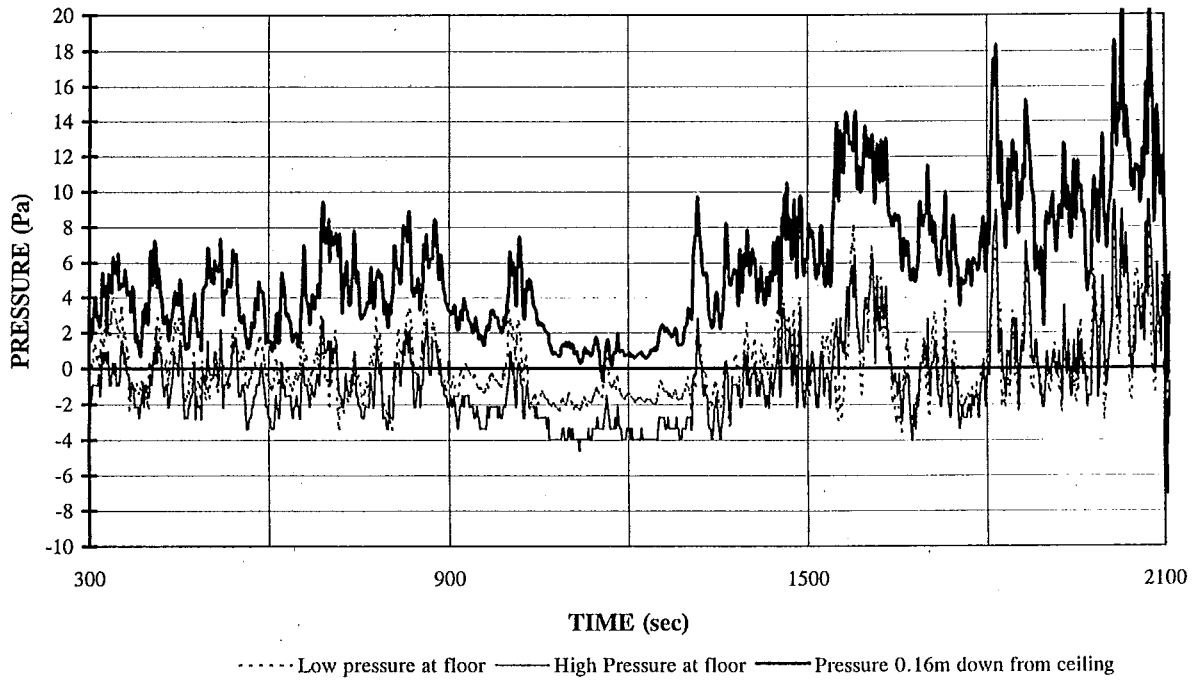
NZP2E04

MASS LOSS HISTORY



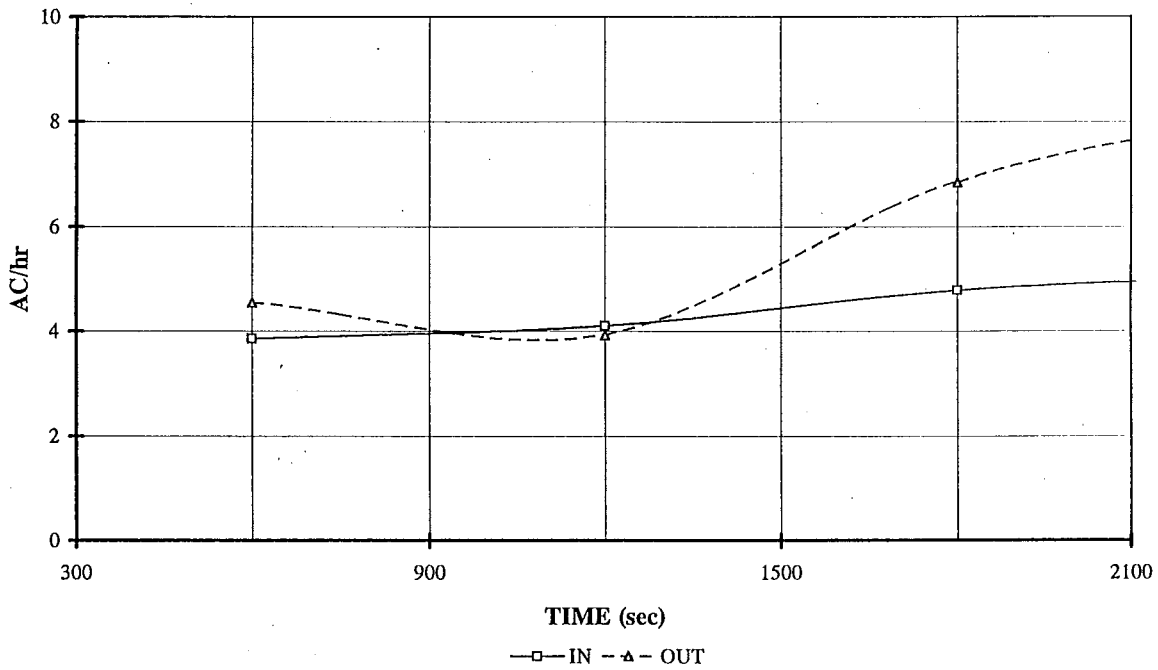
NZP2E04

COMPARTMENT PRESSURE HISTORY



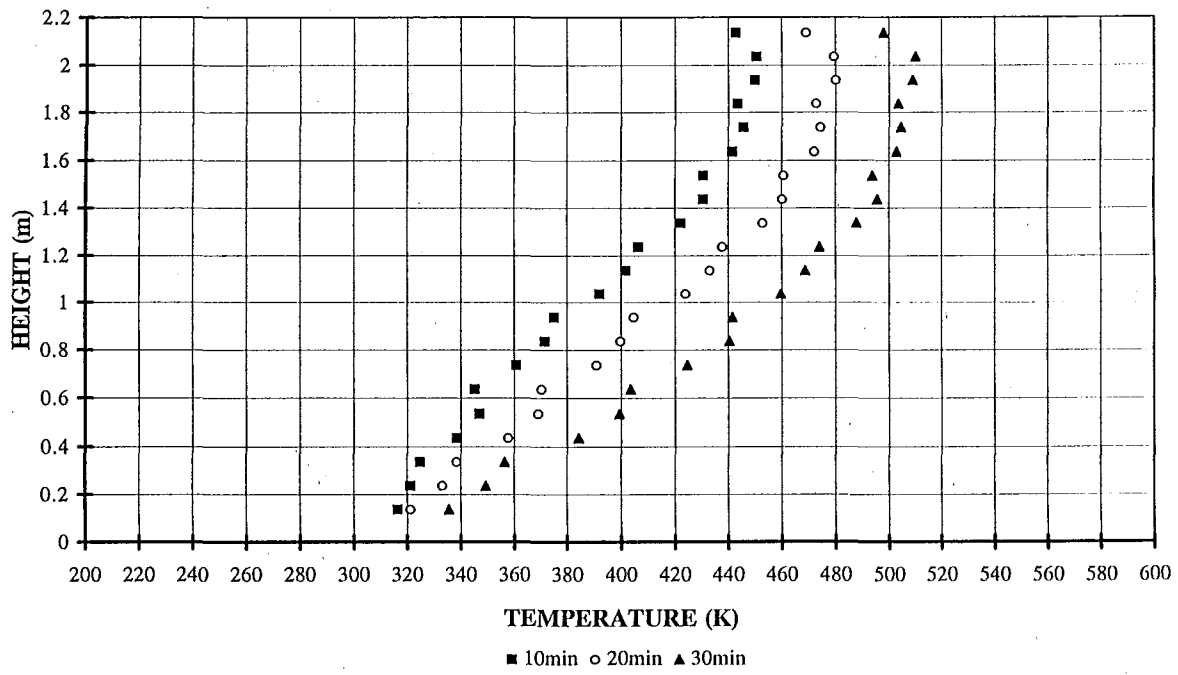
NZP2E04

COMPARTMENT FLOW HISTORY 10 MINUTE AVERAGES



NZP2E04

TEMPERATURE PROFILES

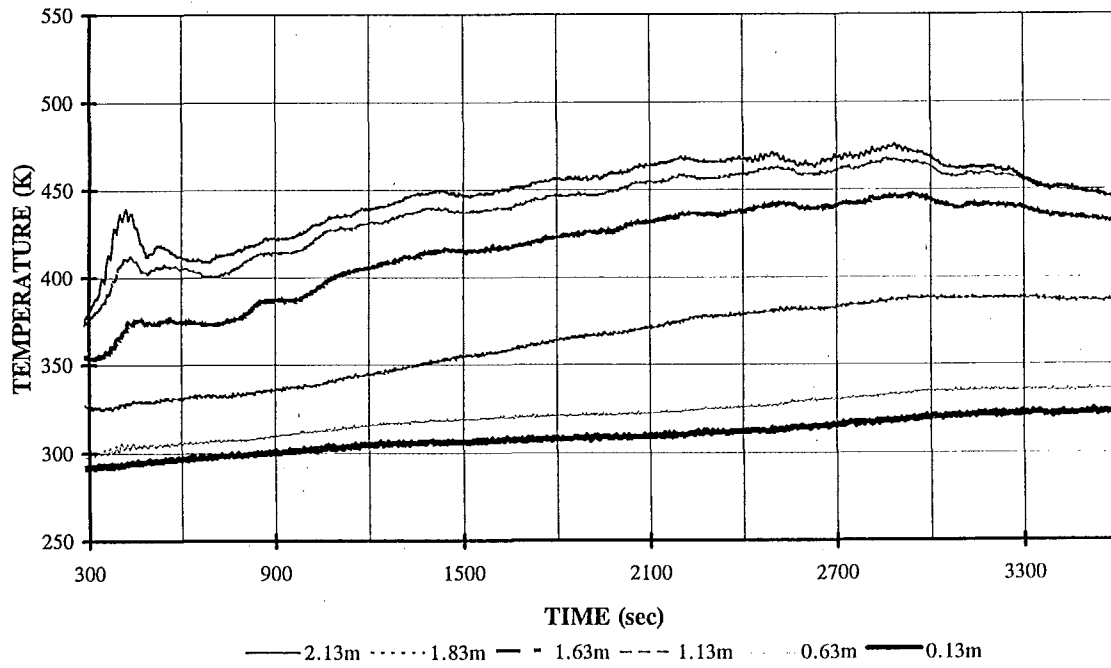


<u>EXPERIMENT</u>		NZP2E05
Vents (m ²)	top	0.0079
	bottom	0.0154
<u>WEATHER CONDITIONS</u>		
Relative Humidity (%)		62
Ambient Temperature (K)		288
Conditions		50 MPH, North Easterly.
<u>WOOD</u>		
Moisture Content (%)		14
Weight of paper used for ignition (kg)		1
Weight of timber cribs (kg)		161.1
<u>EVENTS</u>		
Start Computer (s)		-60
Sparks on (s)		-5
LPG on (s)		0
LPG off (s)		40
Sparks off (s)		40
Sparking procedure during test ¹ (time starts from when LPG on)		at 300s intervals for 10s duration
<u>OPENING</u> ²		3600s, then closed top vent and ran until 7200s

OBSERVATIONS AND IRREGULARITIES

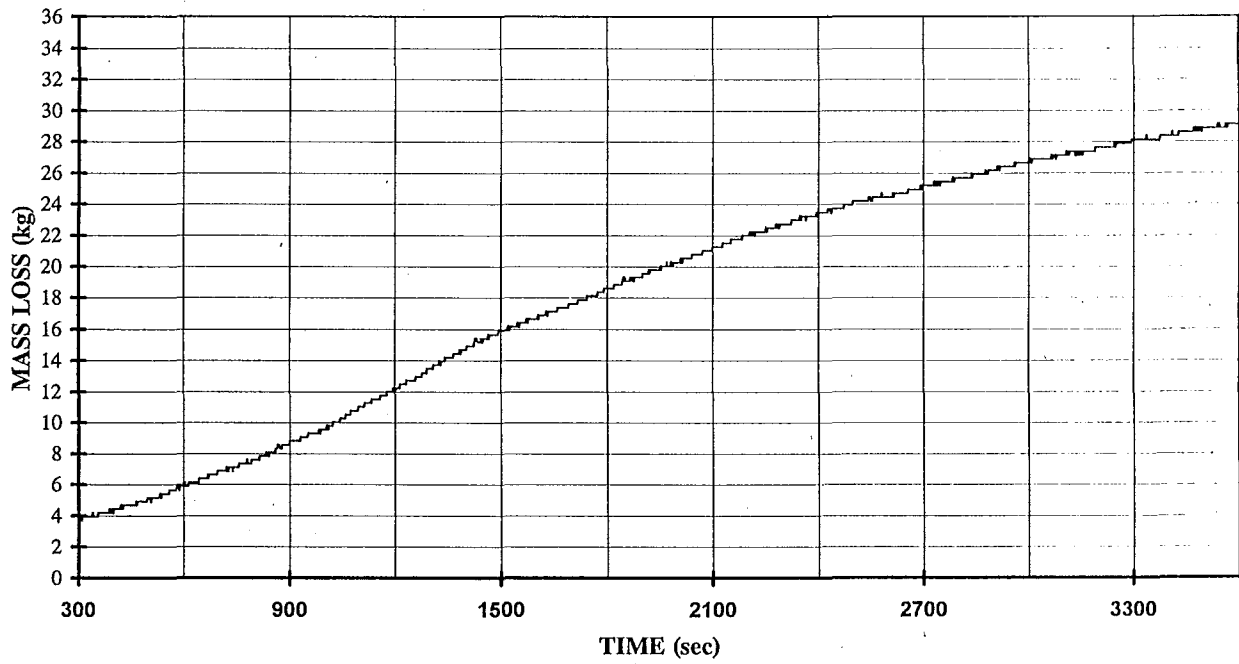
- Before the test we replaced the Kaowool completely around the pressure relief panel
- Not as much leakage as in the previous tests. May be due to lower internal pressure caused by low temperatures.
- Appeared if more water was coming off between 900s and 1200s.
- Felt as if more water produced than normal, possibly more efficient burning.
- ¹Missed 3000s spark.
- At 3300s the layer height was measured to be 880mm (350mm above top of box beam on window).
- ²After opening the door at 3600s, it was not closed again until 3720s.
- ¹Sparks in the second phase were operated at the following times for 10s, 3840s, 3690s, 4140s and then every 120s.
- Right hand crib burned, left was literally unaffected.

TEMPERATURE HISTORY - TC TREE DATA



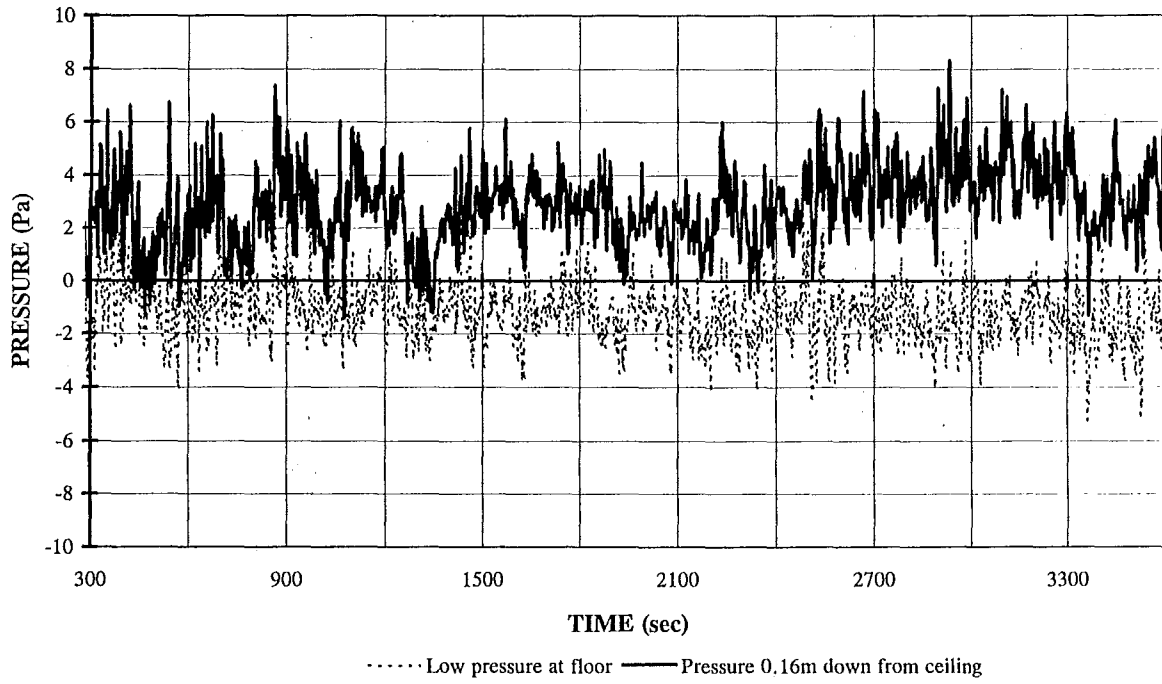
NZP2E05

MASS LOSS HISTORY



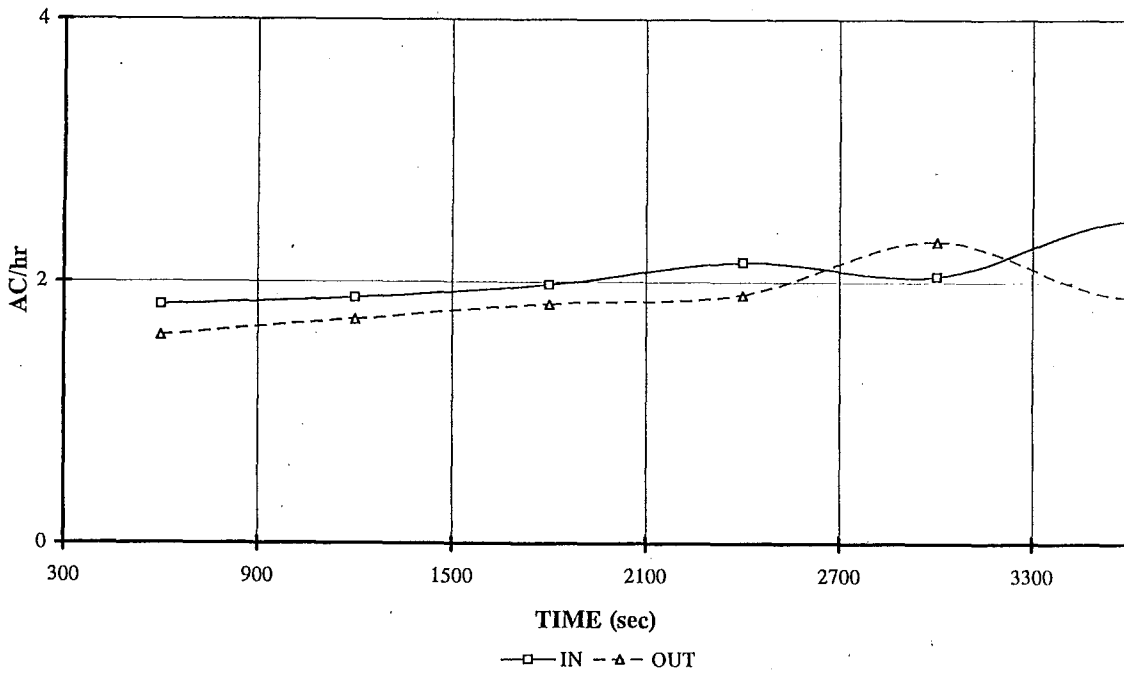
NZP2E05

COMPARTMENT PRESSURE HISTORY



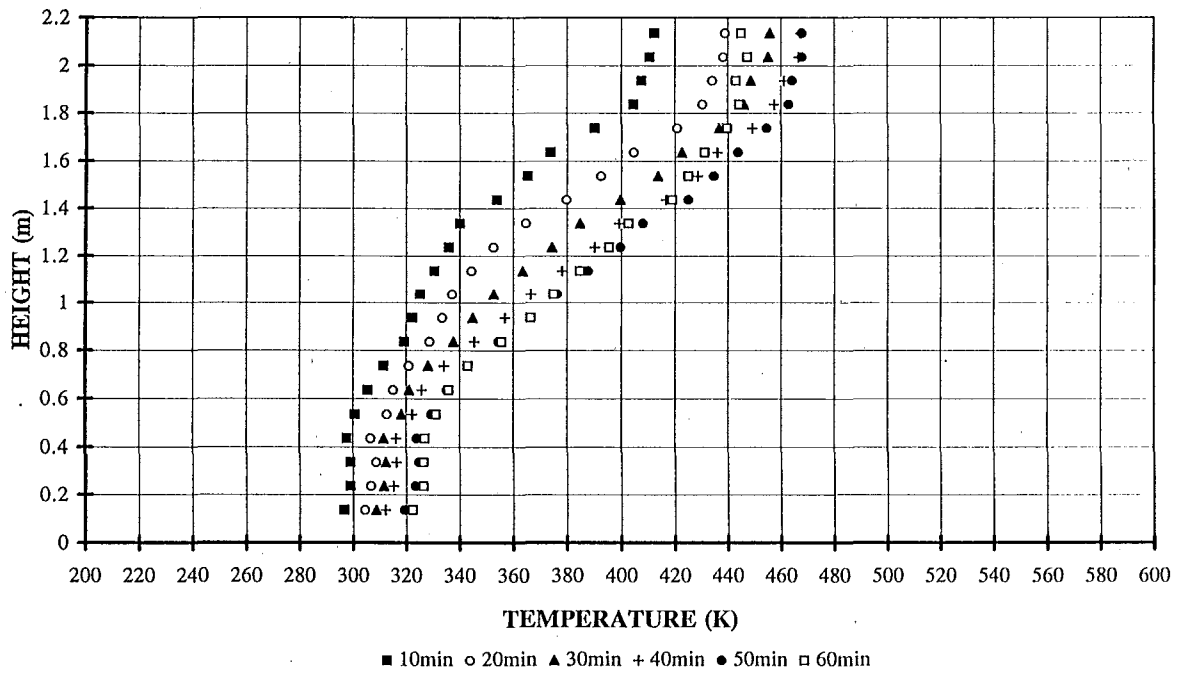
NZP2E05

COMPARTMENT FLOW HISTORY 10 MINUTE AVERAGES



NZP2E05

TEMPERATURE PROFILES

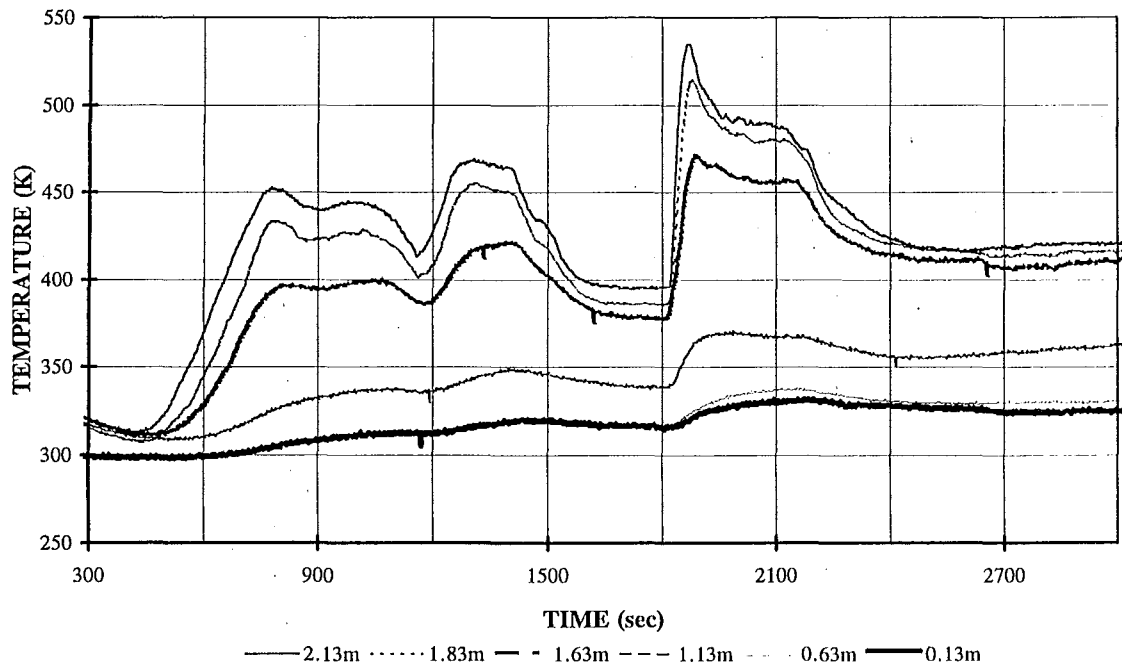


<u>EXPERIMENT</u>		NZP2E06
Vents (m ²)	top	0.0000
	central	0.0079
	bottom	0.0154
<u>WHEATHER CONDITIONS</u>		
Relative Humidity (%)		83
Ambient Temperature (K)		288
Conditions		50 MPH, North Easterly.
<u>WOOD</u>		
Moisture Content (%)		14
Weight of paper used for ignition (kg)		0.7
Weight of timber cribs (kg)		161.4
<u>EVENTS</u>		
Start Computer (s)		-60
Sparks on (s)		-5
LPG on (s)		0
LPG off (s)		15
Sparks off (s)		20
Sparking procedure during test ¹ (time starts from when LPG on)		at 300s intervals for 10s duration
<u>OPENING</u> ²		3020s, 7200s

OBSERVATIONS AND IRREGULARITIES

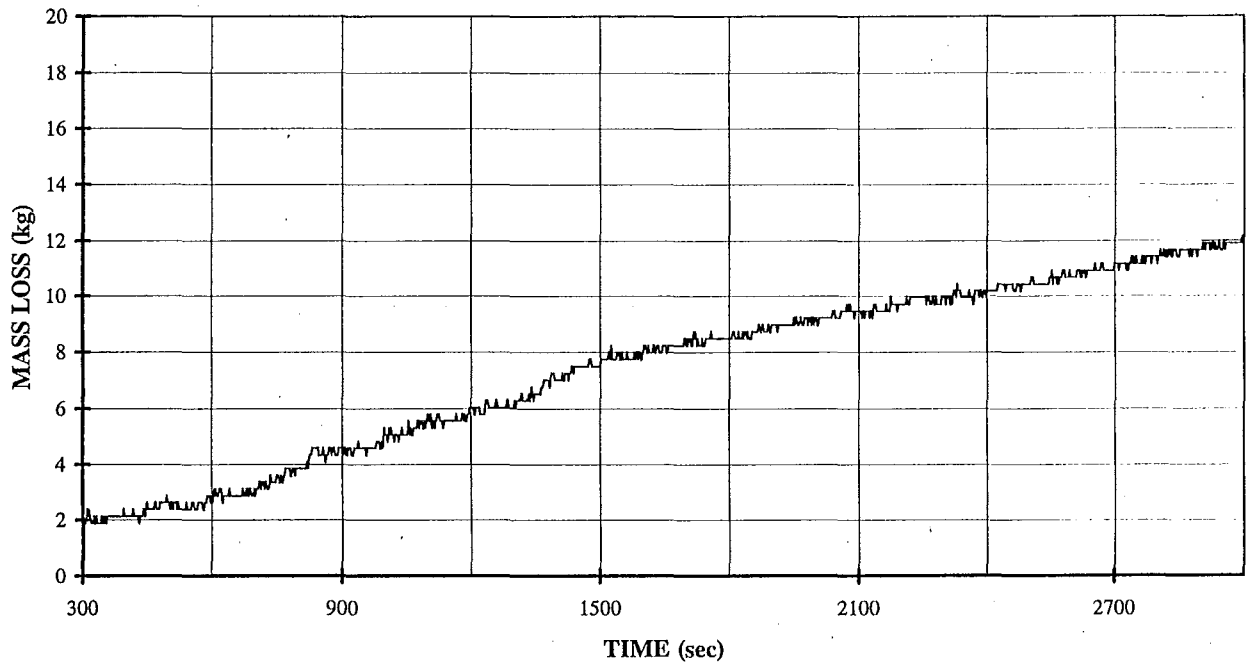
- The fire appeared to have gone out within the first 300s but it became steady again by around 600s.
- ¹First sparked at 900s.
- ¹Sparked at 2160s not 2100s.
- The layer height was measured to be 880mm (350mm above top of box beam on window) and a second layer at 1110mm(780mm above b.beam)
- ²After opening the door at the end of phase 1 it was left open for approxiametly 120s before closing to initiate phase 2.
- ¹After 3660s the sparks were left on continuously.
- At 4560s smoke began venting out leakage areas. It is thought that some of the gases may have ignited causing expansion of the gases.
- At 4920s the data acquisition was stopped and a new file (NZP2E06b) was started.
- Right hand crib burned, left was literally unaffected.

TEMPERATURE HISTORY - TC TREE DATA



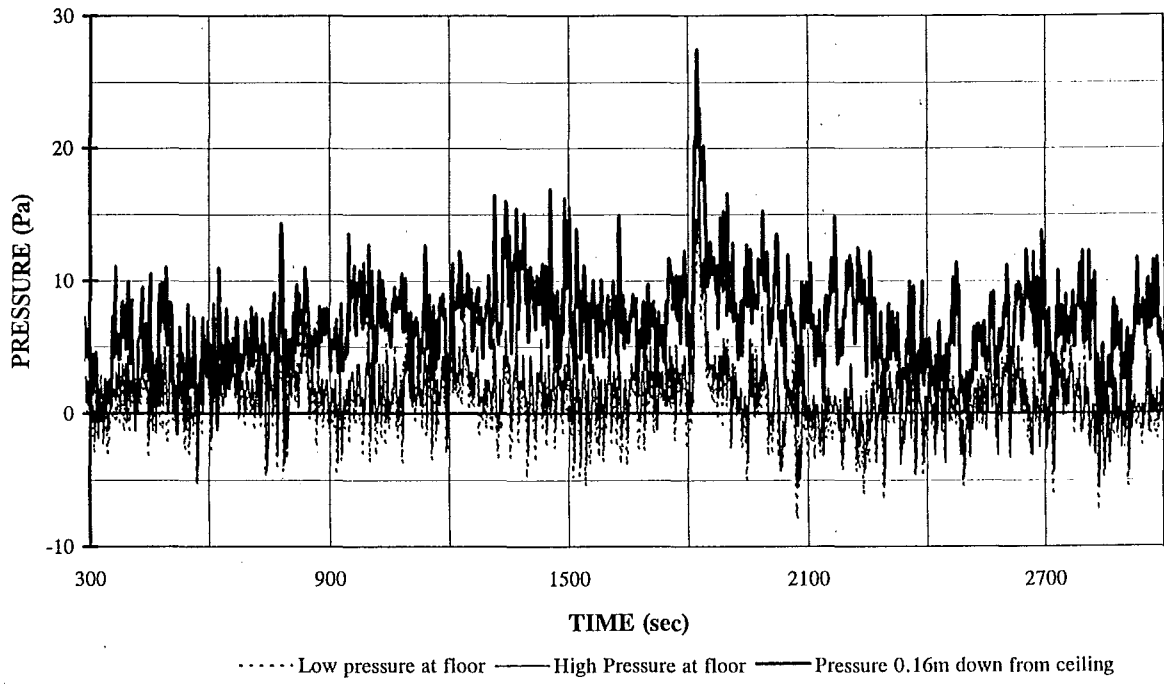
NZP2E06

MASS LOSS HISTORY



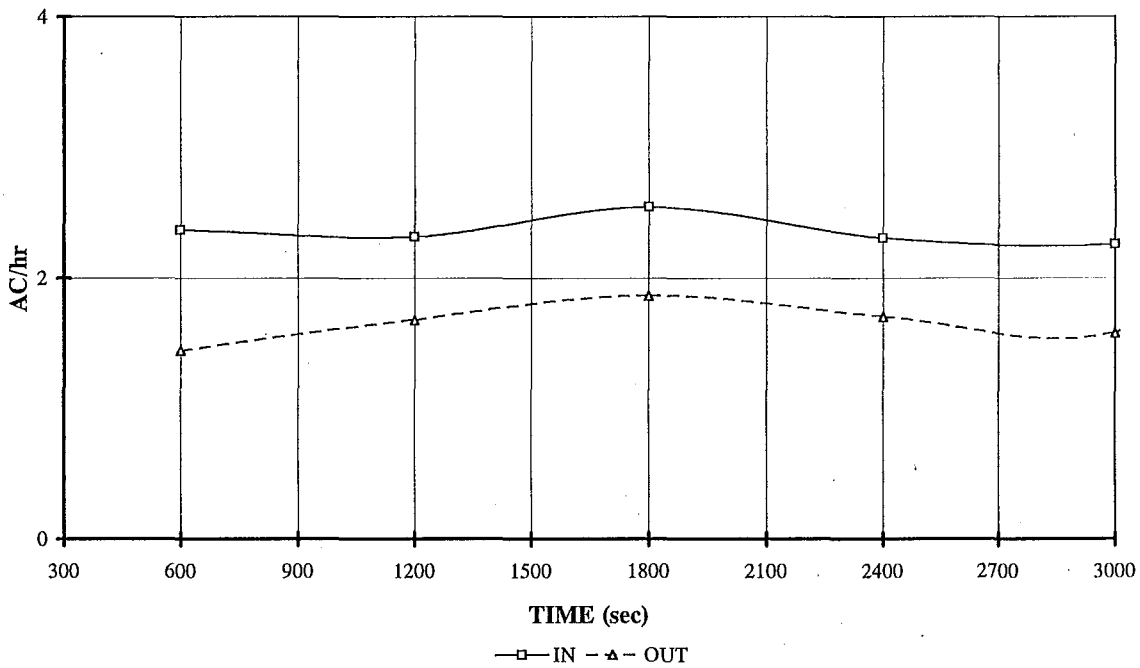
NZP2E06

COMPARTMENT PRESSURE HISTORY



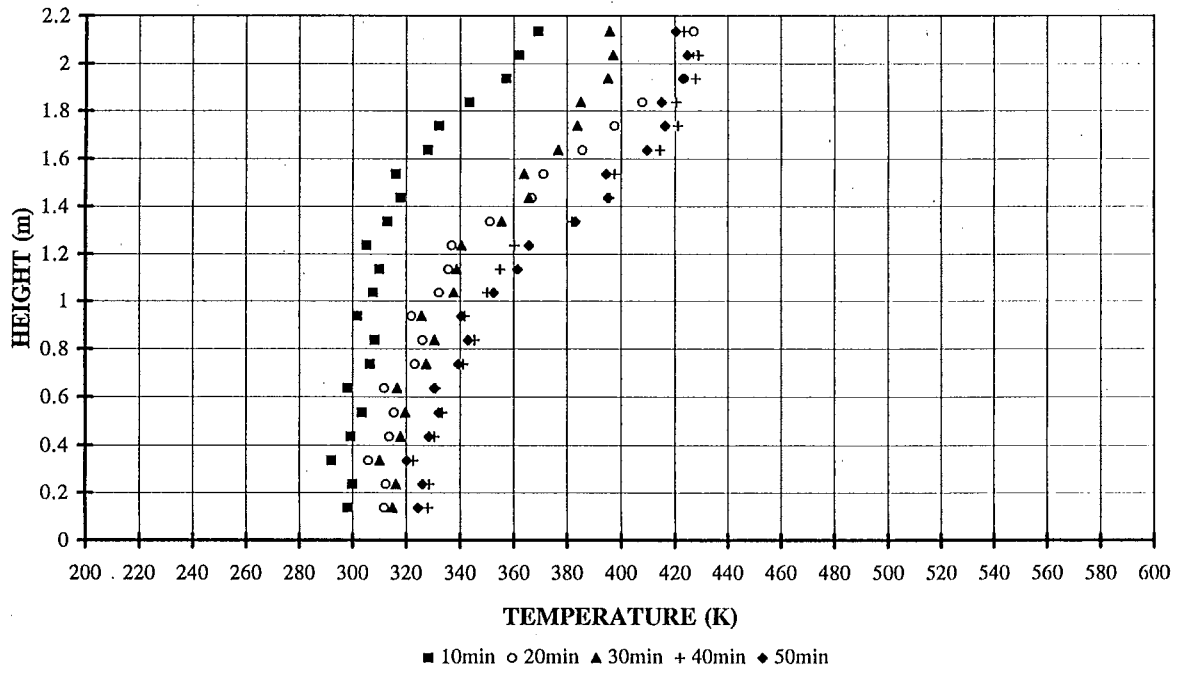
NZP2E06

COMPARTMENT FLOW HISTORY 10 MINUTE AVERAGES



NZP2E06

TEMPERATURE PROFILES

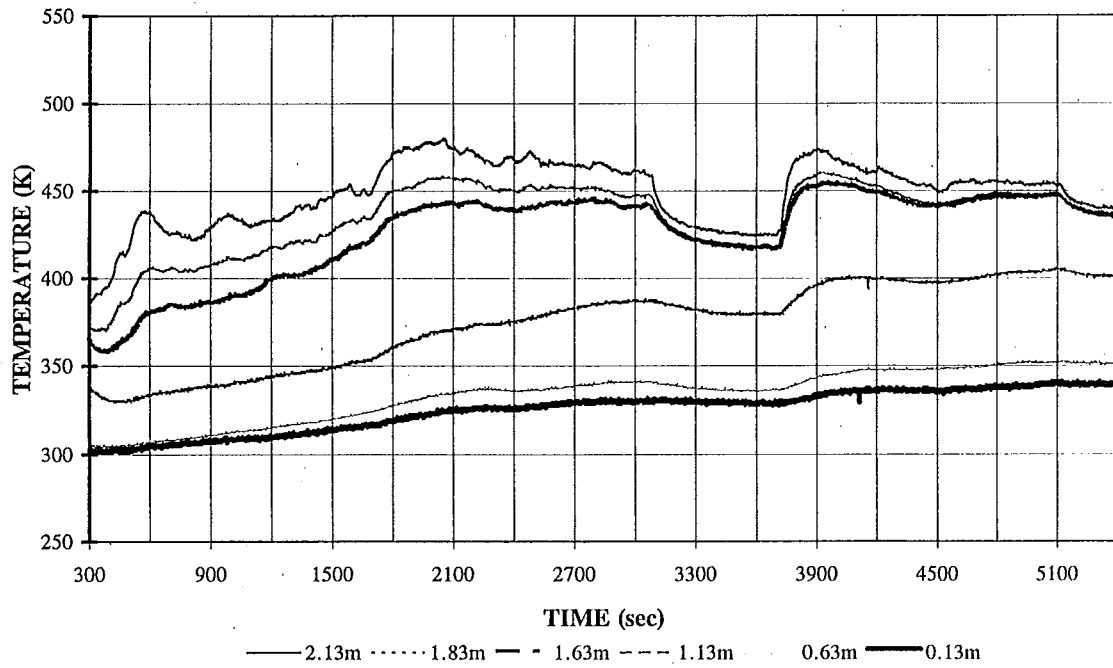


<u>EXPERIMENT</u>		NZP2E07
Vents (m ²)	top	0.0000
	central	0.0079
	bottom ²	0.0154
<u>WEATHER CONDITIONS</u>		
Relative Humidity (%)		25
Ambient Temperature (K)		297
Conditions ³		50 MPH, North Easterly.
<u>WOOD</u>		
Moisture Content (%)		14
Weight of paper used for ignition (kg)		1.8
Weight of timber cribs (kg)		165.9
<u>EVENTS</u>		
Start Computer (s)		-60
Sparks on (s)		-5
LPG on (s)		0
LPG off (s)		240
Sparks off (s)		45
Sparkling procedure during test ¹ (time starts from when LPG on)		at 480s intervals for 120s duration
<u>OPENING</u> ²		5400s, 7200s

OBSERVATIONS AND IRREGULARITIES

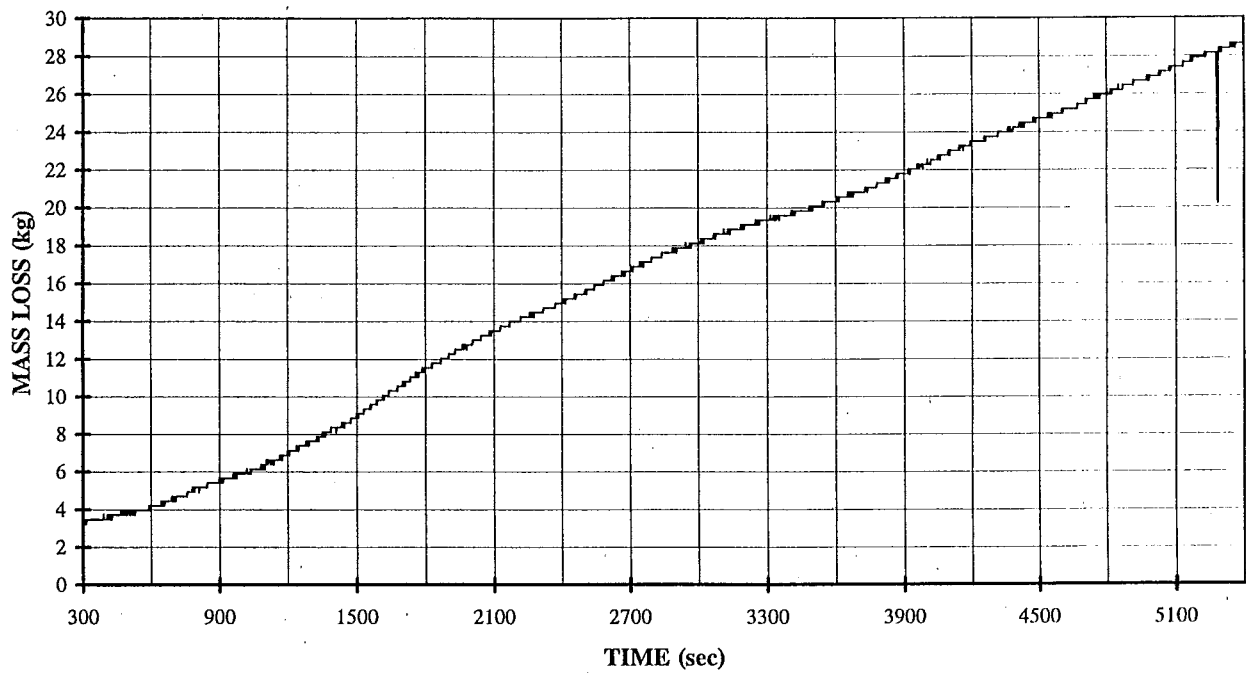
- ³1800s the wind appeared to drop to zero.
- ¹Sparks left on continuously between 4080s and 4800s.
- After 4320s it was noticed that the gas sample line was leaking, it was repaired between 4320s and 4800s.
- At 5020s the load cell was accidentally interfered with.
- ²At 5400s the bottom vent was changed to 0.066m², the hatch was not opened.
- At 7020s the data acquisition was stopped and a new file (NZP2E07b) was started.
- Right hand crib burned, left was literally unaffected.

TEMPERATURE HISTORY - TC TREE DATA



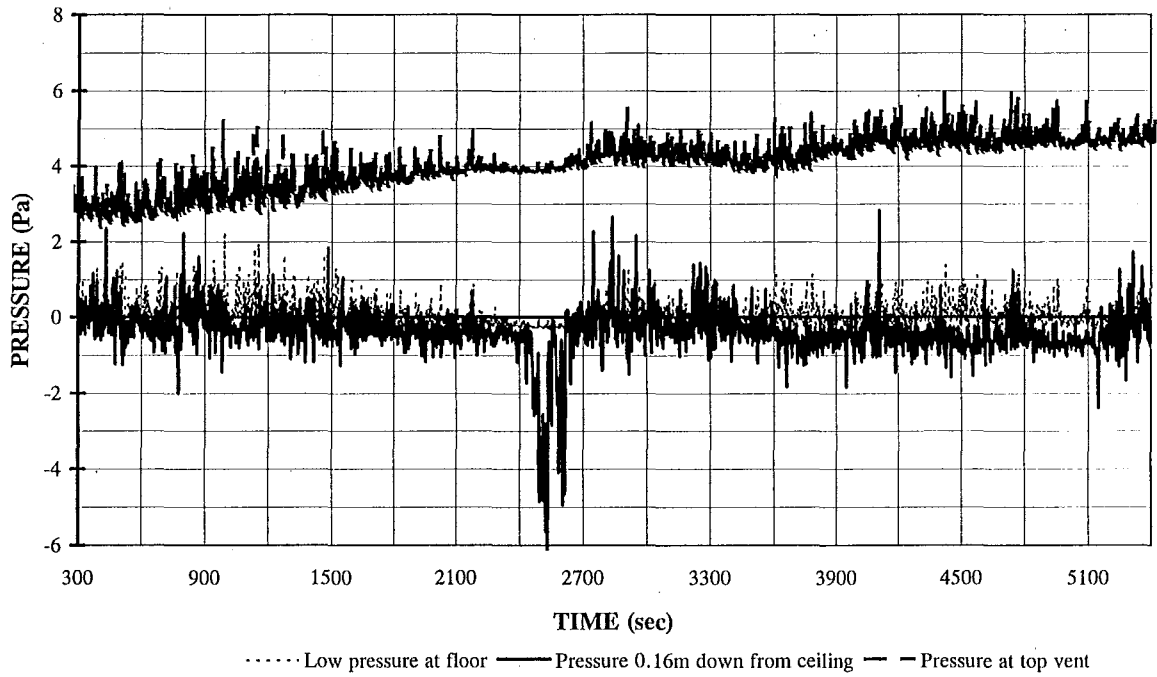
NZP2E07

MASS LOSS HISTORY



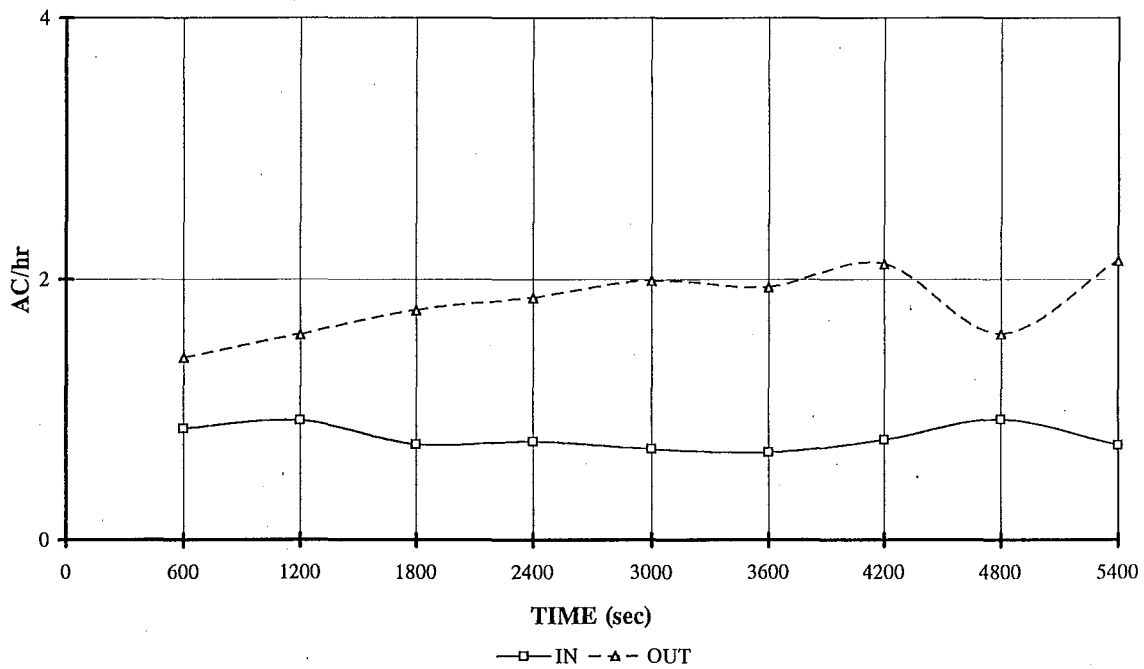
NZP2E07

COMPARTMENT PRESSURE HISTORY



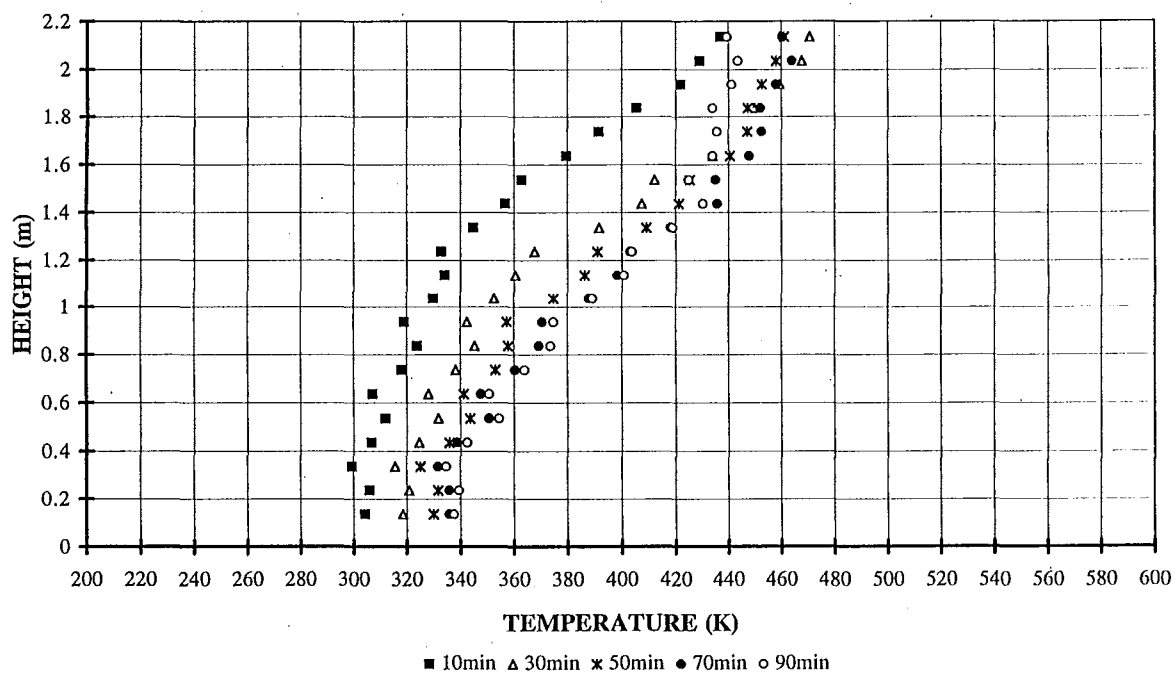
NZP2E07

COMPARTMENT FLOW HISTORY 10 MINUTE AVERAGES



NZP2E07

TEMPERATURE PROFILES

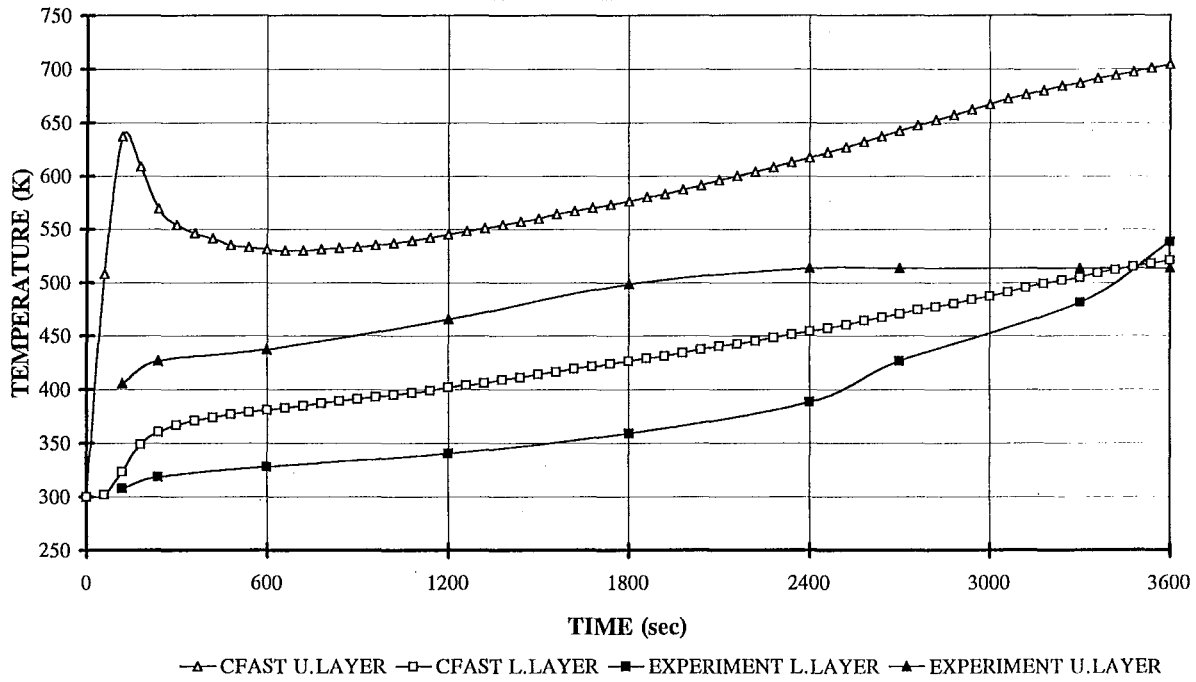


APPENDIX C

GRAPHS OF THE RESULTS MADE BETWEEN CFAST AND EXPERIMENTS

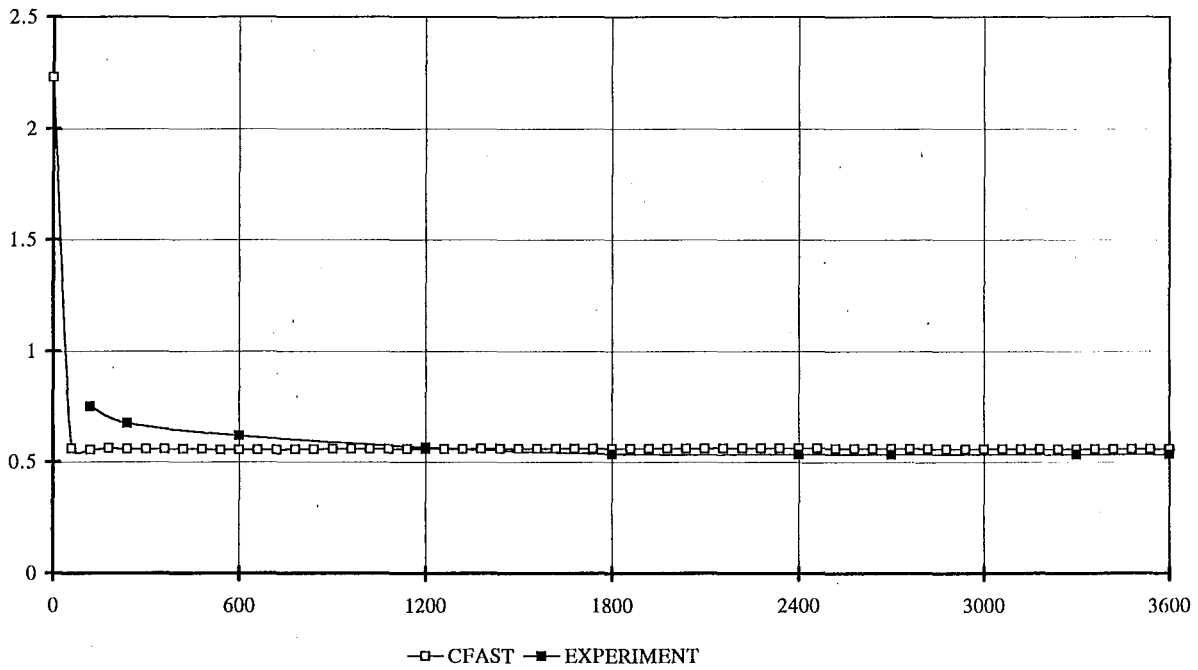
SCENARIO 2

CFAST COMPARISON LAYER TEMPERATURES



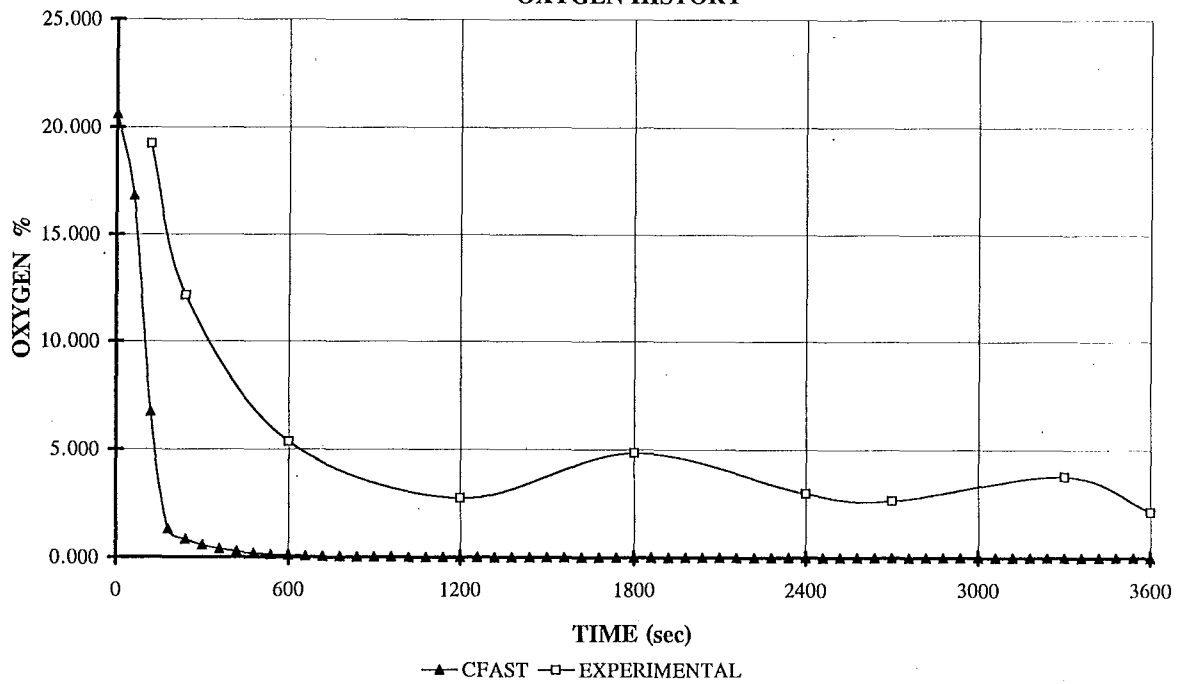
NZP2E2

LAYER HEIGHT



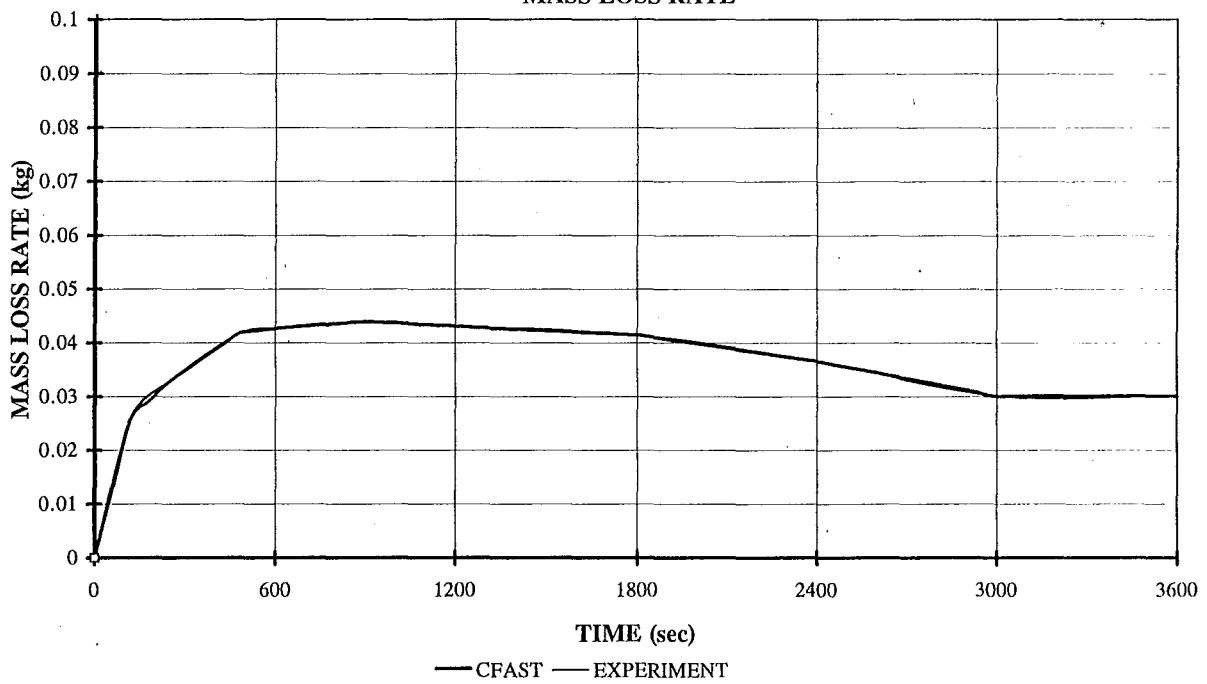
NZP2E2

CFAST COMPARISON OXYGEN HISTORY



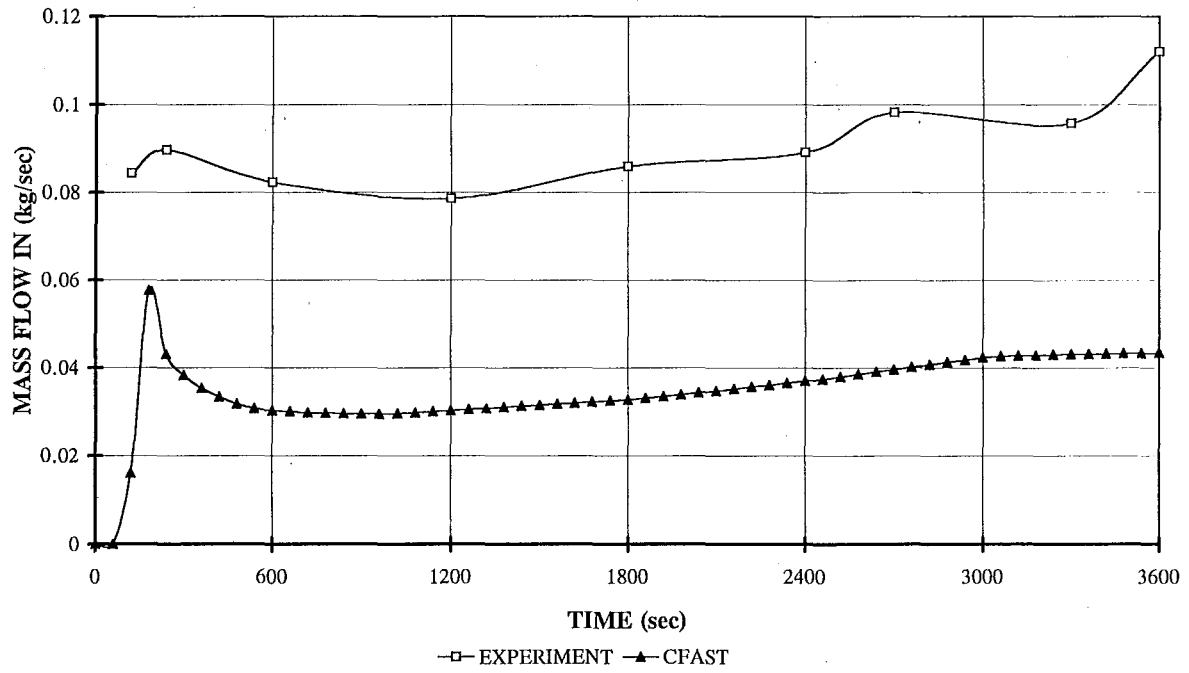
NZP2E2

CFAST COMPARISON MASS LOSS RATE



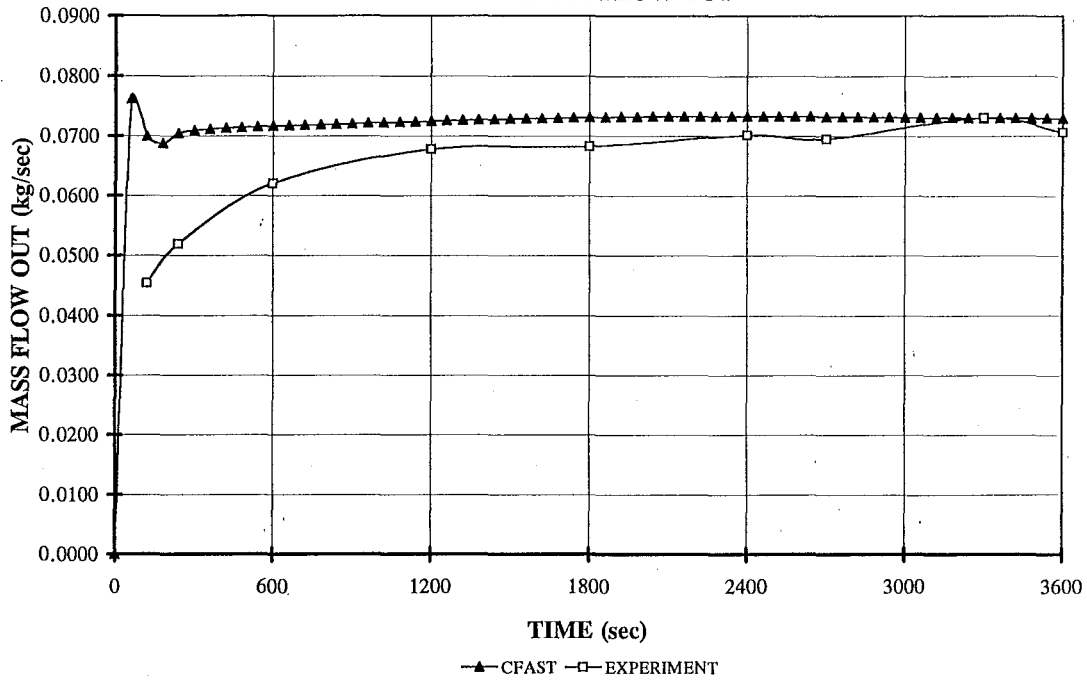
NZP2E2

CFAST COMPARISON **MASS FLOW IN**



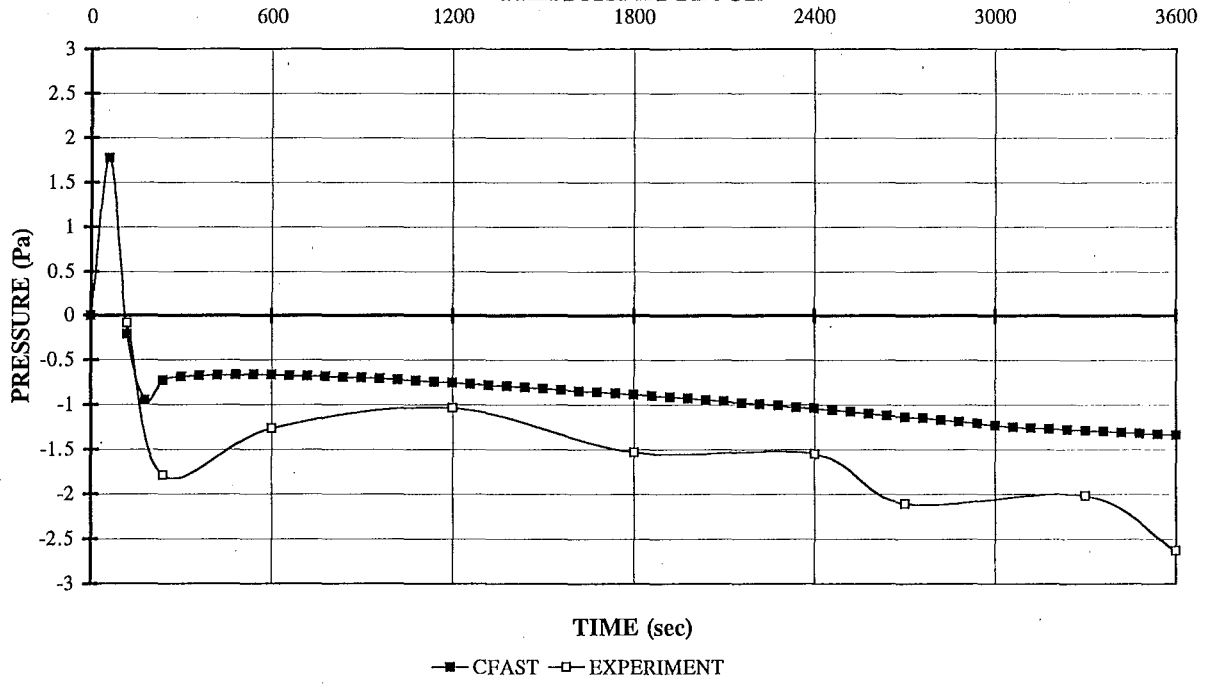
NZP2E2

CFAST COMPARISON **MASS FLOW OUT**



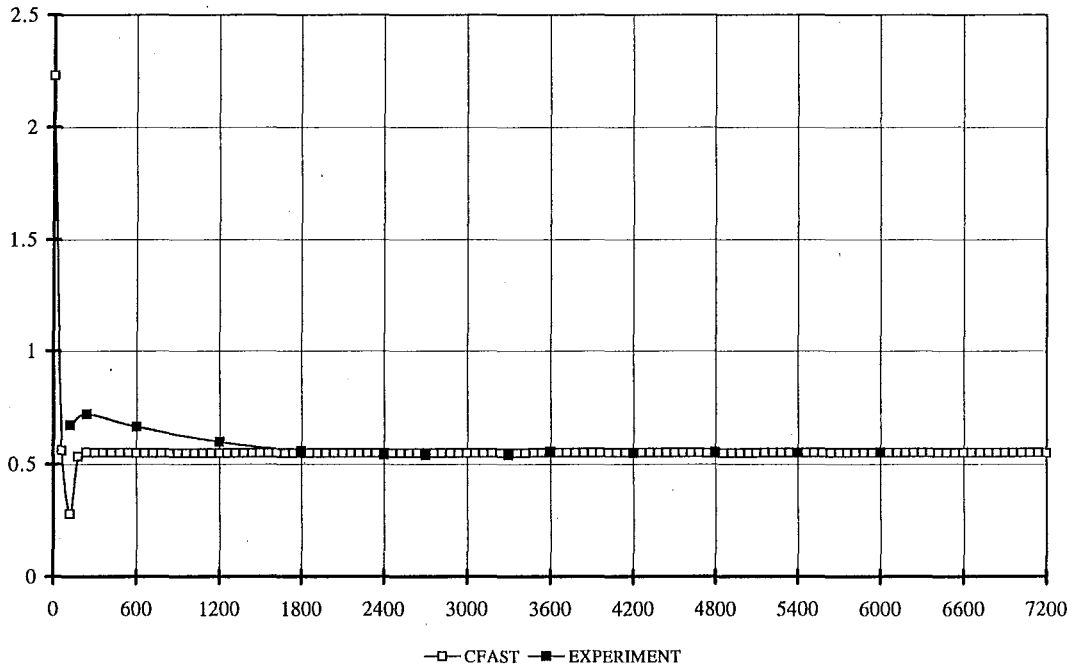
NZP2E2

CFAST COMPARISON
PRESSURE AT FLOOR



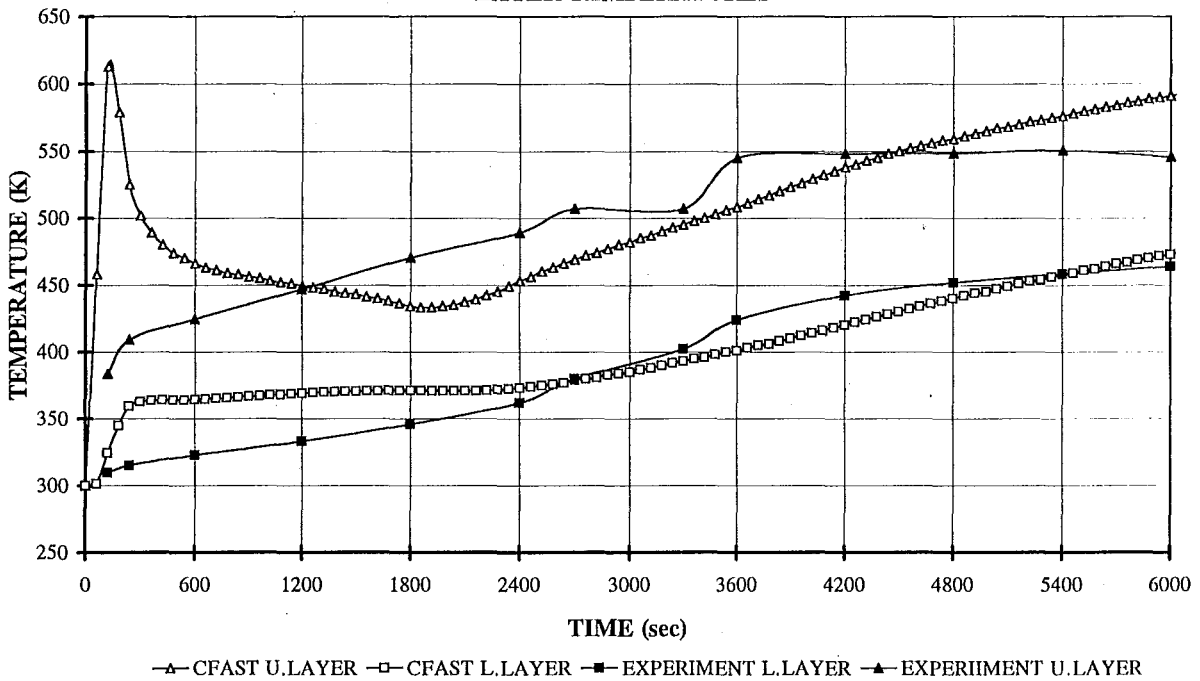
SCENARIO 3

LAYER HEIGHT



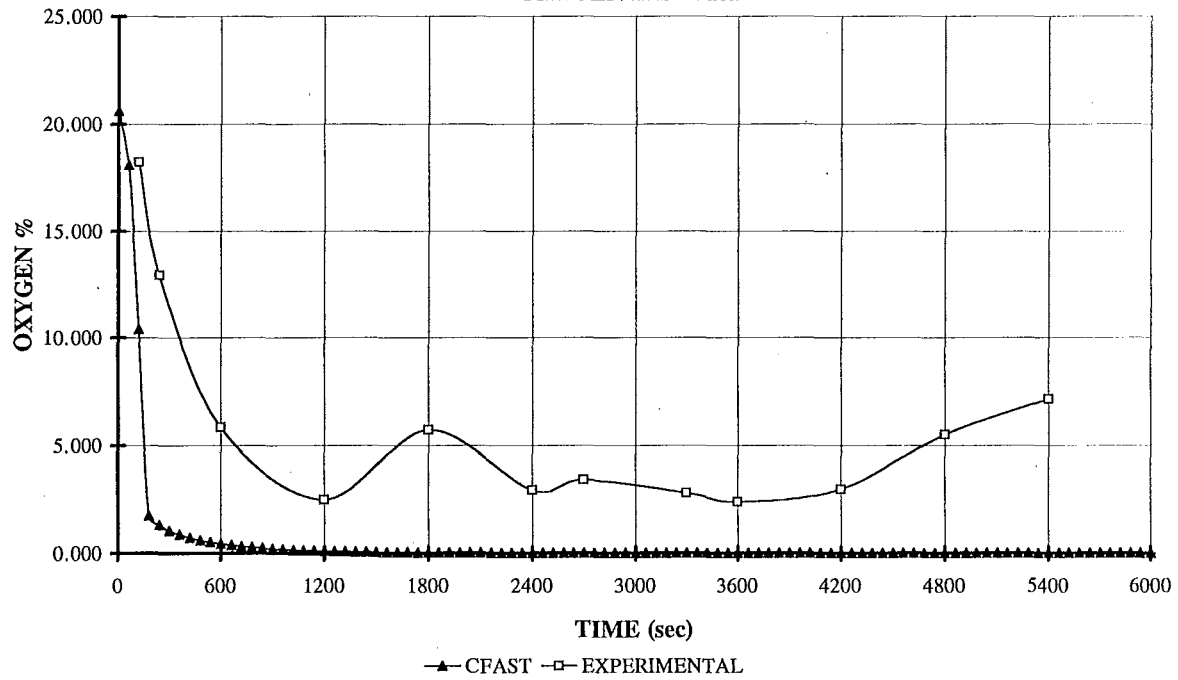
NZP2E3

CFAST COMPARISON LAYER TEMPERATURES



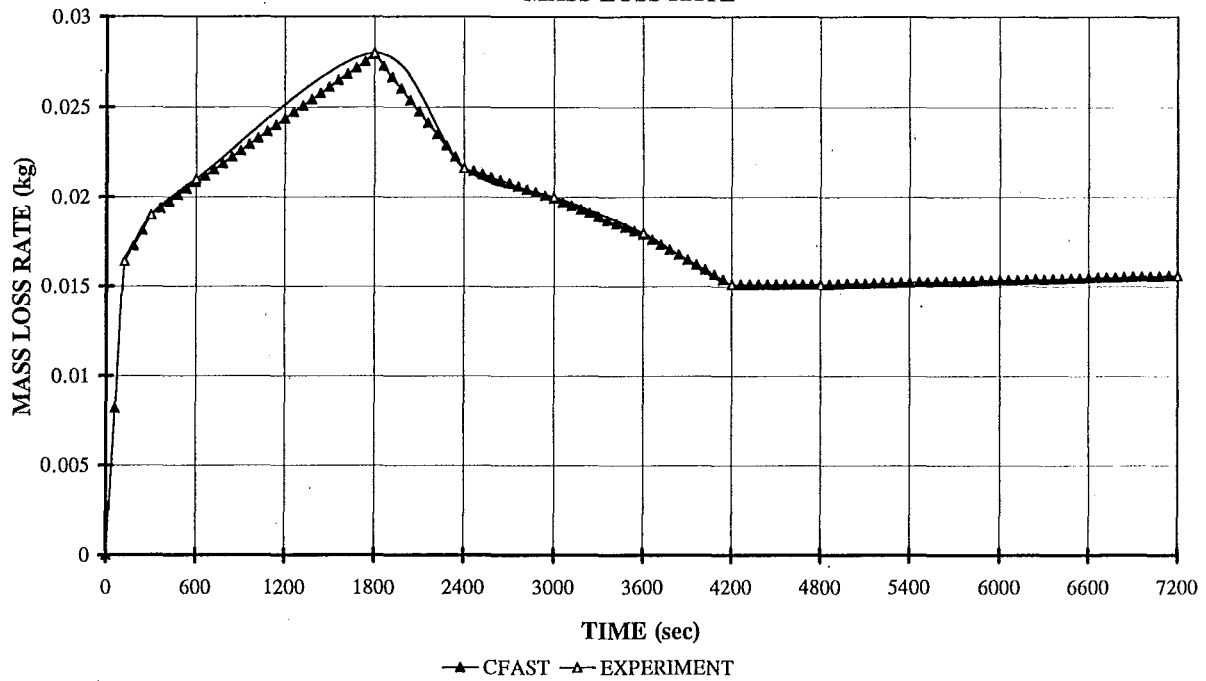
NZP2E3

CFAST COMPARISON OXYGEN HISTORY



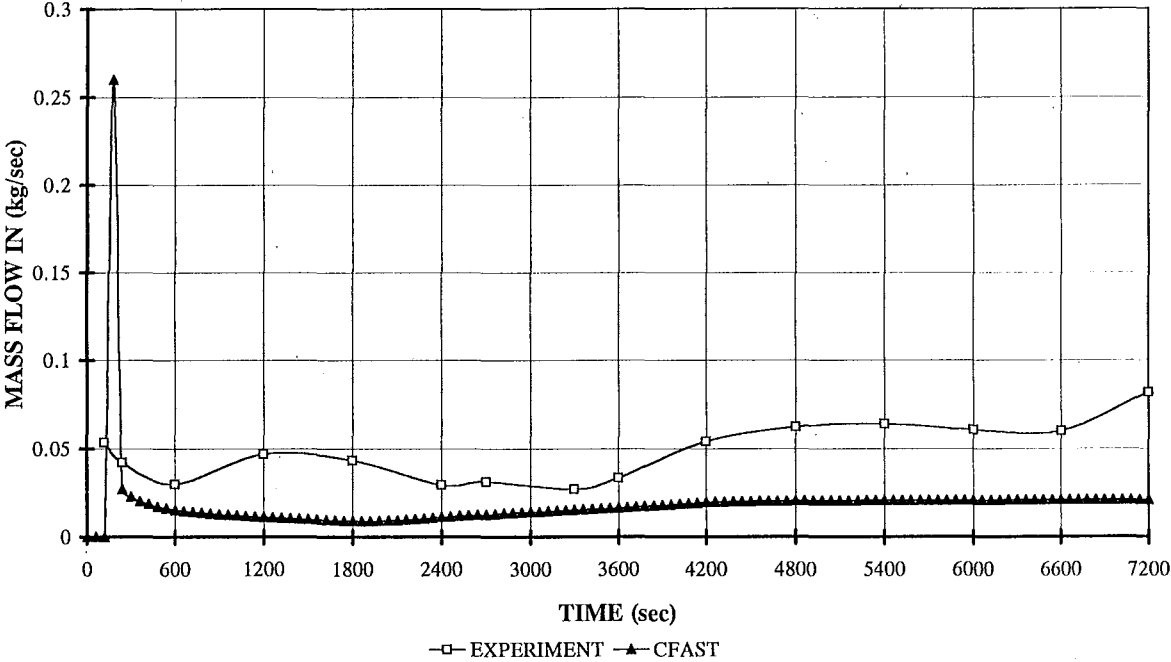
NZP2E3

CFAST COMPARISON MASS LOSS RATE



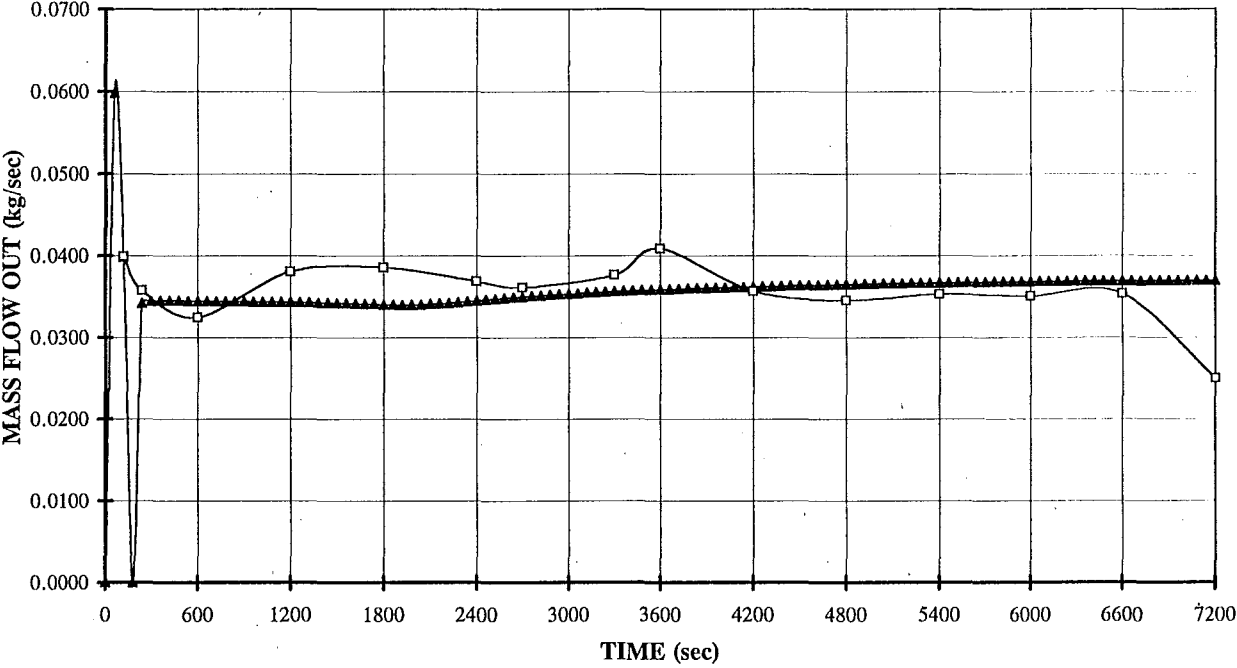
NZP2E3

CFAST COMPARISON
MASS FLOW IN



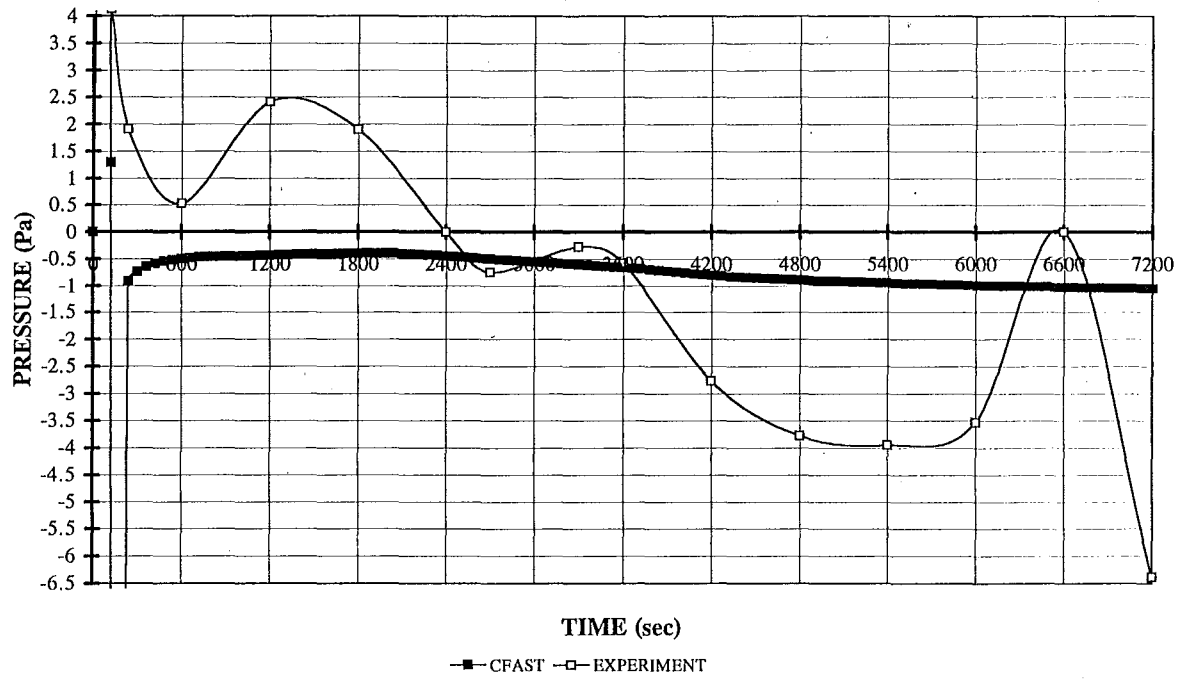
NZP2E3

CFAST COMPARISON
MASS FLOW OUT



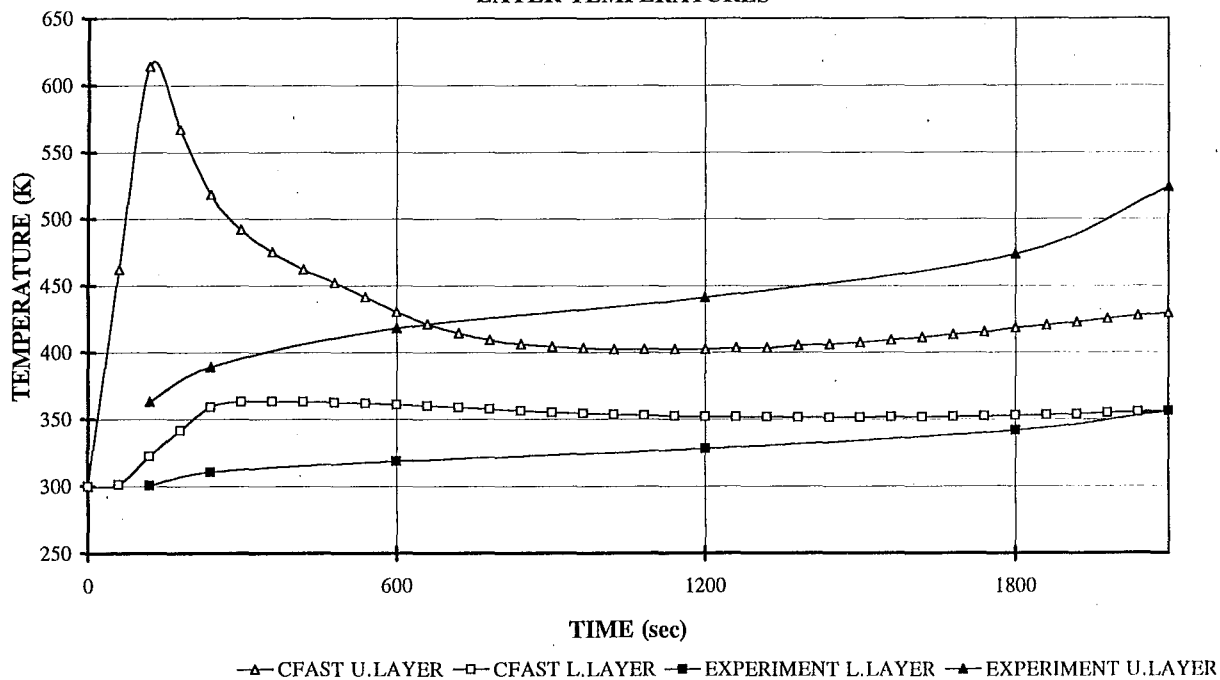
NZP2E3

CFAST COMPARISON PRESSURE AT FLOOR



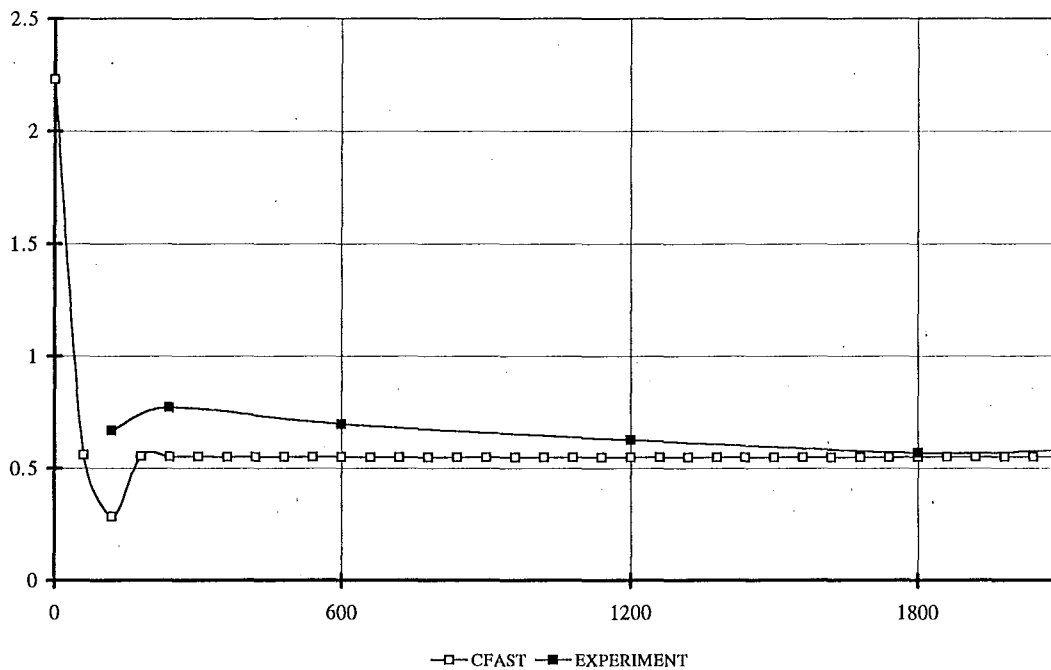
SCENARIO 4

CFAST COMPARISON LAYER TEMPERATURES



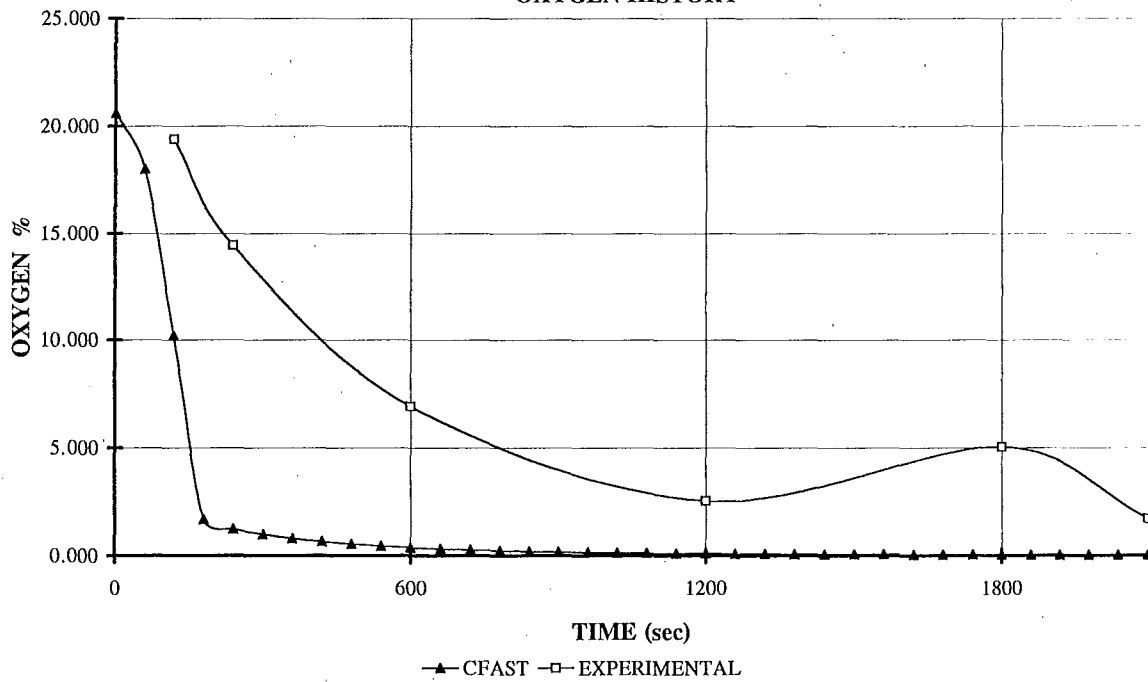
NZP2E4

LAYER HEIGHT



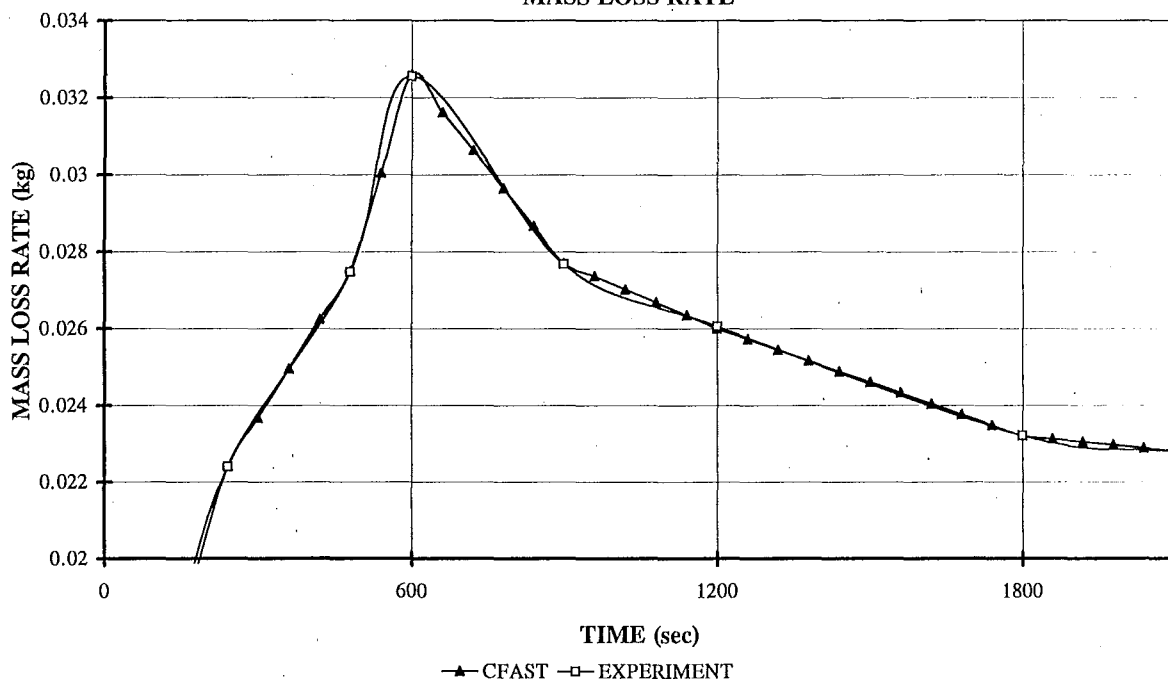
NZP2E4

CFAST COMPARISON OXYGEN HISTORY



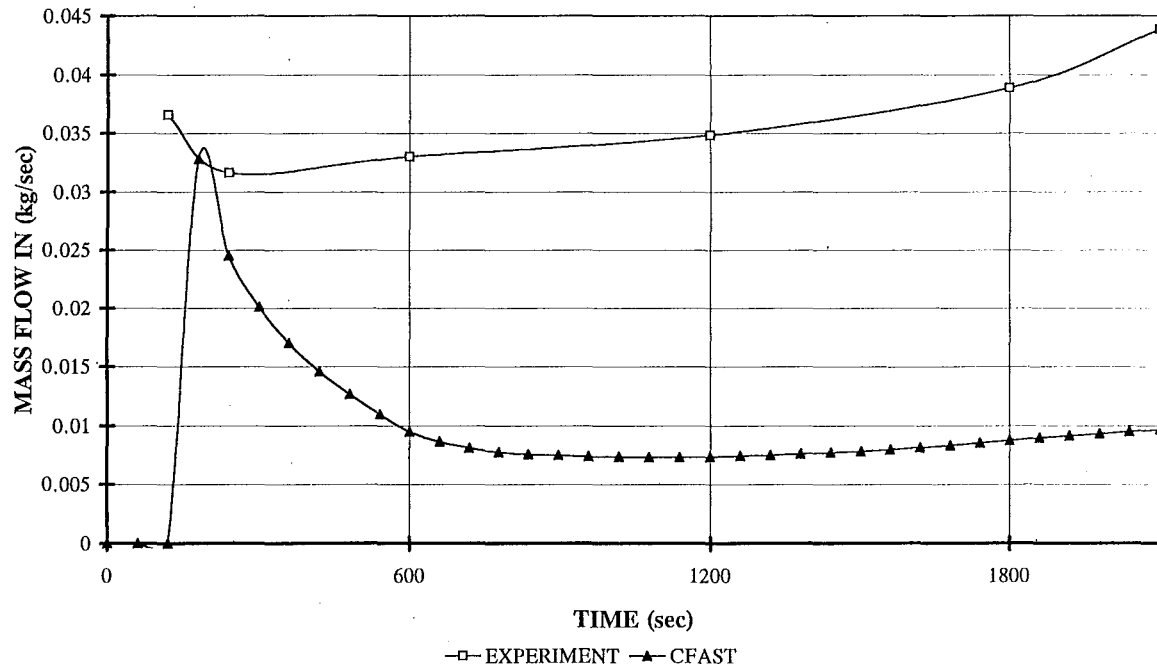
NZP2E4

CFAST COMPARISON MASS LOSS RATE



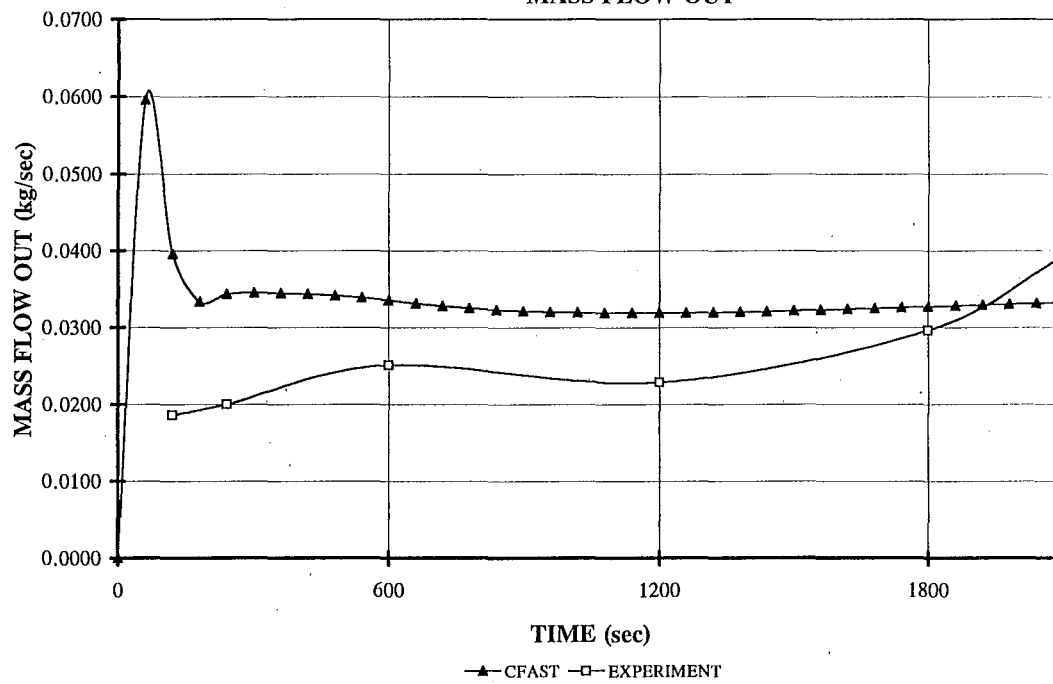
NZP2E4

CFAST COMPARISON MASS FLOW IN



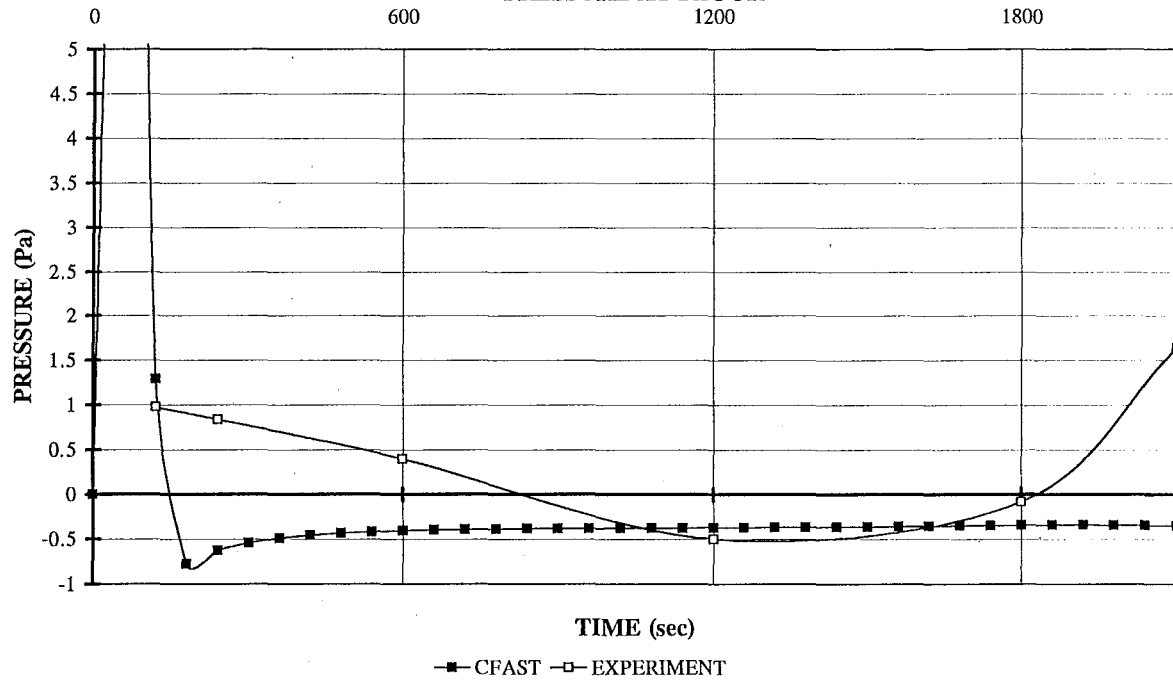
NZP2E4

CFAST COMPARISON MASS FLOW OUT



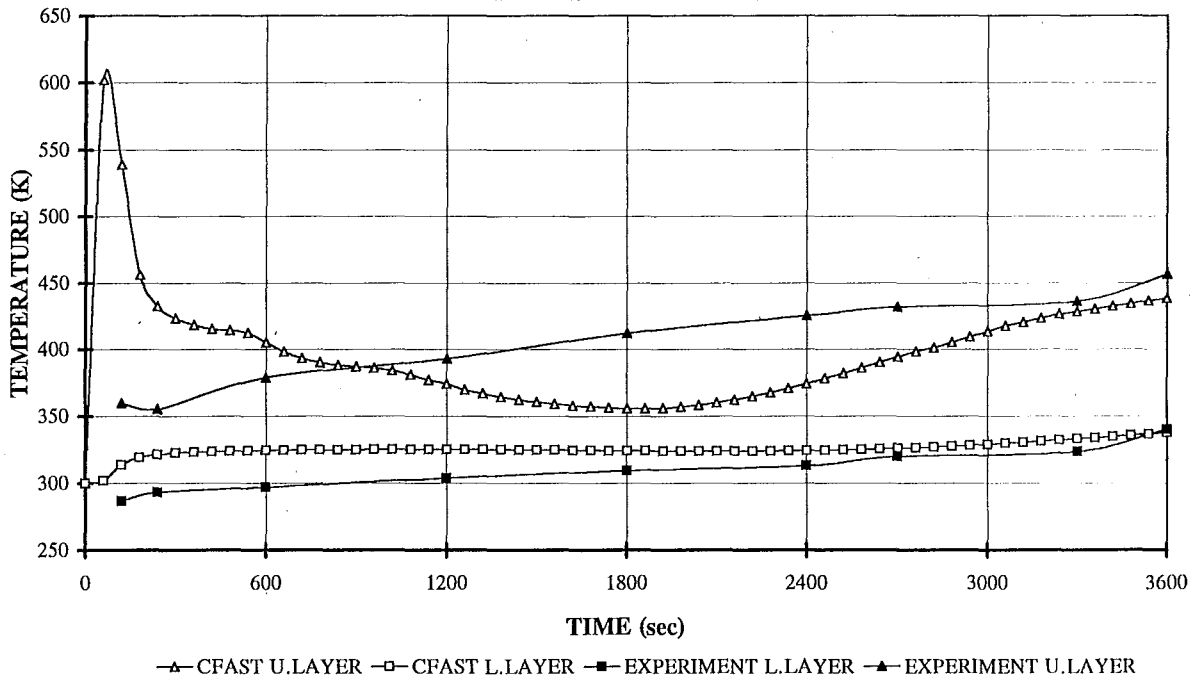
NZP2E4

CFAST COMPARISON PRESSURE AT FLOOR



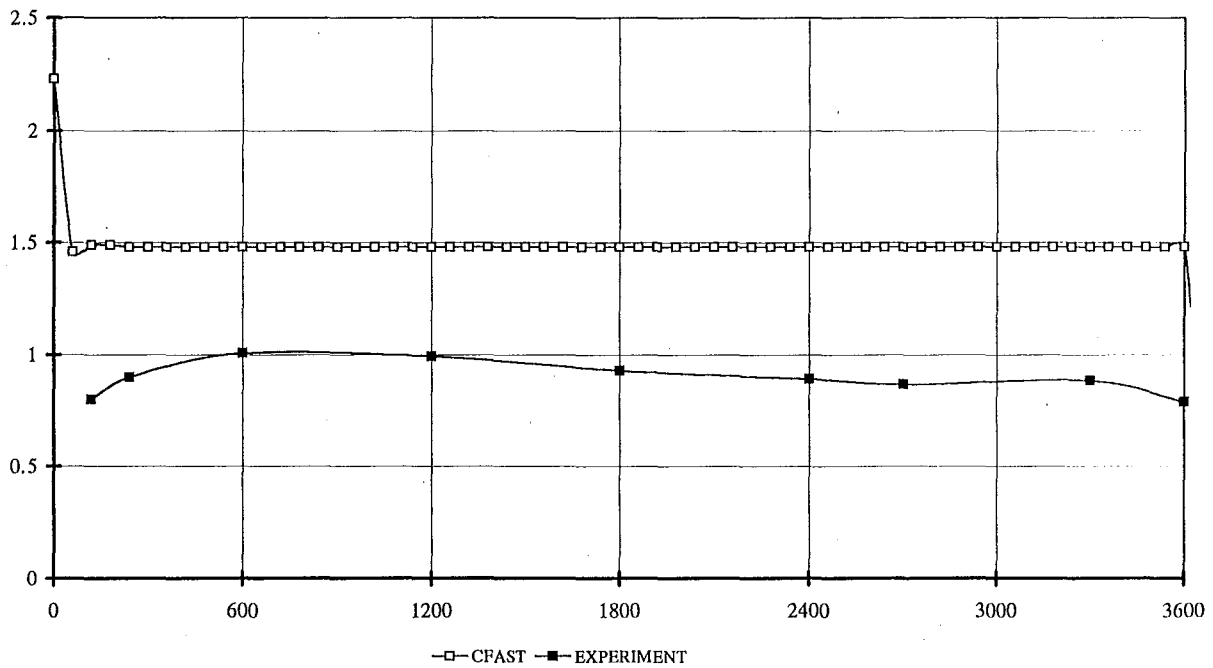
SCENARIO 5

CFAST COMPARISON LAYER TEMPERATURES



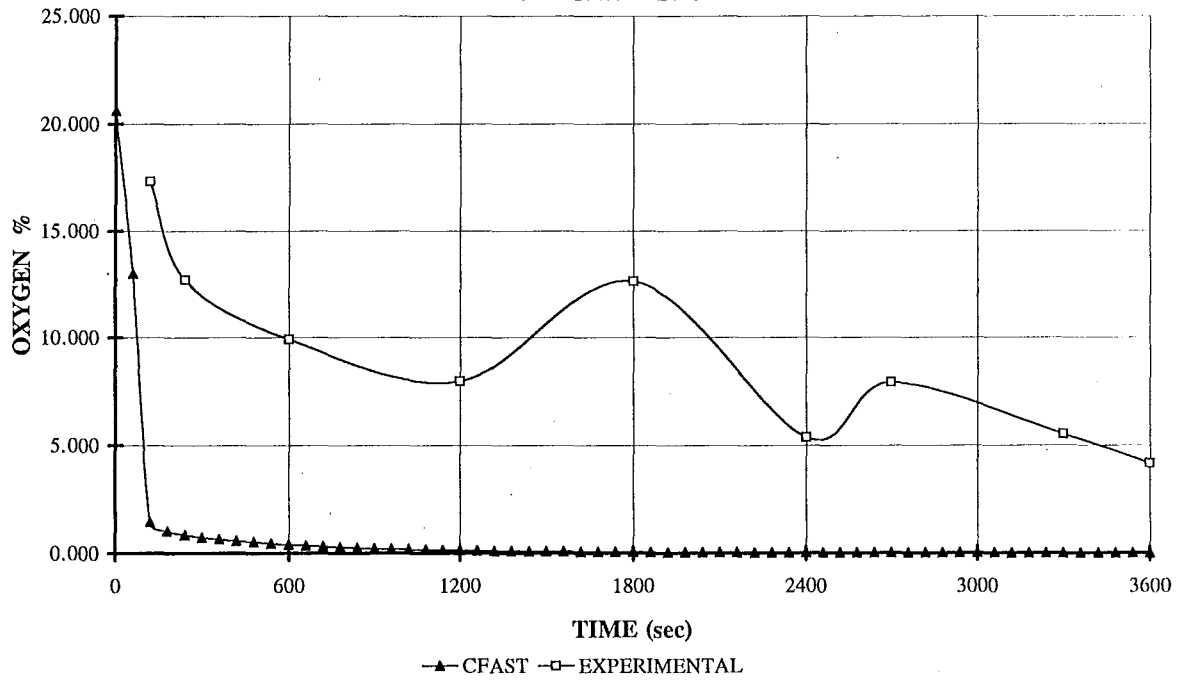
NZP2E5

LAYER HEIGHT



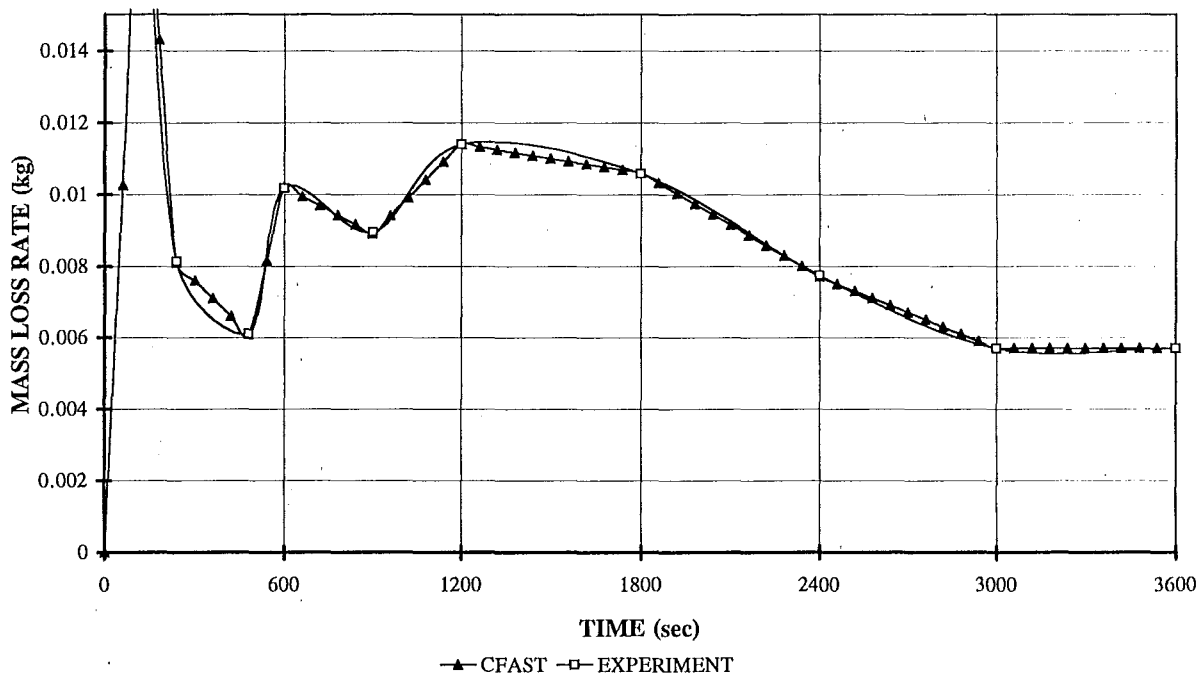
NZP2E5

CFAST COMPARISON OXYGEN HISTORY



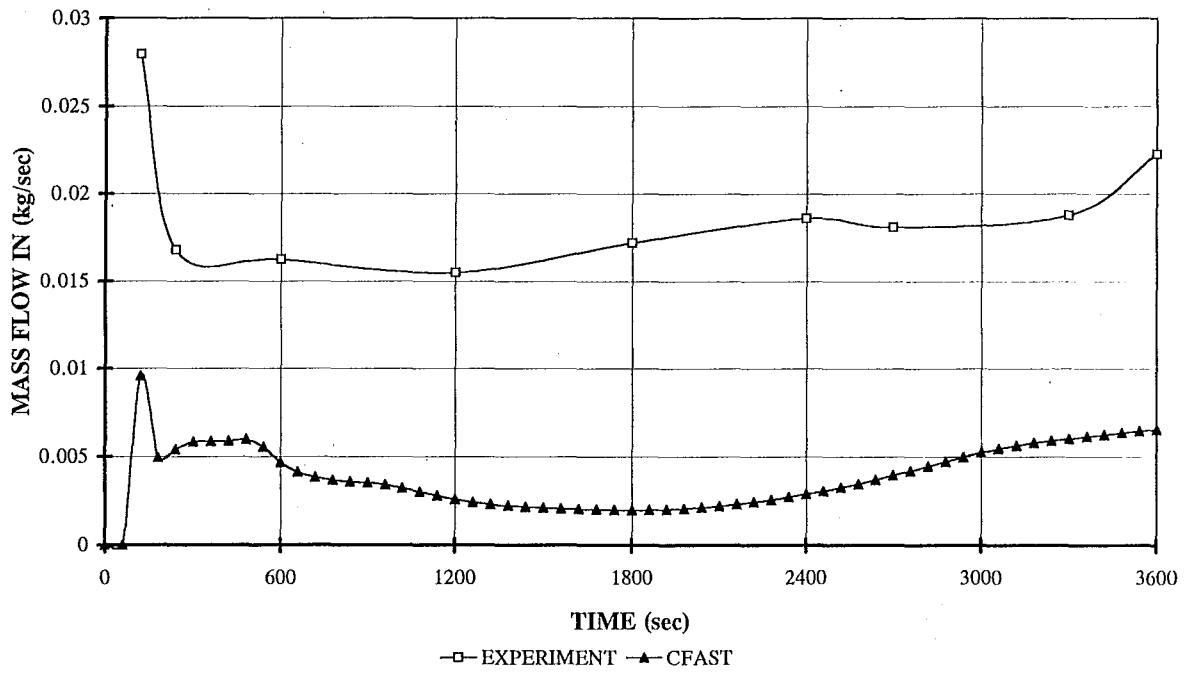
NZP2E5

CFAST COMPARISON MASS LOSS RATE



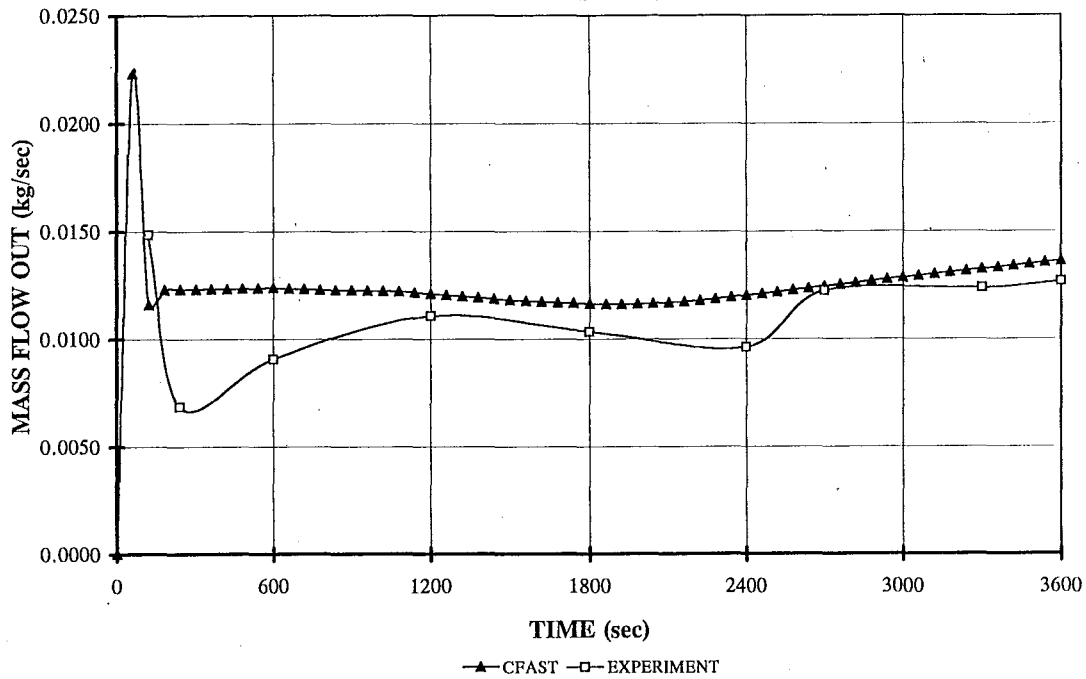
NZP2E5

CFAST COMPARISON MASS FLOW IN

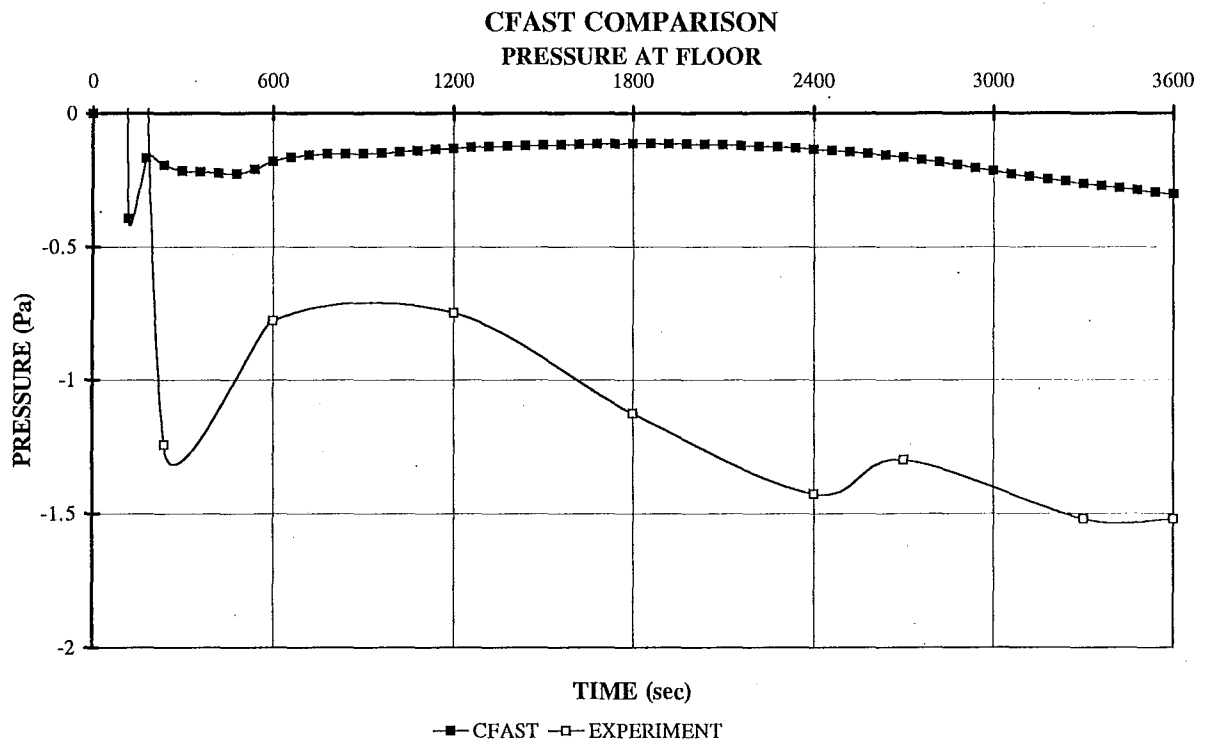


NZP2E5

CFAST COMPARISON MASS FLOW OUT

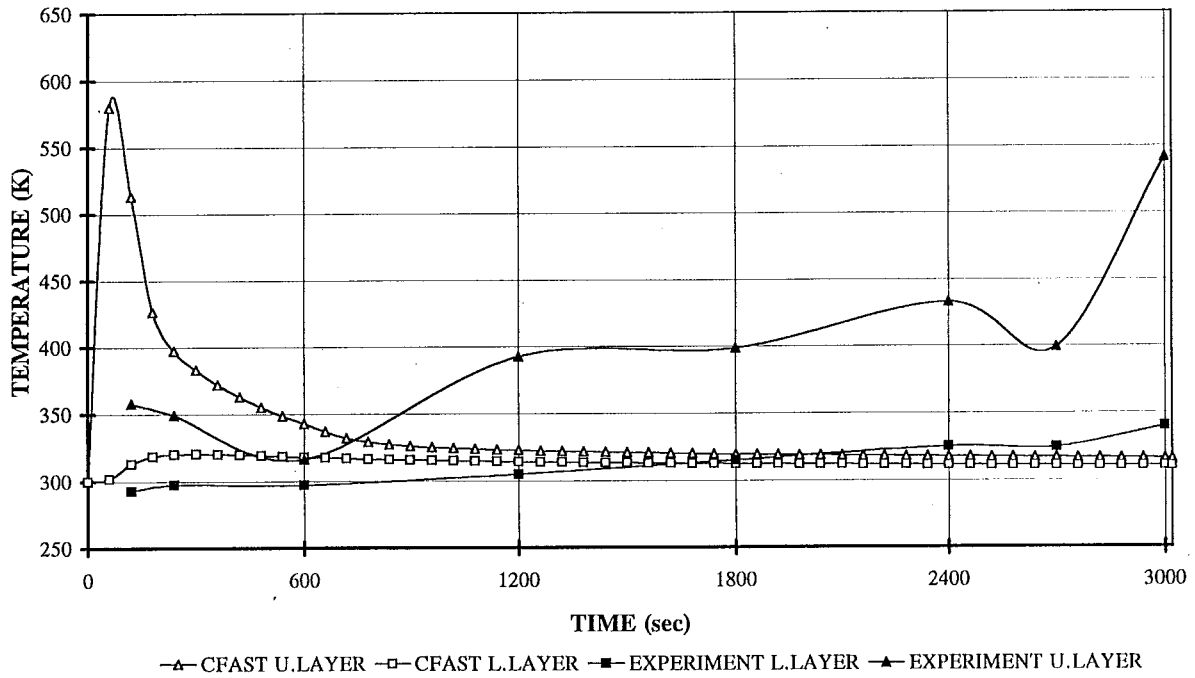


NZP2E5



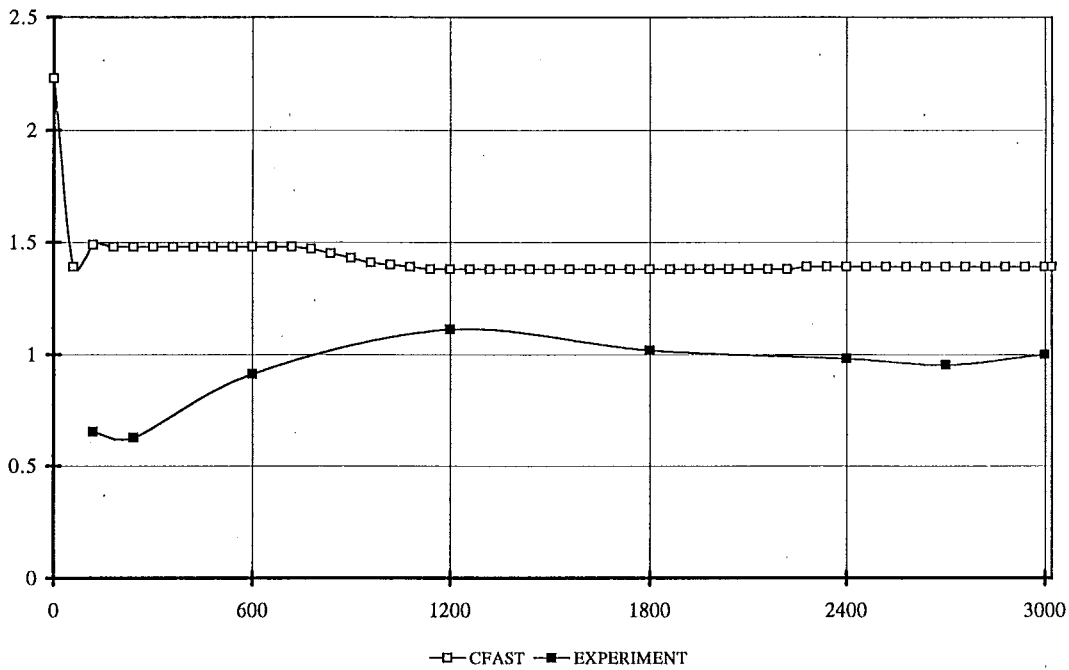
SCENARIO 6

CFAST COMPARISON LAYER TEMPERATURES



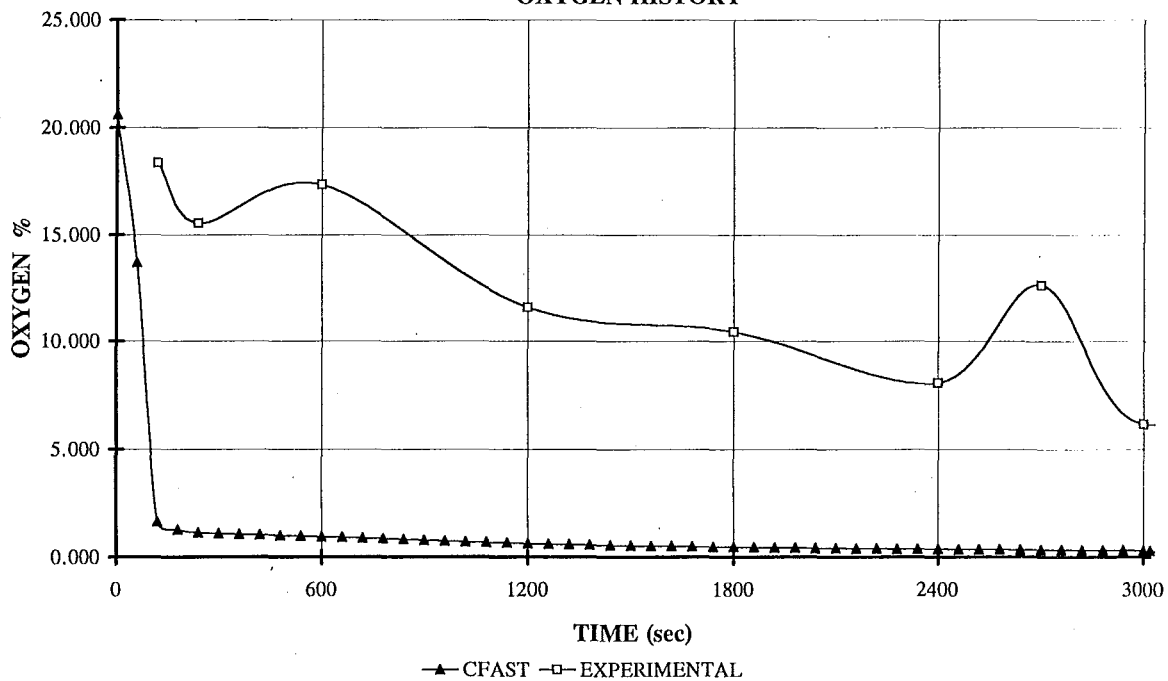
NZP2E6

LAYER HEIGHT



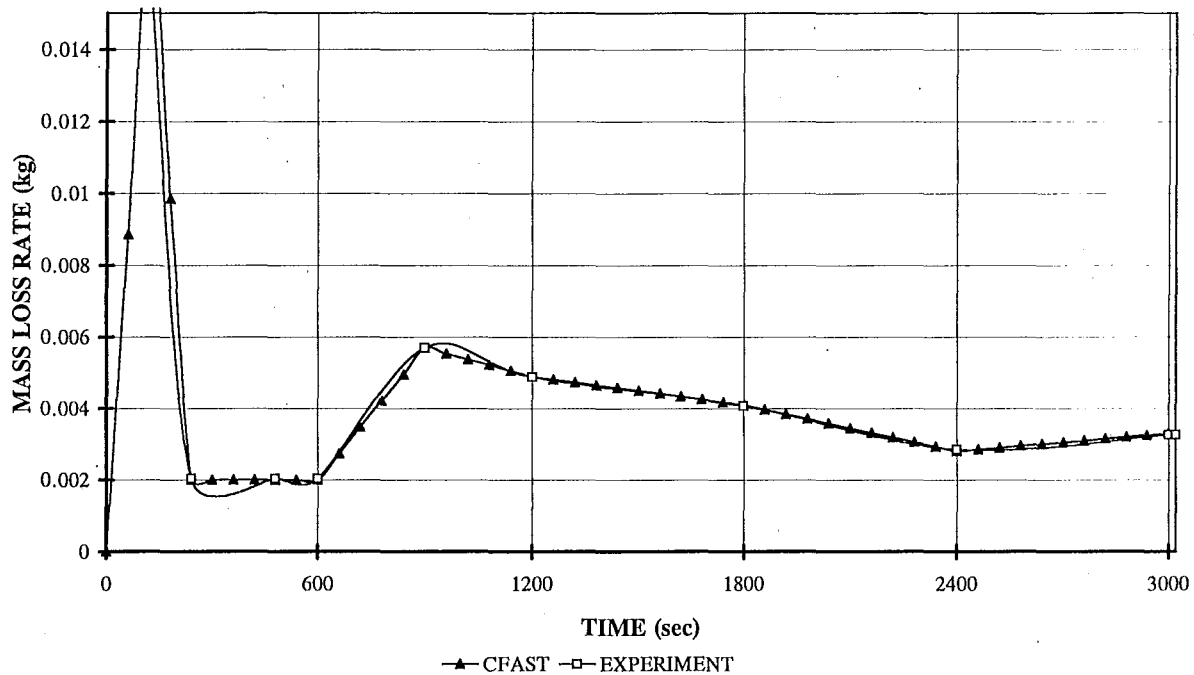
NZP2E6

CFAST COMPARISON OXYGEN HISTORY



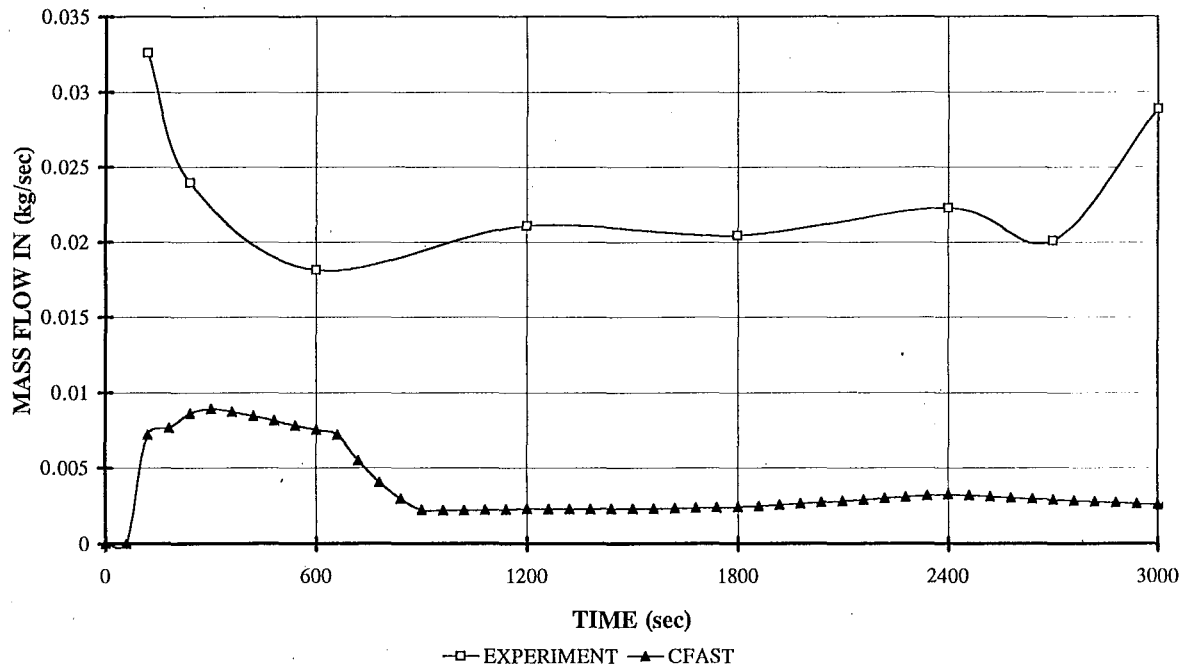
NZP2E6

CFAST COMPARISON MASS LOSS RATE



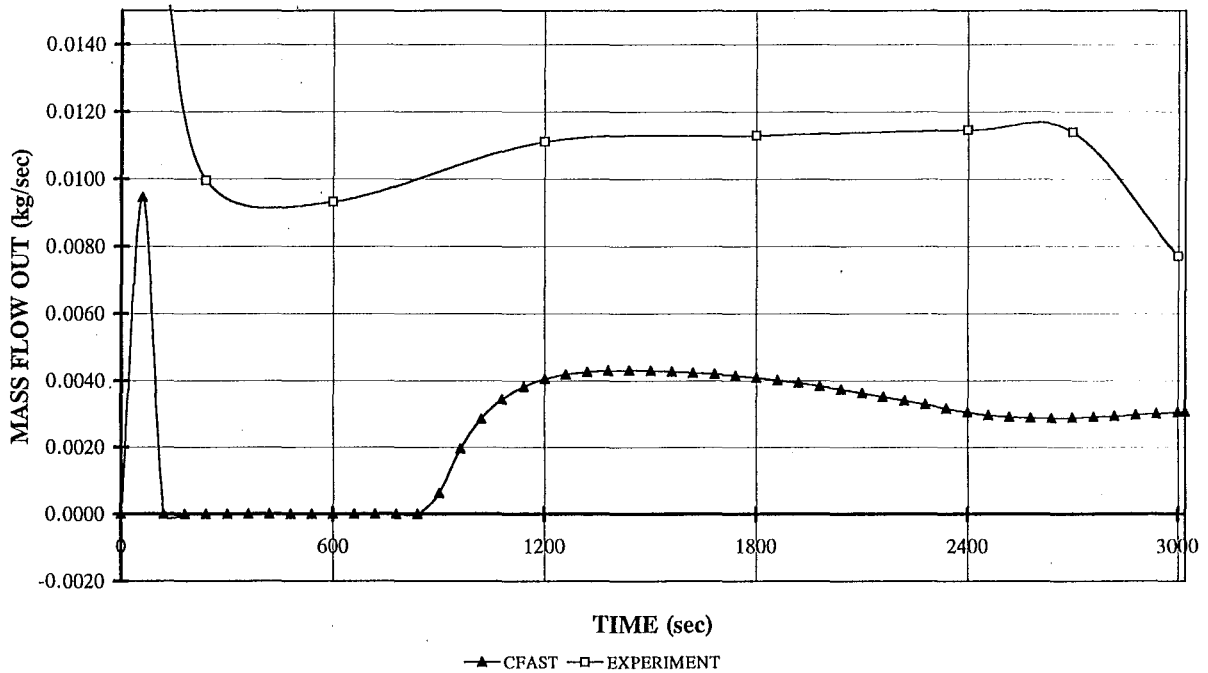
NZP2E6

CFAST COMPARISON **MASS FLOW IN**



NZP2E6

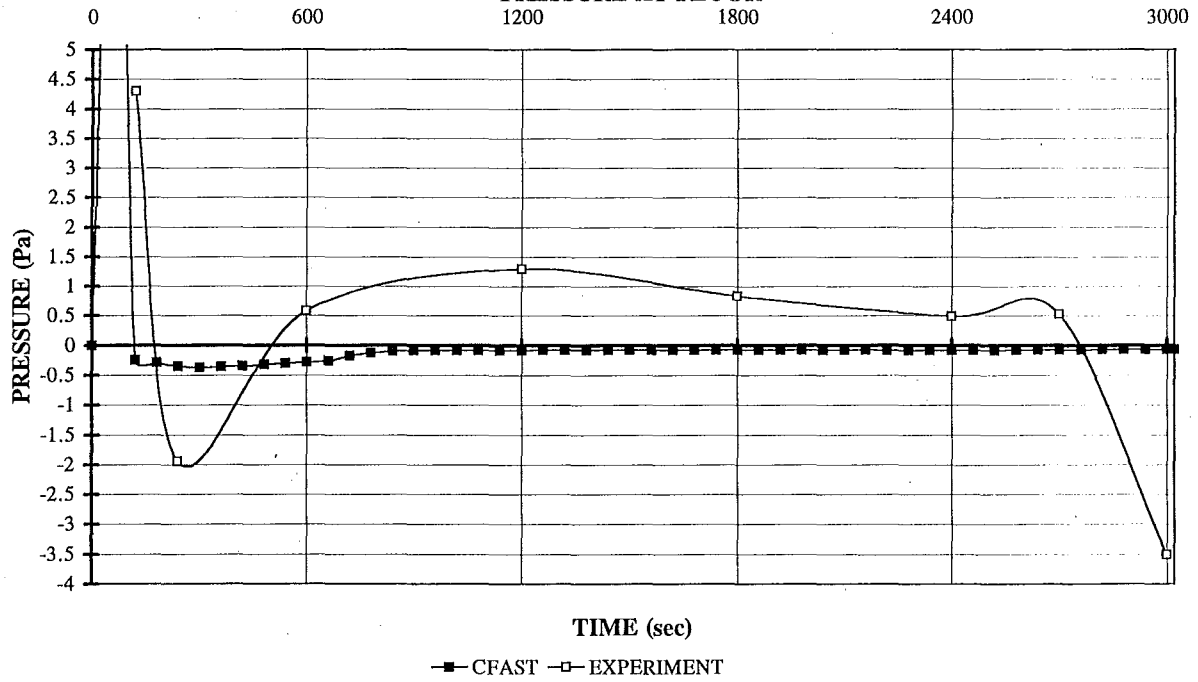
CFAST COMPARISON **MASS FLOW OUT**



NZP2E6

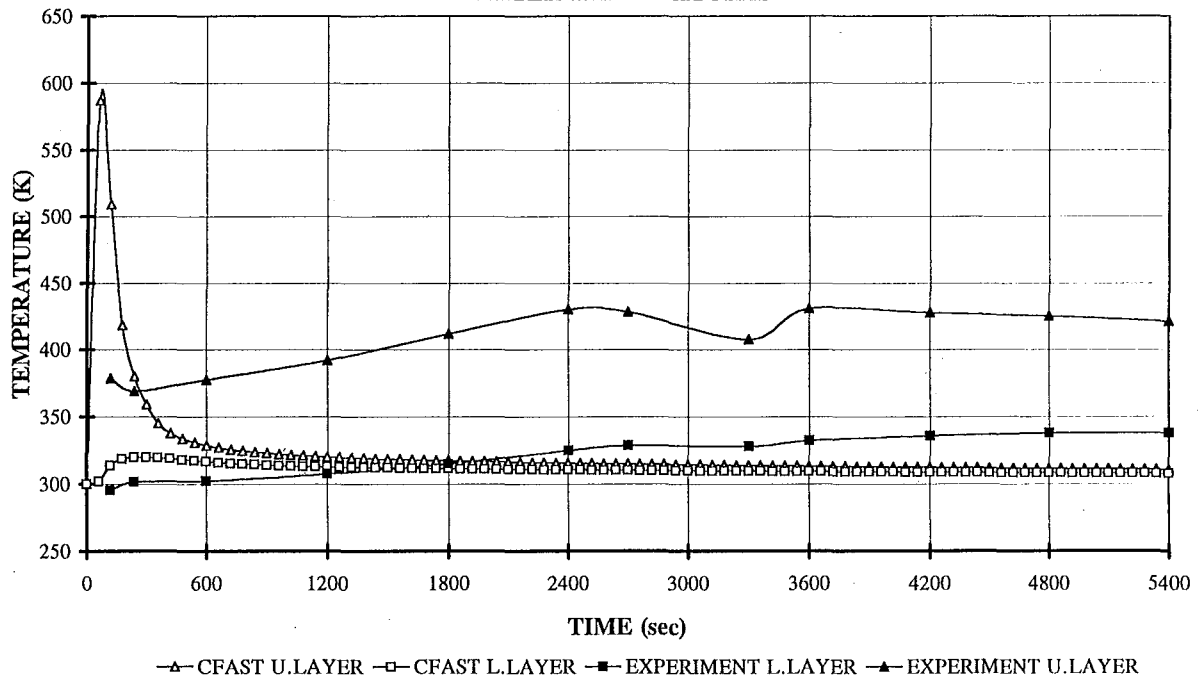
CFAST COMPARISON

PRESSURE AT FLOOR



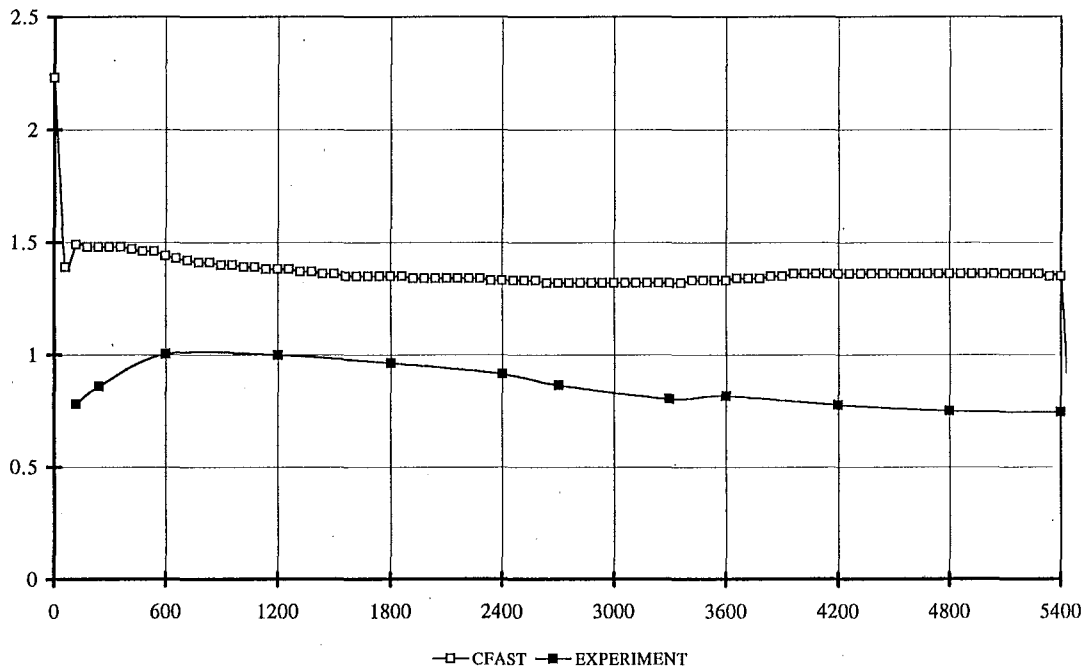
SCENARIO 7

CFAST COMPARISON LAYER TEMPERATURES



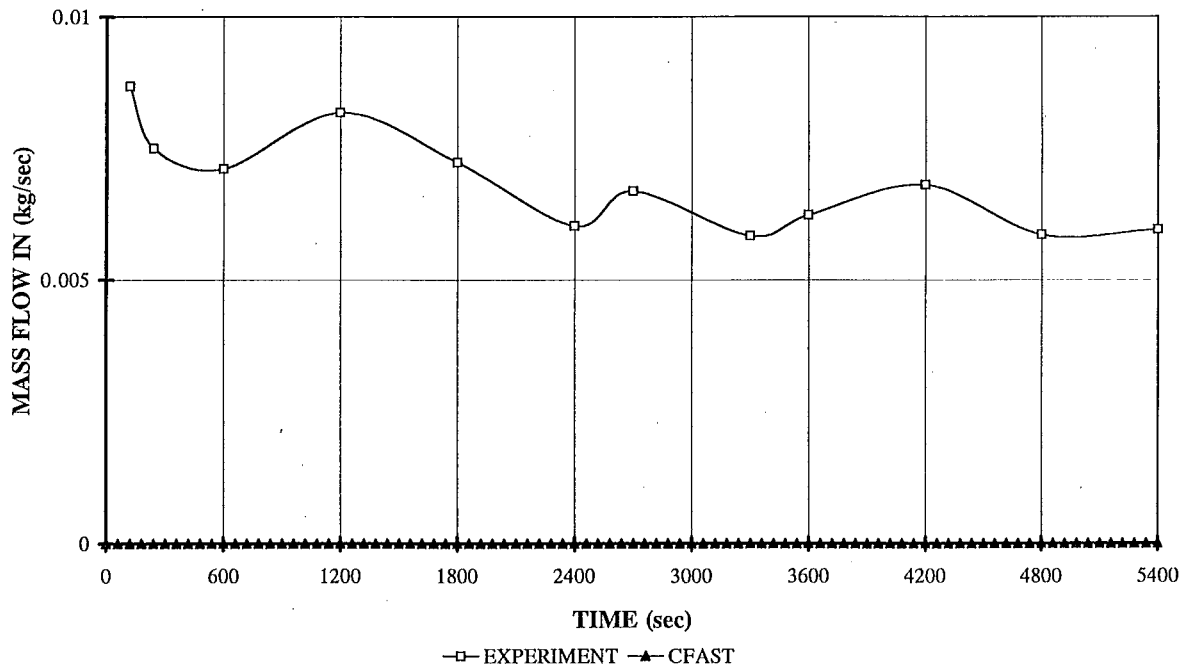
NZP2E7

LAYER HEIGHT



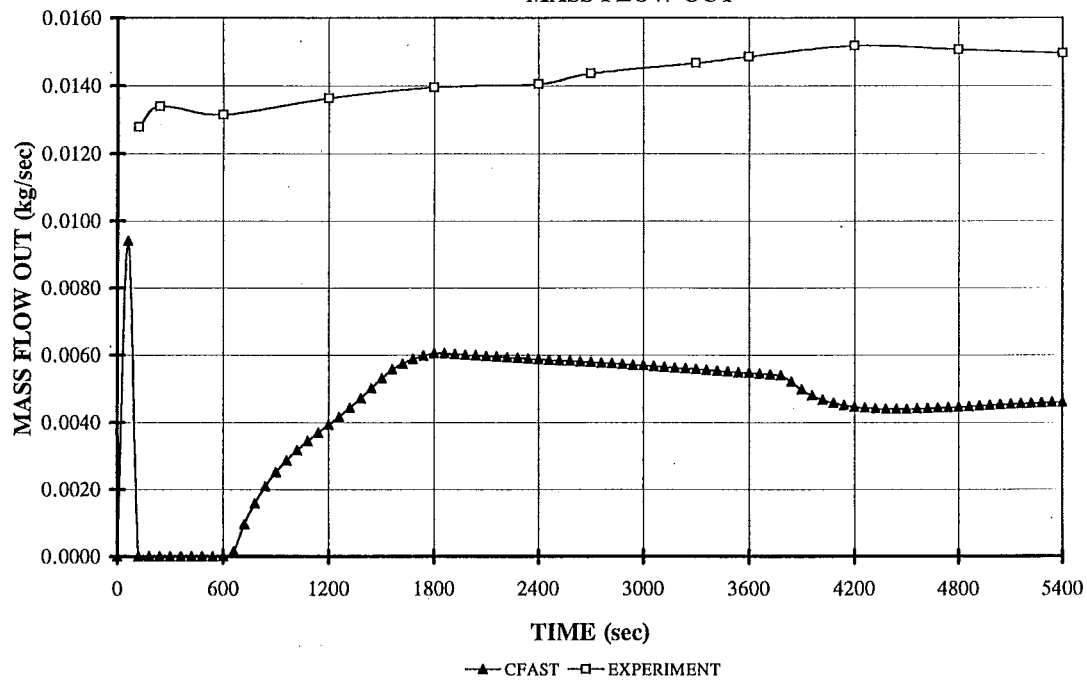
NZP2E7

CFAST COMPARISON MASS FLOW IN



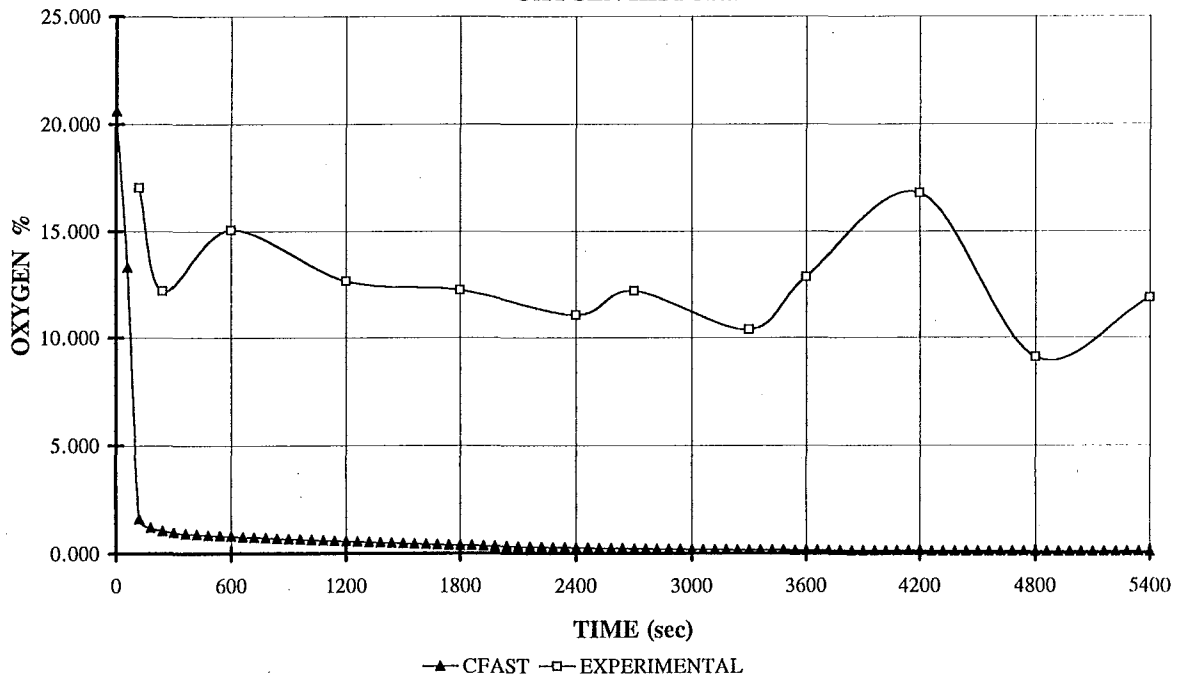
NZP2E7

CFAST COMPARISON MASS FLOW OUT



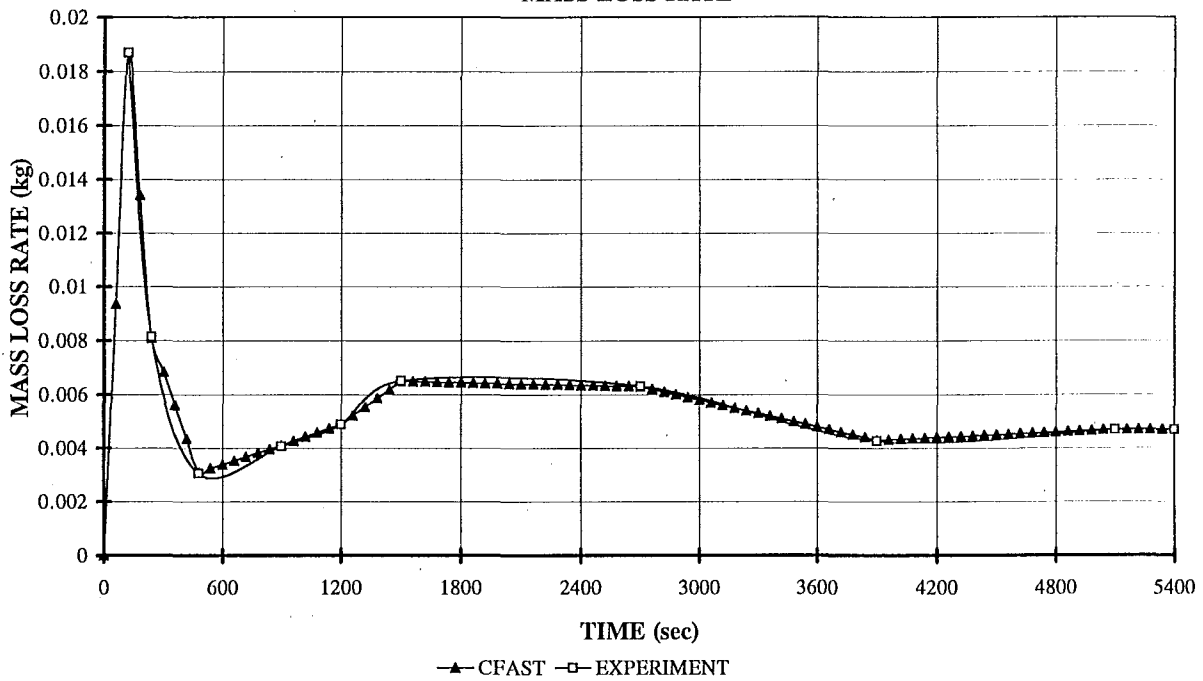
NZP2E7

CFAST COMPARISON OXYGEN HISTORY

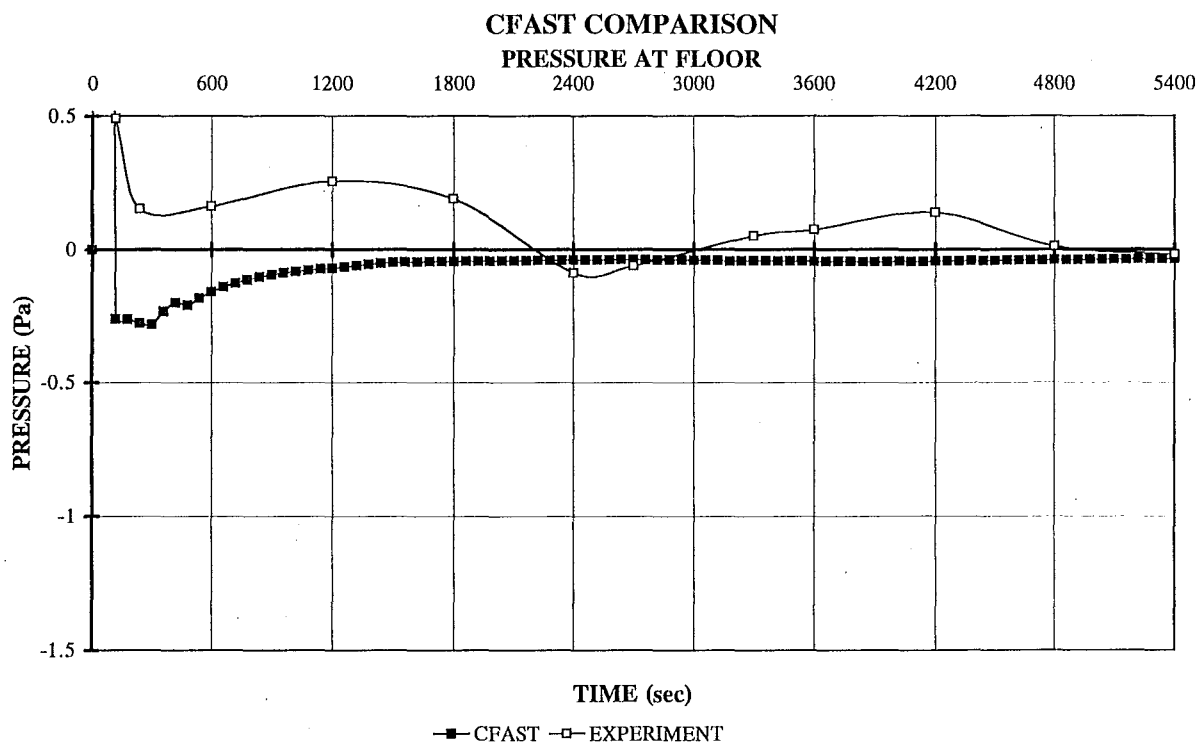


NZP2E7

CFAST COMPARISON MASS LOSS RATE



NZP2E7



APPENDIX D

DATA AND RESULT FILES FROM CFAST

```

VERSN 2MLR. 2 EXACT test number two
TIMES 3600 600 60 10 0
TAMB 300. 101300. 0.
EAMB 300. 101300. 0.
HI/F 0.00
WIDTH 2.23
DEPTH 5.40
HEIGH 2.23
HVENT 1 2 1 0.177 2.130 1.953 0.000
HVENT 1 2 2 0.257 0.307 0.050 0.000
CVENT 1 2 1 1.00 1.00 1.00 1.00 1.00 1.00 1.00 1.00
=> 1.00 1.00
CVENT 1 2 2 1.00 1.00 1.00 1.00 1.00 1.00 1.00 1.00
=> 1.00 1.00
CEILI GYPROCK GYPROCK gYP3/4
WALLS GYPROCK GYPROCK GYP3/4
FLOOR GYP3/4
CHEMI 16. 20. 2 18000000. 300. 400. 0.000
LFB0 1
LFBT 2
FPOS 0.52 1.05 0.27
FTIME 120. 240. 480. 600. 900. 1200. 1800. 2400. 3000. 36000.
FRASS 0.0000 0.0259 0.0326 0.0418 0.0427 0.0440 0.0431 0.0415 0.0366 0.0301 0.0
=> .301
FHIGH 0.27 0.27 0.27 0.27 0.27 0.27 0.27 0.27 0.27 0.27 0
=> .27
FAREA 0.85 0.85 0.85 0.85 0.85 0.85 0.85 0.85 0.85 0.85 0
=> .85
FODOT 0.00 2.95E+05 3.42E+05 3.75E+05 5.02E+05 3.88E+05 3.58E+05 3.22E+05 2
=> .72E+05 3.36E+05 2.81E+05
CJET all
HCR 0.333 0.333 0.200 0.200 0.100 0.100 0.100 0.100 0.100 0.100 0.100
CO 0.000 0.140 0.189 0.262 0.350 0.314 0.313 0.272 0.222 0.139 0.146
OD 0.130 0.100 0.100 0.100 0.075 0.050 0.050 0.050 0.050 0.050 0.050
STPMAX 5.00
DUMPR 2end.DMP
DEVICE 1
WINDOW 0 0. 0. 1279. 1023. 4095.

```

```

** CFAST Version 2.0.1 Run 3/2/95 **
**                                     **
** A contribution of the             **
** National Institute of Standards and Technology **
** Gaithersburg, MD 20899          **
** Not subject to Copyright         **

```

Time = 0.0 seconds.

Compartment	Upper Temp. (K)	Lower Temp. (K)	Inter. Height (m)	Pyrol Rate (kg/s)	Fire Size (W)
1 Outside	300.0	300.0	2.2	0.000	0.000

Time = 600.0 seconds.

Compartment	Upper Temp. (K)	Lower Temp. (K)	Inter. Height (m)	Pyrol Rate (kg/s)	Fire Size (W)
1 Outside	531.1	381.3	0.55	4.270E-02	8.960E+04 3.146E+05

Time = 1200.0 seconds.

Compartment	Upper Temp. (K)	Lower Temp. (K)	Inter. Height (m)	Pyrol Rate (kg/s)	Fire Size (W)
1 Outside	545.1	401.7	0.56	4.310E-02	8.547E+04 2.825E+05

Time = 1800.0 seconds.

Compartment	Upper Temp. (K)	Lower Temp. (K)	Inter. Height (m)	Pyrol Rate (kg/s)	Fire Size (W)
1 Outside	576.1	426.4	0.56	4.150E-02	9.252E+04 2.411E+05

Time = 2400.0 seconds.

Compartment	Upper Temp. (K)	Lower Temp. (K)	Inter. Height (m)	Pyrol Rate (kg/s)	Fire Size (W)
1 Outside	617.2	454.2	0.56	3.660E-02	1.072E+05 1.832E+05

Time = 3000.0 seconds.

Compartment	Upper Temp. (K)	Lower Temp. (K)	Inter. Height (m)	Pyrol Rate (kg/s)	Fire Size (W)
1 Outside	667.5	487.4	0.56	3.010E-02	1.263E+05 2.250E+05

Time = 3600.0 seconds.

Compartment	Upper Temp. (K)	Lower Temp. (K)	Inter. Height (m)	Pyrol Rate (kg/s)	Fire Size (W)
1 Outside	703.7	521.3	0.56	3.010E-02	1.278E+05 2.098E+05


```

VERSN      2MLR.3 EXACT o2 = 2%, all jets on
TIMES      7200 1200 60 10 0
TAMB      300. 101300. 0.
EAMB      300. 101300. 0.
HI/F       0.00
WIDTH      2.23
DEPTH      5.40
HEIGHT     2.23
HVENT      1 2 1 0.124 2.130 2.006 0.000
HVENT      1 2 2 0.177 0.227 0.050 0.000
CVENT      1 2 1 1.00 1.00 1.00 1.00 1.00 1.00 1.00 1.00
=> 1.00 1.00
CVENT      1 2 2 1.00 1.00 1.00 1.00 1.00 1.00 1.00 1.00
=> 1.00 1.00
CEILI GYPROCK GYPROCK gYP3/4
WALLS GYPROCK GYPROCK GYP3/4
FLOOR GYP3/4
CHENI      16. 20. 2 18000000. 300. 400. 0.000
LFB0       1
LFBT       2
FPOS       0.52 1.05 0.27
FTIME      120. 300. 600. 1800. 2400. 3000. 3600. 4200. 4800. 7200.
FMASS      0.0000 0.0164 0.0190 0.0208 0.0279 0.0216 0.0199 0.0179 0.0151 0.0151 0.0
=> 156
FHIGH      0.27 0.27 0.27 0.27 0.27 0.27 0.27 0.27 0.27 0.27 0
=> 27
FAREA      0.85 0.85 0.85 0.85 0.85 0.85 0.85 0.85 0.85 0.85 0
=> .85
FDDOT      0.00 2.95E+05 3.42E+05 3.75E+05 5.02E+05 3.88E+05 3.58E+05 3.22E+05 2
=> .72E+05 3.36E+05 2.81E+05
CIET all
HCR        0.333 0.333 0.200 0.200 0.100 0.100 0.100 0.100 0.100 0.100 0.100
CD         0.000 0.227 0.384 0.413 0.510 0.491 0.470 0.438 0.264 0.236 0.208
OD         0.130 0.100 0.100 0.100 0.075 0.050 0.050 0.050 0.050 0.050 0.050
STPMAX     5.00
DUMPR 3end.DMP
DEVICE 1
WINDOW 0 0. 0. 1279. 1023. 4095.

```

```

** CFAST Version 2.0.1 Run 2/26/95 **
**                                     **
** A contribution of the              **
** National Institute of Standards and Technology **
** Gaithersburg, MD 20899           **
** Not subject to Copyright          **

```

Time = 0.0 seconds.

Compartment	Upper Temp. (K)	Lower Temp. (K)	Inter. Height (m)	Pyrol Rate (kg/s)	Fire Size (W)
1	300.0	300.0	2.2	0.000	0.000
Outside					0.000

Time = 1200.0 seconds.

Compartment	Upper Temp. (K)	Lower Temp. (K)	Inter. Height (m)	Pyrol Rate (kg/s)	Fire Size (W)
1	449.4	369.2	0.55	2.435E-02	3.253E+04
Outside					3.184E+05

Time = 2400.0 seconds.

Compartment	Upper Temp. (K)	Lower Temp. (K)	Inter. Height (m)	Pyrol Rate (kg/s)	Fire Size (W)
1	452.6	373.1	0.55	2.160E-02	3.221E+04
Outside					4.229E+05

Time = 3600.0 seconds.

Compartment	Upper Temp. (K)	Lower Temp. (K)	Inter. Height (m)	Pyrol Rate (kg/s)	Fire Size (W)
1	508.3	401.3	0.55	1.790E-02	5.080E+04
Outside					3.181E+05

Time = 4800.0 seconds.

Compartment	Upper Temp. (K)	Lower Temp. (K)	Inter. Height (m)	Pyrol Rate (kg/s)	Fire Size (W)
1	559.5	439.9	0.55	1.510E-02	6.277E+04
Outside					2.849E+05

Time = 6000.0 seconds.

Compartment	Upper Temp. (K)	Lower Temp. (K)	Inter. Height (m)	Pyrol Rate (kg/s)	Fire Size (W)
1	591.5	473.2	0.55	1.535E-02	6.367E+04
Outside					2.502E+05

Time = 7200.0 seconds.

Compartment	Upper Temp. (K)	Lower Temp. (K)	Inter. Height (m)	Pyrol Rate (kg/s)	Fire Size (W)
1	616.9	499.8	0.55	1.560E-02	6.375E+04
Outside					2.204E+05

```

VERSN      ZMLR. 4 EXACT test number FOUR
TIMES      2100 600 60 10 0
TAMB       300. 101300. 0.
EAMB       300. 101300. 0.
HI/F       0.00
WIDTH      2.23
DEPTH      5.40
HEIGHT     2.23
HVENT      1 2 1 0.124 2.130 2.006 0.000
HVENT      1 2 2 0.177 0.227 0.050 0.000
CVENT      1 2 1 1.00 1.00 1.00 1.00 1.00 1.00 1.00 1.00 1.00
=> 1.00 1.00
CVENT      1 2 2 1.00 1.00 1.00 1.00 1.00 1.00 1.00 1.00 1.00
=> 1.00 1.00
CEILI GYROCK GYROCK gYP3/4
WALLS GYROCK GYROCK GYP3/4
FLOOR GYP3/4
CHEMI      16. 20. 2 18000000. 300. 400. 0.000
LFBO       1
LFBT       2
FPOS       0.52 1.05 0.27
FTIME      120. 240. 480. 600. 900. 1200. 1800. 2100. 3000. 36000.
FHASS      0.0000 0.0171 0.0224 0.0275 0.0326 0.0277 0.0260 0.0232 0.0228 0.0228 0.0
=> .228
FHIGH      0.27 0.27 0.27 0.27 0.27 0.27 0.27 0.27 0.27 0.27 0
=> .27
FAREA      0.85 0.85 0.85 0.85 0.85 0.85 0.85 0.85 0.85 0.85 0
=> .85
FDDOT      0.00 2.95E+05 3.42E+05 3.75E+05 5.02E+05 3.88E+05 3.58E+05 3.22E+05 2
=> .72E+05 3.36E+05 2.81E+05
CJET all
HCR        0.333 0.333 0.200 0.200 0.100 0.100 0.100 0.100 0.100 0.100 0.100
CD         0.000 0.276 0.384 0.422 0.537 0.432 0.403 0.342 0.286 0.259 0.218
OD         0.130 0.100 0.100 0.100 0.075 0.050 0.050 0.050 0.050 0.050 0.050
STPMAX     5.00
DUMPR 4END.DMP
DEVICE 1
WINDOW 0 0. 0. 1279. 1023. 4095.

```

```

** CFAST Version 2.0.1 Run 2/26/95 **
**                                     **
** A contribution of the             **
** National Institute of Standards and Technology **
** Gaithersburg, MD 20899          **
** Not subject to Copyright         **

```

Time = 0.0 seconds.

Compartment	Upper Temp. (K)	Lower Temp. (K)	Inter. Height (m)	Pyrol Rate (kg/s)	Fire Size (W)
1 Outside	300.0	300.0	2.2	0.000	0.000 0.000

Time = 600.0 seconds.

Compartment	Upper Temp. (K)	Lower Temp. (K)	Inter. Height (m)	Pyrol Rate (kg/s)	Fire Size (W)
1 Outside	430.3	361.1	0.55	3.260E-02	2.517E+04 2.031E+05

Time = 1200.0 seconds.

Compartment	Upper Temp. (K)	Lower Temp. (K)	Inter. Height (m)	Pyrol Rate (kg/s)	Fire Size (W)
1 Outside	402.0	352.0	0.55	2.600E-02	1.680E+04 2.959E+05

Time = 1800.0 seconds.

Compartment	Upper Temp. (K)	Lower Temp. (K)	Inter. Height (m)	Pyrol Rate (kg/s)	Fire Size (W)
1 Outside	417.6	352.8	0.55	2.320E-02	2.380E+04 3.248E+05

Time = 2100.0 seconds.

Compartment	Upper Temp. (K)	Lower Temp. (K)	Inter. Height (m)	Pyrol Rate (kg/s)	Fire Size (W)
1 Outside	428.8	356.1	0.55	2.280E-02	2.758E+04 2.752E+05

```

VERSN      ZMLR. 5 EXACT test number FIVE
TIMES      3600 600 60 10 0
TAMB       300. 101300. 0.
EAMB       300. 101300. 0.
HI/F       0.00
WIDTH      2.23
DEPTH      5.40
HEIGHT     2.23
HVENT      1 2 1 0.089 2.130 2.041 0.000
HVENT      1 2 2 0.124 0.174 0.050 0.000
CVENT      1 2 1 1.00 1.00 1.00 1.00 1.00 1.00 1.00 1.00 1.00
=> 1.00 1.00
CVENT      1 2 2 1.00 1.00 1.00 1.00 1.00 1.00 1.00 1.00 1.00
=> 1.00 1.00
CEILI GYPROCK GYPROCK GYP3/4
WALLS GYPROCK GYPROCK GYP3/4
FLOOR GYP3/4
CHEMI      16. 20. 2 18000000. 300. 400. 0.000
LFBO       1
LFBT       2
FPOS       0.52 1.05 0.74
FTIME      120. 240. 480. 600. 900. 1200. 1800. 2400. 3000. 36000.
FRASS      0.0000 0.0205 0.0081 0.0061 0.0102 0.0089 0.0114 0.0106 0.0077 0.0057 0.0
=> 057
FHIGH      0.74 0.74 0.74 0.74 0.74 0.74 0.74 0.74 0.74 0.74 0
=> .74
FAREA      0.85 0.85 0.85 0.85 0.85 0.85 0.85 0.85 0.85 0.85 0
=> .85
FQDOT      0.00 2.95E+05 3.42E+05 3.75E+05 5.02E+05 3.88E+05 3.58E+05 3.22E+05 2
=> .72E+05 3.36E+05 2.81E+05
CJET all
HCR        0.333 0.333 0.200 0.200 0.100 0.100 0.100 0.100 0.100 0.100 0.100
CO         0.000 0.412 0.291 0.201 0.329 0.333 0.408 0.349 0.225 0.145 0.134
OD         0.130 0.100 0.100 0.100 0.075 0.050 0.050 0.050 0.050 0.050 0.050
STPMAX     5.00
DUMPR SEND.DMP
DEVICE 1
WINDOW 0 0. 0. 1279. 1023. 4095.

```

```

** CFAST Version 2.0.1 Run 2/26/95 **
**                                     **
** A contribution of the             **
** National Institute of Standards and Technology **
** Gaithersburg, MD 20899          **
** Not subject to Copyright         **

```

Time = 0.0 seconds.

Compartment	Upper Temp. (K)	Lower Temp. (K)	Inter. Height (m)	Pyrol Rate (kg/s)	Fire Size (W)
1 Outside	300.0	300.0	2.2	0.000	0.000 0.000

Time = 600.0 seconds.

Compartment	Upper Temp. (K)	Lower Temp. (K)	Inter. Height (m)	Pyrol Rate (kg/s)	Fire Size (W)
1 Outside	404.6	324.4	1.5	1.020E-02	1.483E+04 2.226E+05

Time = 1200.0 seconds.

Compartment	Upper Temp. (K)	Lower Temp. (K)	Inter. Height (m)	Pyrol Rate (kg/s)	Fire Size (W)
1 Outside	373.5	325.1	1.5	1.140E-02	6.781E+03 0.000

Time = 1800.0 seconds.

Compartment	Upper Temp. (K)	Lower Temp. (K)	Inter. Height (m)	Pyrol Rate (kg/s)	Fire Size (W)
1 Outside	355.7	324.2	1.5	1.060E-02	3.734E+03 0.000

Time = 2400.0 seconds.

Compartment	Upper Temp. (K)	Lower Temp. (K)	Inter. Height (m)	Pyrol Rate (kg/s)	Fire Size (W)
1 Outside	374.4	324.3	1.5	7.700E-03	8.844E+03 0.000

Time = 3000.0 seconds.

Compartment	Upper Temp. (K)	Lower Temp. (K)	Inter. Height (m)	Pyrol Rate (kg/s)	Fire Size (W)
1 Outside	413.3	328.9	1.5	5.700E-03	1.796E+04 4.965E+05

Time = 3600.0 seconds.

Compartment	Upper Temp. (K)	Lower Temp. (K)	Inter. Height (m)	Pyrol Rate (kg/s)	Fire Size (W)
1 Outside	438.2	337.7	1.5	5.700E-03	2.243E+04 4.054E+05

```

VERSN      2MLR. 6 EXACT test number SIX
TIMES      3020 600 60 10 0
TAMB       300. 101300. 0.
EAMB       300. 101300. 0.
HI/F       0.00
WIDTH      2.23
DEPTH      5.40
HEIGHT     2.23
HVENT      1 2 1 0.089 1.435 1.346 0.000
HVENT      1 2 2 0.124 0.174 0.050 0.000
CVENT      1 2 1 1.00 1.00 1.00 1.00 1.00 1.00 1.00 1.00 1.00
=> 1.00 1.00
CVENT      1 2 2 1.00 1.00 1.00 1.00 1.00 1.00 1.00 1.00 1.00
=> 1.00 1.00
CEILI GYPROCK GYPROCK gYP3/4
WALLS GYPROCK GYPROCK GYP3/4
FLOOR GYP3/4
CHEMI      16. 20. 2 18000000. 300. 400. 0.000
LFB0       1
LFBT       2
FPOS       0.52 1.05 0.74
FTIME      120. 240. 480. 600. 900. 1200. 1800. 2400. 3000. 3020.
FMASS      0.0000 0.0177 0.0020 0.0020 0.002 0.0057 0.0049 0.0041 0.0028 0.0033 0.00
=> 326
FHIGH      0.74 0.74 0.74 0.74 0.74 0.74 0.74 0.74 0.74 0.74 0
=> .74
FAREA      0.85 0.85 0.85 0.85 0.85 0.85 0.85 0.85 0.85 0.85 0
=> .85
FODOT      0.00 2.95E+05 3.42E+05 3.75E+05 5.02E+05 3.88E+05 3.58E+05 3.22E+05 2
=> .72E+05 3.36E+05 2.81E+05
CJET all
HER        0.333 0.333 0.200 0.200 0.100 0.100 0.100 0.100 0.100 0.100 0.100
CO         0.000 0.291 0.002 0.007 0.002 0.102 0.084 0.054 0.011 0.028 0.028
OD         0.130 0.100 0.100 0.100 0.075 0.050 0.050 0.050 0.050 0.050 0.050
STPMAX     5.00
DUMPR 6END.DMP
DEVICE 1
WINDOW 0 0. 0. 1279. 1023. 4095.

```

```

XX CFAST Version 2.0.1 Run 2/26/95 XX
XX                                     XX
XX A contribution of the             XX
XX National Institute of Standards and Technology XX
XX Gaithersburg, MD 20899          XX
XX Not subject to Copyright         XX

```

Time = 0.0 seconds.

Compartment	Upper Temp. (K)	Lower Temp. (K)	Inter. Height (m)	Pyrol Rate (kg/s)	Fire Size (W)
1	300.0	300.0	2.2	0.000	0.000
Outside					0.000

Time = 600.0 seconds.

Compartment	Upper Temp. (K)	Lower Temp. (K)	Inter. Height (m)	Pyrol Rate (kg/s)	Fire Size (W)
1	342.9	318.1	1.5	2.000E-03	1.235E+03
Outside					0.000

Time = 1200.0 seconds.

Compartment	Upper Temp. (K)	Lower Temp. (K)	Inter. Height (m)	Pyrol Rate (kg/s)	Fire Size (W)
1	322.8	314.2	1.4	4.900E-03	2.560E-05
Outside					0.000

Time = 1800.0 seconds.

Compartment	Upper Temp. (K)	Lower Temp. (K)	Inter. Height (m)	Pyrol Rate (kg/s)	Fire Size (W)
1	319.6	312.5	1.4	4.100E-03	4.360E-07
Outside					0.000

Time = 2400.0 seconds.

Compartment	Upper Temp. (K)	Lower Temp. (K)	Inter. Height (m)	Pyrol Rate (kg/s)	Fire Size (W)
1	317.7	311.4	1.4	2.800E-03	3.123E-08
Outside					0.000

Time = 3000.0 seconds.

Compartment	Upper Temp. (K)	Lower Temp. (K)	Inter. Height (m)	Pyrol Rate (kg/s)	Fire Size (W)
1	316.1	310.7	1.4	3.300E-03	5.354E-09
Outside					0.000

Time = 3020.0 seconds.

Compartment	Upper Temp. (K)	Lower Temp. (K)	Inter. Height (m)	Pyrol Rate (kg/s)	Fire Size (W)
1	316.1	310.6	1.4	3.260E-03	4.487E-09
Outside					0.000


```

VERSN      2MLR. 6 EXACT test number SEVEN
TIMES      5400 600 60 10 0
TAMB       300. 101300. 0.
EAMB       300. 101300. 0.
HI/F       0.00
WIDTH      2.23
DEPTH      5.40
HEIGHT     2.23
HVENT      1 2 1 0.089 1.435 1.346 0.000
HVENT      1 2 2 0.124 0.174 0.050 0.000
CVENT      1 2 1 1.00 1.00 1.00 1.00 1.00 1.00 1.00 1.00
=> 1.00 1.00
CVENT      1 2 2 1.00 1.00 1.00 1.00 1.00 1.00 1.00 1.00
=> 1.00 1.00
CEILI GYPROCK GYPROCK gYP3/4
WALLS GYPROCK GYPROCK GYP3/4
FLOOR GYP3/4
CHEMI      16. 20. 2 18000000. 300. 400. 0.000
LFBO       1
LFBT       2
FPQS       0.52 1.05 0.74
FTIME      120. 240. 480. 900. 1200. 1500. 2700. 3900. 5100. 5400.
FNASS      0.0000 0.0187 0.0081 0.0031 0.0041 0.0049 0.0065 0.0063 0.0043 0.0047 0.0
=> 0.47
FHIGH      0.74 0.74 0.74 0.74 0.74 0.74 0.74 0.74 0.74 0.74 0
=> .74
FAREA      0.85 0.85 0.85 0.85 0.85 0.85 0.85 0.85 0.85 0.85 0
=> .85
FDDOT      0.00 2.95E+05 3.42E+05 3.75E+05 5.02E+05 3.88E+05 3.58E+05 3.22E+05 2
=> .72E+05 3.36E+05 2.81E+05
CJET all
HCR        0.333 0.333 0.200 0.200 0.100 0.100 0.100 0.100 0.100 0.100 0.100
CO         0.000 0.682 0.507 0.242 0.301 0.326 0.450 0.460 0.396 0.398 0.398
OD         0.130 0.100 0.100 0.100 0.075 0.050 0.050 0.050 0.050 0.050 0.050
STPMAX     5.00
DUMPR 7END.DMP
DEVICE 1
WINDOW 0 0. 0. 1279. 1023. 4095.

```

```

** CFAST Version 2.0.1 Run 2/26/95 **
**                                     **
** A contribution of the               **
** National Institute of Standards and Technology **
** Gaithersburg, MD 20899             **
** Not subject to Copyright            **

```

Time = 0.0 seconds.

Compartment	Upper Temp. (K)	Lower Temp. (K)	Inter. Height (m)	Pyrol Rate (kg/s)	Fire Size (W)
1 Outside	300.0	300.0	2.2	0.000	0.000

Time = 600.0 seconds.

Compartment	Upper Temp. (K)	Lower Temp. (K)	Inter. Height (m)	Pyrol Rate (kg/s)	Fire Size (W)
1 Outside	328.6	316.6	1.4	3.386E-03	9.374E-04

Time = 1200.0 seconds.

Compartment	Upper Temp. (K)	Lower Temp. (K)	Inter. Height (m)	Pyrol Rate (kg/s)	Fire Size (W)
1 Outside	320.2	312.6	1.4	4.900E-03	1.025E-05

Time = 1800.0 seconds.

Compartment	Upper Temp. (K)	Lower Temp. (K)	Inter. Height (m)	Pyrol Rate (kg/s)	Fire Size (W)
1 Outside	317.2	311.3	1.3	6.450E-03	7.734E-08

Time = 2400.0 seconds.

Compartment	Upper Temp. (K)	Lower Temp. (K)	Inter. Height (m)	Pyrol Rate (kg/s)	Fire Size (W)
1 Outside	315.5	310.4	1.3	6.350E-03	1.909E-09

Time = 3000.0 seconds.

Compartment	Upper Temp. (K)	Lower Temp. (K)	Inter. Height (m)	Pyrol Rate (kg/s)	Fire Size (W)
1 Outside	314.2	309.8	1.3	5.800E-03	1.360E-10

Time = 3600.0 seconds.

Compartment	Upper Temp. (K)	Lower Temp. (K)	Inter. Height (m)	Pyrol Rate (kg/s)	Fire Size (W)
1 Outside	313.1	309.2	1.3	4.800E-03	2.216E-11

Time = 4200.0 seconds.

Compartment	Upper Temp. (K)	Lower Temp. (K)	Inter. Height (m)	Pyrol Rate (kg/s)	Fire Size (W)
1 Outside	312.2	308.6	1.4	4.400E-03	6.279E-12

Time = 4800.0 seconds.

Compartment	Upper Temp. (K)	Lower Temp. (K)	Inter. Height (m)	Pyrol Rate (kg/s)	Fire Size (W)
1 Outside	311.4	308.2	1.4	4.600E-03	2.364E-12

Time = 5400.0 seconds.

Compartment	Upper Temp. (K)	Lower Temp. (K)	Inter. Height (m)	Pyrol Rate (kg/s)	Fire Size (W)
1 Outside	310.6	307.8	1.4	4.700E-03	8.856E-13

FIRE ENGINEERING RESEARCH REPORTS

95/1	Full Residential Scale Backdraft	I. B. Bolliger
95/2	A Study of Full Scale Room Fire Experiments	P. A. Enright
95/3	Design of Load-bearing Light Steel Frame Walls for Fire Resistance	J. T. Gerlich
95/4	Full Scale Limited Ventilation Fire Experiments	D. J. Millar
95/5	An Analysis of Domestic Sprinkler Systems for Use in New Zealand	F. Rahmanian

School of Engineering
University of Canterbury
Private Bag 4800
Christchurch, New Zealand

Phone 643 366-7001
Fax 643 364-2758